UNIVERSITY OF CALIFORNIA
RIVERSIDE

Understanding Influenza B Virus Pathology Under Cigarette Smoking Conditions and Development of a New Live Flu Vaccine with Inherited Safety

A Dissertation submitted in partial satisfaction
of the requirements for the degree of

Doctor of Philosophy

in

Genetics, Genomics & Bioinformatics

by

Jerald Rudy Chavez

December 2022

Dissertation Committee:
Dr. Rong Hai, Chairperson
Dr. Sean O'Leary
Dr. Weifeng Gu

The Dissertation of Jerald Rudy Chavez is approved:

Committee Chairperson

University of California, Riverside

ACKNOWLEDGEMENTS

I would like to thank my supervisor and chairperson Dr. Rong Hai for their feedback and mentorship. I would also like to thank my defense and my dissertation committee for their guidance and suggestions over the years. I would also acknowledge the tremendous support from the Tobacco Related Disease Research Program that supported me for years to accomplish components of this work. I would finally like to thank my lab mates Dr. Stephanie Thurmond and Dr. Harrison Dulin whose consistent feedback and scientific conversations shaped me into a better scientist.

Dedication

To my family, friends, and students, I thank you for the years of support and patience with me. I would not be here if not for all of you.

ABSTRACT OF THE DISSERTATION

Understanding Influenza B Virus Pathology Under Cigarette Smoking Conditions and Development of a New Live Flu Vaccine with Inherited Safety

by

Jerald Rudy Chavez

Doctor of Philosophy, Graduate Program in Genetics, Genomics & Bioinformatics
University of California, Riverside, December 2022
Dr. Rong Hai, Chairperson

Influenza B virus (IBV), in conjunction with Influenza A virus (IAV), results in yearly epidemics. While IAV is a well-studied pathogen, IBV lags in understanding of its pathology, replication mechanics, and vaccination use strategies. For example, smoking is a known risk factor for IAV, but little is known regarding its effects on IBV infections and pathology. Second, the IBV nucleoprotein (BNP) fulfills a critical role during replication, but its associated host factors remain largely unclear. Last, live virus vaccinations for IAV during pandemics are considered a potential risk due to the possibility the vaccine virus will reassort with circulating IAV, restoring virulence and exposing a naïve population to a pathogenic virus unintentionally. To fill these gaps, we set out to understand: a) what are the impacts of cigarette smoke on IBV infections b) what host factors are interacting with BNP and how are they involved in replication and c) whether we could attenuate recombinant IBVs (rIBVs) expressing the IAV HA by progressive mutations to the IAV ectodomain. To these ends, we developed an animal model to study the impact of cigarette smoke extract on IBV infections in mice not previously available. We found that low concentration of CSE increased IFN-γ production

in spleenocyte of infected mice, and high concentrations of CSE resulted in lower humoral responses to infection and lower survival rates. Additionally, we confirmed that BNP interacts with the host protein IMPα4, a nuclear import adaptor protein, through yeast-two-hybrid and Co-IP analysis. Further, knockout of IMPα4 expression reduced IBV replication. Finally, progressive mutation of IAV ectodomain using IBV coding sequence did result in attenuation of replication ex vivo, and these candidates could elicit significant humoral and neutralizing responses that protected mice from lethal challenge with homologous strains of IAVs. Together, each of these studies represent a necessary step forward in understanding how lifestyle factors impact IBV infections, the potential specific host-viral protein interactions that could be drug therapeutic targets of the future, and necessary development of innately safe and efficacious live vaccines for use in pandemic scenarios.

Table of Contents

List of Figures

List of Tables

Introduction

Influenza viruses cause seasonal epidemics. In the United States, there are an estimated 9-41 million total infections, 170,000-710,000 hospitalizations, and between 12,000-52,000 deaths annually (1). Worldwide, it results in 260,000 and 650,000 deaths as reported by the World Health Organization (WHO) (2). Resulting symptoms from contracted influenza disease are estimated to cause between 67-74% loss in their workplace productivity (3). Economic burden is estimated to exceed 11 billion dollars (USD) in medical costs annually in the US alone (4). Broken down by virus type, Influenza A virus and influenza B virus account for 63% and 37% of the economic burden across the 2001-2009 seasons (5).

Influenza Disease

Epidemic Influenza virus infections generally occur in the upper respiratory tract. Incubation, or the time it takes between infection and manifestation of symptoms, is generally between 1-4 days (6). These infections lead to direct inflammation and swelling of the tissue of the trachea. Common symptoms of infection include: loss of appetite, fever, cough, runny nose, headache, muscle aches, chills, nausea, and fatigue. These symptoms can last anywhere from 7-10 days on average (7). The disease outcome is greatly influenced by the age. Elderly individuals age 65 and older are most likely to be hospitalized, followed by children under 5 years and adults between 50-65 years of age (8). Additionally, other groups including children under 5 years of age born pre-maturely are at higher risk for complications and hospitalizations compared to their age matched control group (9). These at-risk groups and others with co-morbidities are most likely to experience viral and bacterial pneumonia (10), and in the worst-case

scenario can lead to Acute Respiratory Distress Syndrome (ARDS) and subsequently respiratory failure (11).

Immune Response to Influenza Virus Infection

(This section is adapted from my own published article “Effects of Cigarette Smoking on Influenza Virus/Host Interplay” Chavez, J.; Hai, R. Pathogens 2021, 10, 1636)(12)

In response to infection, the body initiates both an innate and adaptive immune response, in which the non-specific innate response restricts and contains infection, while the targeted adaptive response is responsible for ultimate clearance of the virus (summarized in Figure 1). Influenza viruses first infect upper respiratory airway epithelial cells, where infection is initially detected by recognition of pathogen associated molecular patterns (PAMPs) that are inherent to the virion or produced during infection. These PAMPs, such as viral RNA, are detected by Pattern Recognition Receptors (PRRs). For example, RIG-I is an intracellular receptor (recognizes and binds the influenza viral genomic RNAs (13)), which triggers signaling cascades leading to production of the proinflammatory cytokine interferon (IFN) (14, 15). Type 1 IFNs secreted by infected cells alert neighboring cells to the infection and stimulate transcription of Interferon stimulated genes (ISGs). ISGs in turn produce an antiviral state that restricts virus replication. The release of pro-inflammatory cytokines and chemokines results in the recruitment of circulating immune cells from the blood to the site of infection. For example, NLRP3, activated by multiple Influenza PAMPs(16), results in the formation of the NLRP3 inflammasome and production of pro-inflammatory cytokines that recruit of leukocytes (macrophages, lymphocytes, granulocytes, etc) to the lungs during infection (17). Leukocytes such as neutrophils and macrophages are critical in restriction of the virus, as they serve to phagocytose infectious virus, breaking

them down by lysosomal degradation. Additionally, these cells secrete additional cytokines and chemokines to sustain and increase recruitment of other immune cells to aid in virus restriction and clearance.

Adaptive immune responses are critical for ultimate clearance of infection. Adaptive immunity requires that viral antigens (components of the virus) be presented to adaptive immune cells for activation. The process is completed by antigen presenting cells, including dendritic cells and macrophages. They process viral proteins and present them to $CD4^+$ helper T-cells, resulting in their activation and proliferation. These activated helper T-cells go on to activate B-cells and other effector cells, such as $CD8^+$ T-cells. B-cells produce antibodies that bind influenza virus and prevent the virus entry into susceptible cells (neutralization), while active $CD8^+$ T-cells seek out and kill virus infected cells. Therefore, innate immune response cells like macrophages and dendritic cells represent critical bridges from the innate to the adaptive responses.

While recruitment and activation of innate and adaptive cells are necessary to combat infection, excess inflammation can result in severe damage to the airway and lung tissue. In severe influenza infections, viruses migrate from the upper respiratory tract to the lower respiratory tract, where infection of the lower lung epithelia triggers inflammatory cell recruitment, causing damage to the alveolar epithelial cells responsible for gas exchange in the lungs. Once infection reaches the endothelium in the interstitium, cytokine responses and inflammation are further exacerbated (18). In some severe cases, this exaggerated inflammation and damage can lead to acute respiratory distress syndrome (ARDS) and subsequently, respiratory failure. However, this severe disease is more likely associated with pandemic influenza (such as 2009 H1N1(19, 20)) and strains of Avian influenza (such as H5N1) (21-23). The exacerbated levels of pro-

inflammatory cytokines and chemokines is referred to as a “cytokine storm.” This phenomena is typically not associated with mild, but rather severe cases of influenza. Patients hospitalized with severe influenza due to infection with avian H5N1 exhibit exacerbated levels of circulating pro-inflammatory cytokines including TNF-α, IL-6, sIL-2r, IP-10, and MIG.

Influenza virus infection eventually stimulates molecular and cellular pathways to effect tissue repair of infection damaged airways. For example, Influenza virus infection induces IL-33 expression (24). IL-33 acts on a number of cells including but not limited to ILC2s, T_H2 cells and T-reg cells (25), which drive the type II immune response critical for tissue repair. Thus, the immune response must stimulate enough immune cell recruitment to the local effected area to restrict or clear infection, but not so much that it results in excessive damage that slows or inhibits type II repair responses.

Influenza Virus Types, Replication, and Differences

Influenza Disease is caused by influenza virus infection. These viruses are part of the Orthomyxoviridae family. There are 4 types of Influenza viruses: Influenza A Virus (IAV), Influenza B Virus (IBV), Influenza C Virus (ICV), and Influenza D Virus (IDV). Type A-C all infect humans, with influenza D virus primarily infecting cattle (26). These are negative sense, enveloped, RNA Viruses. The viral genomes of IAV and IBV are segmented, comprised of 8 individual RNA segments. These segments encode a total of at least 10 viral proteins. These RNAs are bound with multiple copies of the viral NP protein and a single copy of the heterotrimeric viral polymerase, forming the viral ribonucleoprotein complex (vRNP). The vRNPs are surrounded by a viral envelope studded with viral hemagglutinin (HA) and neuraminidase (NA). Infection by the virus is initiated by interaction between HA and the cellular receptor Sialic Acid. The virion is

then phagocytosed by the cell, where pH changes result in HA mediated fusion of the endosomal and viral membranes, resulting in release of the viral genomes into the cytoplasm. The vRNPs are subsequently imported into the nucleus where they are transcribed into cRNAs that serve as templates to produce more vRNA. After export to and translation of the RNAs in the cytoplasm, the viral proteins assemble at the cytoplasmic membrane, where budding and release of new virions occur. These viruses are subject to two forms of mutation, termed genetic drift and genetic shift. “Drift” refers to mutations introduced by the viral polymerase during transcription, where “shift” refers to swapping of RNA segments when two genetically distinct viruses infect the same cell. These mutations have resulted in a total of 18 genetically distinct subtypes of HA, and 11 subtypes of NA. Due to their serologic phenotypes, the field has adopted a naming convention based on the combination of HA and NA genetic segments, such as H1N1 or H3N2. We shall see that these mutations and combination of various segments will have significant effects on immune evasion and threat for pandemics as we shall see. IAV and IBV are responsible for seasonal, yearly epidemics. In addition to replicating and causing disease in humans, IAV primarily replicates in avian waterfowl (like ducks), which act a reservoir for year-round replication of the virus. While highly virulent, avian influenza viruses do not transmit well between humans. However, these viruses do transmit well between waterfowl and several terrestrial species, including several livestock animals such as pigs, chickens, and turkeys. Because animals like pigs can be infected by both human and avian IAV, they are thought to serve as “mixing vessels,” producing novel IAVs that could potentially infect and expose a naive human population to a highly virulent and pathogenic virus.

Of the three types of human influenza, IAV is the only type that has historically caused pandemics. Influenza pandemics are defined by the rapid and pathogenic spread of a virus outside of its geographic point of origin, usually resulting from exposure of a population to an antigenically novel viral variant. The most famous of Influenza pandemics, the 1918 H1N1 pandemic, resulted in more than 40 million deaths worldwide, surpassing all countries WWI deaths combined by 2-fold in a much shorter time span than WWI itself (1914-1918). Subsequently, IAV was responsible for additional pandemics in 1957 (H2N2), 1968 (H3N2), and 2009 (H1N1) (27).

IBV has a similar genomic constellation to IAV, with 8 viral RNA segments encoding at least 11 proteins. In comparison to IAV, IBV virus remains relatively understudied. IBV, outside of humans, has only been detected in grey and harbor seals (28) which are not likely to easily pass viruses between themselves and humans. Genetically, IBV has been shown in vitro to have a 3-fold lower mutation rate compared to IAV (29), and the IBV HA head antigenic sites are less tolerant to insertion mutations compared to IAV HA (30). Genetically and antigenically, IBVs are not defined by subtype, but rather by two broad co-circulating lineages: B/Victoria lineage and B/Yamagata (31). Unlike IAV, co-infection of the two IBV lineages under lab conditions is rare, suggesting reassortment between lineages does not frequently occur (32). As such, the prevailing notion is that IBV primarily only infects humans, has no other animal reservoir akin to IAV waterfowl, and has lower mutation rates and potential compared to IAV. Therefore IBV is considered less of a disease and pandemic threat compared to IAV (33). However, despite the reduced pandemic and immune evasion potential, there is evidence that IBV does cause significant yearly morbidity and mortality, and that perhaps treating IBV infections in the same manner as IAV needs to be revisited.

Despite not have the mutational and pandemic potential of IAV, IBV still causes significant numbers of infections in the United States (Table 1) and its differences to IAV genetics, epidemiology, and immunopathology are key to understanding how underestimation could result in unnecessary disease burden. IBV can and does result in hospitalizations, and significantly impacts the health and wellbeing of both people 65 years or older (34, 35) and children (36). Specifically in younger children, Victoria virus was more likely to infect children under 6 years of age, while Yamagata Virus was more likely to affect children older than 6 years of age (37). When we examine hospitalization patterns of IBV, we see the percent of hospitalized IBV patients who were admitted to the intensive care unit exceeded that of IAV patients in the 2005-2006 & the 2011-2012 seasons, and was within 5% of IAV for other seasons studied (38). For hospitalized patients, a line of defense post infection are antiviral drugs, like Oseltamivir. In the event of severe infection (or the possibility of severe infection), reducing and clearing viral loads can be achieved using antiviral drugs like Oseltamivir. Oseltamivir is an NA inhibitor and is an approved treatment for sever Influenza infections. However, while effective as an IAV inhibitor, Oseltamivir has been shown to be 30-40 fold less effective against IBV replication compared to IAV likely to the conformation difference between influenza A and B NAs (39). Some evidence also suggests that IBV may have a different immunopathology than IAV, as IBV induces IRF3 and IFN-λ1 genes almost immediately post infection, compared to IAV delayed activation, even though the associated consequences remains largely unknown (40).

In summary, IBV poses less pandemic, slower mutation rate, and less immune evasion potential compared to IAV. However, IBV can still cause sever disease, and has unique epidemiology, immunopathology, and drug resistance profiles versus IAV. These

facts simultaneously make IBV a worthy vector candidate for potential vaccines without the fear of pandemic spread, but also necessitates further examination on its own merits to prevent excess disease burden due to its differences with IAV. Indeed, outside the United States, the dominant lineage of IBV can shift every 1-3 years, and has been shown to become the dominant circulating virus in areas of Europe and Asia between 2017-2018 (41). IBV has been shown to peak later in the season compared to IAV (42-44) and result in lower vaccine effectiveness (45). As such, it is critical that we contrast the differences with IAV replication, pathology, and epidemiology to tailor responses to each virus to prevent as much disease as possible, and to better treat the already infected.

Vaccination Strategies and the future

Yearly vaccination remains the best strategy to prevent IAV and IBV infection and limit the spread of disease. Despite this, vaccine effectiveness (defined as the reduction of risk for clinical outcomes under real world conditions) on any given year hovers between 40-60% (46). Many factors can affect these protection levels, including the match of vaccine strains and circulating strains, age of the recipient, and the type of vaccine given. There are two basic categories of influenza virus vaccines currently available in the United States, inactivated virus vaccines (IIVs) or live attenuated influenza vaccines (LAIVs). Inactivated vaccines are produced by seeding an attenuated version of a circulating virus into chicken eggs on mass to produce large batch quantities of vaccine. The virus is chemically inactivated with compounds like formalin, and its protein components are subsequently purified to produce vaccine ready doses. Meta-analysis over 12 flu seasons shows that IIVs pooled efficacy is only 59% (47). IIVs protect primarily through induction of humoral (antibody based) immunity. Therefore,

mismatches between the vaccine virus strain used in production and circulating virus strains could lower effectiveness. In addition to lack of vaccination coverage, it is not clear that IIVs activate effective cellular and mucosal immune responses (48). Cellular T cell responses for example can target internal viral proteins that are more conserved than the epitopes of HA which is the immunodominant epitope (49) IIVs are designed around. The absence of cellular responses could result in decreased vaccine effectiveness in the case of vaccine mismatches.

In contrast, LAIVs have the potential to simultaneously activate cellular, humoral, and mucosal immunity. They can achieve this because they simulate real influenza virus infection, as these vaccines employ live attenuated viruses that do infect and replicate, but typically do not cause disease. These vaccines are produced by seeding chicken eggs or cells with a master donor virus and a virus that most closely genetically and antigenically resembles the predicted circulating strain for an upcoming season. The master doner virus possess temperature sensitive and cold adaptive mutations in the PA, PB1, and NP genome segments. The temperature sensitive mutations restrict the vaccine viruses to replicating in the cooler temperatures of the upper respiratory tract, while the cold-adapted mutations allow the virus to replicate at lower temperature during serial passages for production (50). LAIVs are efficacious in children (51-53) and the immuno-naïve and elicit broader humoral and mucosal responses (54). However, reassortment of LIAVs with circulating IAV could restore pathogenicity and virulence to the vaccine virus, and thus expose a naïve large population to highly virulent viruses. Hai et al., addressed this concern by expressing the IAV HA ectodomain in the IBV genomic background, thus preventing reassortment with circulating IAV while still eliciting antibodies against the IAV HA (55). While these candidate viruses do elicit

antibodies to IAV HA and could protect mice from lethal IAV challenge, attenuation was achieved through truncation mutations of NS-1. This leaves the candidate vaccines vulnerable to reassortment with circulating IBV that could restore virulence. Therefore, to address the reassortment concern, we hypothesized that the inherit safety could be achieved through moving the attenuation from NS1 to the HA segment that carries the immunodominant epitope necessary for humoral protection.

Cigarette Smokers, a Population Vulnerable to Infection

(This section is adapted from my own published article “Effects of Cigarette Smoking on Influenza Virus/Host Interplay” Chavez, J.; Hai, R. Pathogens 2021, 10, 1636)(12)

As of 2018, the CDC estimates that current cigarette smokers represent 14% of the US population, representing 34 million Americans (56). Cigarette smoking results in 480,000 annual deaths in the United States and is estimated to have resulted in over 10 times the number of premature deaths than all US fought wars combined (56). Smoking is a well-known cause of pulmonary conditions such as chronic obstructive pulmonary disease (COPD), directly affecting risk and degrees of symptoms. However, besides the direct damage cigarette smoke (CS) can inflict on the pulmonary system, it is also a well-known risk factor for the development and exacerbation of infectious diseases such as influenza virus (57-60). The CS specific mechanism(s) directly responsible for the impact on risk and disease outcome remains unclear. A direct complicating factor to this study of CS induced disease and complications is that CS comprises over 7000 different compounds and toxins. This high number of chemicals makes isolation of a single causative agent for pathologies induced by CS extremely difficult and time-consuming. Additionally, human genetic variability and the fact that smoking can result in other chronic diseases adds further confounding factors to the study of CS exposure and

infection in human populations. The etiology of smoking's impact on infection outcomes remains relatively understudied. Despite this hurdle, a common thread in the CS induced exacerbation of chronic and infectious disease appears to be acute and chronic (dubbed "low-grade") inflammation. Chronic inflammation is a well-studied risk factor in the development of chronic diseases like cardiovascular disease (CVD). Critical immune responses necessary to combat infection depend on induced inflammation, yet it is unclear how or if CS-induced acute and chronic inflammation directly affects infectious disease, or where these sources of inflammation would be coming from. In the following, we will discuss the known impact of CS exposure on immune responses critical to influenza infection, the exacerbation of inflammation (local and systemic) during infection in smokers and smoking models, potential CS induced changes in virus replication due to changes in immune response, and potential impacts of low-grade inflammation on influenza disease outcomes.

Once drawn into the lungs, cigarette smoke particles bombard the respiratory epithelial cells, triggering release of pro-inflammatory cytokines (such as IL-8 and TNF-α) by resident immune cells and epithelial cells alike. This results in elevated recruitment of neutrophils in acute cigarette smoke exposure and increased macrophage levels in the lungs (61-64). Upon arrival, innate immune cells aid in clearance of smoke particles, but also perpetuate inflammation and cellular recruitment by releasing pro-inflammatory cytokines and chemokines in the affected tissue. One could hypothesize that if inflammation and innate immunity are already elevated in smokers prior to infection, that this would aid in preventing infections, or make clearing of infections faster for the host. However, in cigarette mouse models, IAV infection results in worse disease outcomes compared to non-smoking controls. For example, CS exposure and subsequently

infection typically will result in reduced weight gain post infection (65-69), increased lung remodeling (deposition of scar tissue replacing functional lung tissue) (70, 71) and increased mortality (64, 66-68, 72) compared to non-CS infected mice. Similarly, CS exposure in humans is shown to be associated with increased risk of influenza infections (59, 73, 74), increased risk of severe symptoms (59), and decreased efficacy of influenza vaccines (75, 76).

Therefore, worse infection outcomes could be due to at least two factors: a) CS compromises immune responses necessary for antiviral defense and thus the host incurs more direct viral damage and/or b) IAV infection/replication is not affected, but rather a response to viral infection triggers an exaggerated inflammatory response compared to healthy individuals, resulting in more damage during infection and prolonged recovery. If the former is true, we would look for evidence that shows a) compromising of known immune responses necessary for containment and clearance of influenza virus b) evidence of more viral replication in smokers or smoking models compared to healthy individuals or controls, and c) longer viral clearance times for CS exposed individuals vs non-CS controls. Reports do indicate that specific immune responses important to viral insult response may be altered. Hans et al. has shown that cytokines and chemokines like TNF-α, IL-6, IL-4, IL-5, IL-10, and IFN-γ levels were elevated (between 2-10-fold) in the mice lungs after 3 weeks of CS exposure followed by IAV infection (67). These cytokines represent a mixture of both pro and anti-inflammatory cytokines. For example, IL-4, 5, and 10 are classic T-helper type 2 (T_H2) specific cytokines that normally push specific cells to commit to the T_H2 response. The T_H2 immune response function varies depending on the cells involved. Generally, they handle three broad processes: a) response to and clearance of allergens, b)

intracellular parasites defense, and c) tissue homeostasis and repair. Because long term smoking repeatedly introduces noxious elements to the lungs (as smoke particles) that need to be removed and cause excessive pulmonary inflammation, cigarette smoking is likely engaging both the T_H2 allergen clearance and tissue repair mechanisms. Indeed, smoking is associated with a higher risk for allergens and asthma (77), representing engagement of the allergic T_H2 responses. To activate the allergen response, dendritic cells (professional antigen presenting cells) uptake the allergen or noxious element and subsequently activate naive T-cells. These activated T-cells (now T_H2 cells) migrate to lymph nodes where they further differentiate and secrete IL-4, inducing class switching in B-Cells to produce IgE specific antibodies. Additionally, these T_H2 cells can egress from the lymph nodes and infiltrate tissue, where they can begin to produce IL-5 and IL-13. IL-5 stimulates activation and recruitment of eosinophils, which subsequently aid in further T_H2 recruitment and proliferation of T-cell cytokine production (reviewed in (78)). IL-13 is an anti-inflammatory cytokine, inhibiting pro-inflammatory cytokine production (79-81) and may represent engagement of repair mechanisms. In smoking models of COPD, however, IL-13 is primarily responsible for induction of emphysema (82). Chronically engaging these aspects of T_H2 immunity through smoking may likely result in poor response to viral infection upon challenge, as restriction and clearance of viruses like Influenza A and B viruses rely primarily on T_H1 pro-inflammatory responses, which are antagonistic to T_H2 responses (83). Indeed, exogenous IL-4 administered to mice results in slower viral clearance of IAV and reduced activation of $CD8^+$ T-cells (84), which are necessary for clearance of virus infected cells. In addition to lower activation of antiviral cytotoxic T-cells, it's possible a significant portion of B-cells in smokers are producing IgE due to engagement of T_H2 responses. T_H1 mediated antiviral defenses

activate B-cells to produce virus specific IgG antibodies, which block virus entry into the cell (neutralization) and thus halt infections while $CD8^+$ T-cells seek out and kill virus-infected cells to clear infection. Thus, in smokers, if T_H2 responses were primarily engaged before infection, there may be a lag time for B-cells to undergo class switching to IgG to combat influenza virus infection compared to healthy individuals. While adaptive immune responses to IAV after CS exposure are less well characterized compared to innate responses, chronic CS exposure (>2 weeks) leads to decreased IFN production by $CD4^+$ and $CD8^+$ T cells (66), no change to sera (IgG) IAV-specific antibodies 6 weeks post infection (72), but decreased levels of IAV IgA (68, 85). Effector T-cells secrete cytokines like IFN-γ in order to carry out their function. Lower IFN production could be predictive of decreased viral clearance and lower activation of subsequent adaptive immune cells like B-cells. No change in serum antibodies in CS exposed models compared to non-CS groups could suggest that if skewing of adaptive immunity is occurring, it is at a level that does not have a significant impact on IgG IAV antibodies. However, it should be noted that the kinetics of antibody responses to IAV infection in CS models to our knowledge has not been examined, potentially missing critical early effects of smoking on serum antibody responses. Reduced levels of IAV IgA antibodies on the other hand indicates at a minimum that smoking is having an impact on mucosal immunity. IgA antibodies are secreted into the mucosal lining of the respiratory tract, where they can intercept their viral target prior to it reaching the epithelium, preventing infection. As such, a decrease in IgA response in CS models during Influenza infection represents a direct compromise of the viral immune response (86).

So, if immune responses necessary for containment and clearance of Influenza viruses are compromised, the follow-up question would be whether viral replication has been affected? A/WSN/1933(H1N1) IAV had higher infectivity levels in human small airway epithelial cells exposed to cigarette smoke compared to air exposed controls (86). Similarly, Calu-3 cells (lung epithelial cell line) exposed to CS supported 1-log higher replication of H1N1 IAV compared to non-CS controls (87). Comparing viral replication in nasal epithelia cells isolated from smokers versus non-smokers, it was reported that there was a six-fold higher virus replication in cells from smokers compared to healthy controls (88). However, mouse model data regarding viral loads with CS exposure is less compelling. Gualano et al reports 4-day CS exposure increases H3N2 viral replication compared to controls, though only to a moderate degree with a ~3.5 fold increase (65). Other groups reported CS exposure having little to no effect on viral replication (64, 66, 72, 89). This suggests that worse disease outcome may result from other factors (such as exaggerated inflammation) rather than compromised immune responses in smokers. However, it should be noted that these results may be just a consequence of a lack of standardization in model systems, as CS exposure length, cigarette type and number, mouse genotype background, IAV infection MOI, and IAV strain used do not have any standard in the field. For example, CS exposure in mouse models of infection can range from 3 days (90) to 6 months (85) prior to infection.

If viral loads are not significantly affected by CS exposure, then could clearance of IAV infection be compromised? Mebratu et al showed, using mouse adapted H3N2- HK X31 at $1X10^3$ PFU/mouse with up to 1 month CS exposure, that CS exposed mice had 1 log higher titers at 14dpi (as measured by qPCR) compared to air control mice (91). Similarly, Hong et al. noted that, with H3N2 at 25 TCID50 with 3-month CS exposure,

CS exposed mice had 100-fold higher live virus titers at 10dpi vs the no CS controls, suggesting viral clearance had been impeded (68). Interestingly, Lee et al. has shown, using PR8 IAV at 100 PFU per mouse with 2 weeks CS exposure, that early viral titers at three days post infection were higher in CS mice vs controls, but peak viral titers and post peak clearance for CS and controls were identical in contrast to previous studies (69). While seemingly conflicting, we would assume that these conflicting clearance results are more potentially due to variability in IAV dose, CS exposure, and viral genotype rather than being in direct contradiction. As such, it is important that further studies conducted on the effects of CS on viral loads and clearance standardize a set CS exposure amount and virus type, while titrating viral doses. This would be beneficial not only to determine if CS affects viral burden and clearance with a single IAV strain, but may also help parse the effects of smoking in both mild and severe infections.

If we examine the latter option, CS exposure may exacerbate infection outcomes by exaggerated inflammatory responses to pulmonary insults (like infection). Airway epithelial cells harvested from smokers have lower levels of Type I and II IFN in response to IAV infection compared to healthy cells (88), while exposure to CS extract (water soluble contents of cigarette smoke) results in lower type I and type II IFN, IP-10, IL-6, and RIG-I transcription and expression (92, 93), suggesting CS has an inhibitory effect on innate immune responses to viral insult in humans. Oddly, these results suggest the opposite of the proposed exaggerated response mechanism. However, the length of years smoking and the packs smoked per day may have a significant impact on local and systemic inflammation responses. In mice, response to IAV infection with sub-chronic CS exposure (<2 weeks) appears to have a suppressive effect on a range of cytokines (TNF-α, lL-1B, IL-6, and IP-10) (65) and are reported to have increased BALF

and lymph node $CD4^+$ and $CD8^+$ T cells numbers. In contrast, chronic CS exposure (>2 weeks) results in exaggerated cytokine responses (TNF-α, IFN-y, IL-6, IL-12, IL-23, IL-1, IL-5, IL-10, KC, MIP-1a, IL-17, IL-1B) (67, 68, 71, 72, 85) with infection compared to non-smoking infected controls. In addition to elevated cytokine profiles, chronic exposure is also associated with increased local pulmonary inflammation including increased lung tissue and BALF neutrophils (65, 68, 69, 71, 72, 89), macrophages (65, 69, 71, 72, 91, 94), and lymphocytes (71, 91, 94) compared to non-CS exposed animals.

In summary, there is evidence that innate and adaptive responses to influenza infection are altered in CS patients, which was confirmed in CS animal models. However, reports are inconclusive as to whether CS exposure cause higher than normal viral burden or longer than average viral clearance. Irrespective of the virological response, there are increased pro-inflammatory cytokine profiles in chronic CS exposure models, with increased pulmonary cellular recruitment in acute and chronic CS exposure. This reflects an exaggerated response to infection in which IAV infection in chronic CS models, resulting in increased pro-inflammatory cytokine production, and subsequently exaggerated recruitment of inflammatory immune cells. These will ultimately cause more tissue damage and worse disease outcomes to infection compared to non-CS individuals. Conflicting data on virological responses most likely reflects lack of standardization for multiple experimental parameters withing CS models, meaning care should be taken when interpreting conclusions about virological responses. It should be noted however that there is next to no information or model data on how IBV epidemiology, replication, or pathology are affected by cigarette smoking. There is no data regarding how CS impacts IBV viral loads.

Influenza B Virus NP and its interaction with nuclear import machinery.

As noted above, the lack of information regarding IBV in general represents a critical gap in the field, which hinders the development of more efficient medical intervention for IBV infection. In this case, wholesale treatment of IBV infections as if they were IAV infections in smokers without model of observational data is likely to lead to undesirable patient outcomes. At minimum, in vitro and in vivo model data is required to set the foundation for effective develop and implementation of treatments. Antiviral drug treatments and development require such model data. These potential antiviral drug targets often begin by examining the interactions between viral proteins and host cell proteins (95, 96). These targets should ideally be well conserved at the amino acid level to prevent immune escape from viral mutations. The viral nucleoprotein (NP) is a well conserved viral factor (97) and its interactions with both viral and cellular factors are essential for viral replication. During replication, viral genomic RNAs (vRNAs) bind to a single heterotrimeric viral polymerase complex and multiple copies of the viral NP protein to form a viral ribonucleoprotein complex (vRNP), one NP per 24 nucleotides (98). These vRNPs will be packaged into new virions for subsequent virus RNA replication. Interactions between viral proteins like NP and host factors represent promising antiviral drug targets. For example, IAV NP (ANP) nuclear export is mediated by interaction with the CRM-1 nuclear export pathway (99-101). Subsequently, this interaction has been targeted as a potential antiviral target (102, 103). Numerous proteomic studies have examined the interactions of the IAV NP and vRNP with host cell factors (104-108), however, as above, the systematic studies on IBV host protein interactions, specifically for IBV NP (BNP) remain lacking.

BNP is a 560 amino acid long viral protein absolutely required for virus replication. Comparison of available BNP proteins from the past 20 Flu seasons (2000-2020) indicates BNP is well conserved, sharing 94% sequence identity (appendix Figure S3). However, its N-terminus region shares little sequence homology with IAV NP (ANP), with 38% total amino acid sequence identity with ANP, and remains relatively understudied in comparison. While a putative nuclear localization signal (NLS) has been reported in the flexible N-terminus region of BNP (109, 110) (amino acids 44-47), conflicting reports exists disputing if the N-terminus amino acids 1-70 are required for BNP nuclear import (111). Nuclear localization of proteins from the cytoplasm to the nucleus is facilitated by interaction of the cytoplasmic cargo proteins with importin α proteins (110). A NLS is required for the cargo to interact with Importin α protein's "Armadillo" domains (ARMs), which tether the cargo to Importin α proteins that mediate nuclear translocation through the nuclear pore complex (NPC). While IBV NP is translocated to the nucleus (111), it's not clear whether BNP is involved in nuclear import of B vRNAs and what host proteins are involved. We recently identified Importin α4 (IMPα4), a nuclear import subunit (112-114), as an interaction partner to BNP via a yeast two hybrid (Y2H) screen, suggesting BNP may play a role in vRNP nuclear import. It remained unclear however if said interaction occurred in human cells, and to what extent this interaction played in viral replication.

Specific AIMs

In the following chapters, we shall examine 3 distinct, but connected projects. Our objectives were: a) to investigate the interaction between BNP and IMPα4 and characterize its involvement in viral replication b) develop a method to attenuate

influenza viruses that would be safe and efficacious vaccines for pandemic situations c) establish a smoking mouse model to study the impact of IBV infection on smoker's health, virus replication and pulmonary damage.

Aim I: Confirm BNP & IMPα4 interactions and determine its role in viral replication. We mapped the interacting domains of BNP and IMPα4 by generating a panel of constructs. Each construct expressed a different truncated form of BNP or IMPα4, which we used for conducting co-IP analysis. In essence, HEK293T cells were transfected with pairs of BNP and IMPα4, wt and mutant-expressing plasmids, and based on the immunoprecipitation (IP) readout, we determined the essential domains required for interaction. We hypothesized the ARM domains of IMPα4 and the putative NLS of BNP mediate the interaction between these two proteins.

Finally, to examine the role of IMPα4 in virus replication, we will compare virus replication profiles with and without IMPα4 expression during IBV infection. A549 (lung epithelium cells) wild type or IMPα4 KO A549 cells will be infected with IBV and virus growth kinetics will be measured over time using plaque assays. We observed that without IMPα4 expression, overall virus replication will be impaired, indicating the importance of IMPα4 in the viral replication.

Aim II: Attenuate a chimeric live influenza virus vaccine by modifying HA membrane proximal region. We generated a recombinant B virus expressing the IAV HA. The C-terminal membrane proximal region of the IAV HA stalk was progressively replaced with the IBV stalk region to attenuate viral replication. We selected the most attenuated candidates by comparing their replication to WT IBV's replication (their genetic backbone) using a multistep growth curve analysis. These candidates were used to infect mice and monitor them for safety factors (weight loss, mortality rates, and

pulmonary viral replication) & correlates of protection (Anti-IAV HA IgG production and virus neutralization). Subsequently, vaccinated mice were challenged with vaccine matched IAV and monitored for weight loss, mortality, and pulmonary viral clearance. Candidate LAIV's safety, correlates of protection, and challenge results was directly compared to WT IBV and PBS mock controls. We observed that progressive introduction of IBV stalk sequence into the MPR of the IAV ectodomain: a) attenuated these viruses in-vitro b) did not cause disease and induce positive correlates of protection c) protect mice from IAV challenge.

Aim III. Develop a small animal model to study smoking's effects on IBV infection. We hypothesize CS exposed mice will have more respiratory inflammation and overall worse disease outcomes when infected with IBV compared to control mice. Mice were exposed to sub chronic CSE levels for 2 weeks and monitored for changes in overall weight gain and lung proinflammatory cytokines in comparison to non-CS exposed mice as a positive control for clinical signs of smoking. 3 & 6 days post sublethal IBV infection, bronchoalveolar lavage fluid (BALF) was used to determine mucosal IgA antibody response by ELISA, cytokine expression profiles (TNF-α, IL-6, IFN Type I & II). Lung tissue sections were examined for inflammation damage and cell death via lung histology. Virus clearance rates were monitored by extracting lungs at day 3 & 6 post infection and quantified pulmonary viral contents via standard plaque assay.

In summary, my research advanced our understanding of the function of essential IBV viral factor, NP protein, established a robust experimental platform to dissect the IBV infection under the influence of a smoking condition, and developed a proof-of-concept new IBV vector based LAIV with inherited safety. This knowledge will better prepare us for future influenza outbreaks likely around the corner.

Acknowledgements

The text of this dissertation's introduction, in part, is a reprint of the material as it appears in "Effects of Cigarette Smoking on Influenza Virus/Host Interplay" Chavez, J.; Hai, R. Pathogens 2021, 10, 1636. The co-author, Rong Hai, listed in that publication directed and supervised the research which forms the basis for this dissertation.

References

1 Control, C. f. D. CDC Disease Burden of Flu Factsheet. (2022).

2 Organization, W. H. WHO Influenza Seasonal Factsheet 2020. (2020).

3 Van Wormer, J. J., King, J. P., Gajewski, A., McLean, H. Q. & Belongia, E. A. Influenza and Workplace Productivity Loss in Working Adults. J Occup Environ Med 59, 1135-1139, doi:10.1097/Jom.0000000000001120 (2017).

4 Putri, W. C. W. S., Muscatello, D. J., Stockwell, M. S. & Newall, A. T. Economic burden of seasonal influenza in the United States. Vaccine 36, 3960-3966, doi:10.1016/j.vaccine.2018.05.057 (2018).

5 Yan, S. K., Weycker, D. & Sokolowski, S. US healthcare costs attributable to type A and type B influenza. Human Vaccines & Immunotherapeutics 13, 2041-2047, doi:10.1080/21645515.2017.1345400 (2017).

6 Control, C. f. D. CDC How Flu Spreads Factsheet.

7 Taubenberger, J. K. & Morens, D. M. The pathology of influenza virus infections. Annu Rev Pathol-Mech 3, 499-522, doi:10.1146/annurev.pathol.3.121806.154316 (2008).

8 Thompson, W. W. et al. Influenza-associated hospitalizations in the United States. Jama-J Am Med Assoc 292, 1333-1340, doi:DOI 10.1001/jama.292.11.1333 (2004).

9 Hauge, S. H., de Blasio, B. F., Haberg, S. E. & Oakley, L. Influenza hospitalizations during childhood in children born preterm. Influenza Other Respir Viruses 16, 247-254, doi:10.1111/irv.12908 (2022).

10 Ramsey, C. D. & Kumar, A. Influenza and endemic viral pneumonia. Crit Care Clin 29, 1069-1086, doi:10.1016/j.ccc.2013.06.003 (2013).

11 Short, K. R., Kroeze, E., Fouchier, R. A. M. & Kuiken, T. Pathogenesis of influenza-induced acute respiratory distress syndrome. Lancet Infect Dis 14, 57-69, doi:10.1016/S1473-3099(13)70286-X (2014).

12 Chavez, J. & Hai, R. Effects of Cigarette Smoking on Influenza Virus/Host Interplay. Pathogens 10, doi:10.3390/pathogens10121636 (2021).

13 Liu, G. Q. et al. Nuclear-resident RIG-I senses viral replication inducing antiviral immunity. Nature Communications 9, doi:10.1038/s41467-018-05745-w (2018).
14 Liu, G. Q., Park, H. S., Pyo, H. M., Liu, Q. & Zhou, Y. Influenza A Virus Panhandle Structure Is Directly Involved in RIG-I Activation and Interferon Induction. Journal of Virology 89, 6067-6079, doi:10.1128/Jvi.00232-15 (2015).

15 Liu, G. Q. & Zhou, Y. Cytoplasm and Beyond: Dynamic Innate Immune Sensing of Influenza A Virus by RIG-I. Journal of Virology 93, doi:ARTN e02299-1810.1128/JVI.02299-18 (2019).

16 Allen, I. C. et al. The NLRP3 Inflammasome Mediates In Vivo Innate Immunity to Influenza A Virus through Recognition of Viral RNA. Immunity 30, 556-565, doi:10.1016/j.immuni.2009.02.005 (2009).

17 Thomas, P. G. et al. The Intracellular Sensor NLRP3 Mediates Key Innate and Healing Responses to Influenza A Virus via the Regulation of Caspase-1. Immunity 30, 566-575, doi:10.1016/j.immuni.2009.02.006 (2009).

18 Teijaro, J. R. et al. Endothelial Cells Are Central Orchestrators of Cytokine Amplification during Influenza Virus Infection. Cell 146, 980-991, doi:10.1016/j.cell.2011.08.015 (2011).

19 Davies, A. et al. Extracorporeal Membrane Oxygenation for 2009 Influenza A(H1N1) Acute Respiratory Distress Syndrome. Jama-J Am Med Assoc 302, 1888-1895, doi:10.1001/jama.2009.1535 (2009).

20 To, K. K. W. et al. Delayed Clearance of Viral Load and Marked Cytokine Activation in Severe Cases of Pandemic H1N1 2009 Influenza Virus Infection. Clinical Infectious Diseases 50, 850-859, doi:10.1086/650581 (2010).

21 Cheung, C. Y. et al. Induction of proinflammatory cytokines in human macrophages by influenza A (H5N1) viruses: a mechanism for the unusual severity of human disease? Lancet 360, 1831-1837, doi:10.1016/s0140-6736(02)11772-7 (2002).

22 Gao, R. B. et al. Human Infection with a Novel Avian-Origin Influenza A (H7N9) Virus. New Engl J Med 368, 1888-1897, doi:10.1056/NEJMoa1304459 (2013).

23 Gao, H. N. et al. Clinical Findings in 111 Cases of Influenza A (H7N9) Virus Infection. New Engl J Med 368, 2277-2285, doi:10.1056/NEJMoa1305584 (2013).

24 Le Goffic, R. et al. Infection with influenza virus induces IL-33 in murine lungs. Am J Respir Cell Mol Biol 45, 1125-1132, doi:10.1165/rcmb.2010-0516OC (2011).

25 Cayrol, C. & Girard, J. P. IL-33: an alarmin cytokine with crucial roles in innate immunity, inflammation and allergy. Curr Opin Immunol 31, 31-37, doi:10.1016/j.coi.2014.09.004 (2014).

26 Luo, J. R. et al. Serological evidence for high prevalence of Influenza D Viruses in Cattle, Nebraska, United States, 2003-2004. Virology 501, 88-91, doi:10.1016/j.virol.2016.11.004 (2017).

27 Kilbourne, E. D. Influenza pandemics of the 20th century. Emerging Infectious Diseases 12, 9-14, doi:10.3201/eid1201.051254 (2006).

28 Fouchier, R. A. M., Bestebroer, T. M., Martina, B. E. E., Rimmelzwaan, G. F. & Osterhaus, A. in 4th World Congress on Options for the Control of Influenza. 225-231 (2001).

29 Nobusawa, E. & Sato, K. Comparison of the mutation rates of human influenza A and B viruses. Journal of Virology 80, 3675-3678, doi:10.1128/Jvi.80.7.3675-3678.2006 (2006).

30 Fulton, B. O., Sun, W. N., Heaton, N. S. & Palese, P. The Influenza B Virus Hemagglutinin Head Domain Is Less Tolerant to Transposon Mutagenesis than That of the Influenza A Virus. Journal of Virology 92, doi:10.1128/jvi.00754-18 (2018).

31 Rota, P. A. et al. Cocirculation of 2 Distinct Evolutionary Lineages of Influenza Type-B Virus since 1983. Virology 175, 59-68, doi:Doi 10.1016/0042-6822(90)90186-U (1990).

32 Laurie, K. L. et al. Evidence for Viral Interference and Cross-reactive Protective Immunity Between Influenza B Virus Lineages. Journal of Infectious Diseases 217, 548-559, doi:10.1093/infdis/jix509 (2018).

33 Jackson, D., Elderfield, R. A. & Barclay, W. S. Molecular studies of influenza B virus in the reverse genetics era. Journal of General Virology 92, 1-17, doi:10.1099/vir.0.026187-0 (2011).

34 Sharabi, S. et al. Epidemiological and Virological Characterization of Influenza B Virus Infections. Plos One 11, doi:10.1371/journal.pone.0161195 (2016).

35 Dwyer, D. E. et al. Comparison of the Outcomes of Individuals With Medically Attended Influenza A and B Virus Infections Enrolled in 2 International Cohort Studies Over a 6-Year Period: 2009-2015. Open Forum Infectious Diseases 4, doi:10.1093/ofid/ofx212 (2017).

36 Daley, A. J., Nallusamy, R. & Isaacs, D. Comparison of influenza A and influenza B virus infection in hospitalized children. Journal of Paediatrics and Child Health 36, 332-335, doi:10.1046/j.1440-1754.2000.00533.x (2000).

37 Jung, S. W., Kim, Y. J., Han, S. B., Lee, K. Y. & Kang, J. H. Differences in the age distribution of influenza B virus infection according to influenza B virus lineages in the Korean population. Postgraduate Medicine 133, 82-88, doi:10.1080/00325481.2020.1825295 (2021).

38 Su, S. et al. Comparing Clinical Characteristics Between Hospitalized Adults With Laboratory-Confirmed Influenza A and B Virus Infection. Clinical Infectious Diseases 59, 252-255, doi:10.1093/cid/ciu269 (2014).

39 Farrukee, R., Mosse, J. & Hurt, A. C. Review of the clinical effectiveness of the neuraminidase inhibitors against influenza B viruses. Expert Review of Anti-Infective Therapy 11, 1135-1145, doi:10.1586/14787210.2013.842466 (2013).

40 Makela, S. M. et al. RIG-I Signaling Is Essential for Influenza B Virus-Induced Rapid Interferon Gene Expression. Journal of Virology 89, 12014-12025, doi:10.1128/jvi.01576-15 (2015).

41 Brottet, E. et al. Influenza season in Reunion dominated by influenza B virus circulation associated with numerous cases of severe disease, France, 2014. Eurosurveillance 19, 2-5, doi:10.2807/1560-7917.es2014.19.39.20916 (2014).

42 Appiah, G. D. et al. Influenza Activity - United States, 2014-15 Season and Composition of the 2015-16 Influenza Vaccine. Mmwr-Morbidity and Mortality Weekly Report 64, 583-590 (2015).

43 Blanton, L. et al. Update: Influenza Activity in the United States During the 2016-17 Season and Composition of the 2017-18 Influenza Vaccine. Mmwr-Morbidity and Mortality Weekly Report 66, 668-676, doi:10.15585/mmwr.mm6625a3 (2017).

44 Epperson, S. et al. Influenza Activity - United States, 2013-14 Season and Composition of the 2014-15 Influenza Vaccines. Mmwr-Morbidity and Mortality Weekly Report 63, 483-490 (2014).

45 Kissling, E. et al. I-MOVE multicentre case-control study 2010/11 to 2014/15: Is there within-season waning of influenza type/subtype vaccine effectiveness with increasing time since vaccination? Eurosurveillance 21, 13-24, doi:10.2807/1560-7917.es.2016.21.16.30201 (2016).

46 Trombetta, C. M., Kistner, O., Montomoli, E., Viviani, S. & Marchi, S. Influenza Viruses and Vaccines: The Role of Vaccine Effectiveness Studies for Evaluation of the Benefits of Influenza Vaccines. Vaccines (Basel) 10, doi:10.3390/vaccines10050714 (2022).

47 Osterholm, M. T., Kelley, N. S., Sommer, A. & Belongia, E. A. Efficacy and effectiveness of influenza vaccines: a systematic review and meta-analysis. Lancet Infect Dis 12, 36-44, doi:10.1016/S1473-3099(11)70295-X (2012).

48 Sridhar, S., Brokstad, K. A. & Cox, R. J. Influenza Vaccination Strategies: Comparing Inactivated and Live Attenuated Influenza Vaccines. Vaccines (Basel) 3, 373-389, doi:10.3390/vaccines3020373 (2015).

49 Altman, M. O., Angeletti, D. & Yewdell, J. W. Antibody Immunodominance: The Key to Understanding Influenza Virus Antigenic Drift. Viral Immunology 31, 142-149, doi:10.1089/vim.2017.0129 (2018).

50 Martinez-Sobrido, L., Peersen, O. & Nogales, A. Temperature Sensitive Mutations in Influenza A Viral Ribonucleoprotein Complex Responsible for the Attenuation of the Live Attenuated Influenza Vaccine. Viruses 10, doi:10.3390/v10100560 (2018).

51 Rhorer, J. et al. Efficacy of live attenuated influenza vaccine in children: A meta-analysis of nine randomized clinical trials. Vaccine 27, 1101-1110, doi:10.1016/j.vaccine.2008.11.093 (2009).

52 Ambrose, C. S., Wu, X. H., Knuf, M. & Wutzler, P. The efficacy of intranasal live attenuated influenza vaccine in children 2 through 17 years of age: A meta-analysis of 8 randomized controlled studies. Vaccine 30, 886-892, doi:10.1016/j.vaccine.2011.11.104 (2012).

53 Belshe, R. B., Ambrose, C. S., Wu, X. & Pilsudski, R. Relative Efficacy of Live Attenuated and Inactivated Influenza Vaccines in Children as a Function of Time Postvaccination. Pediatr Res 68, 274-275, doi:Doi 10.1203/00006450-201011001-00537 (2010).

54 Thompson, W. W. et al. Mortality associated with influenza and respiratory syncytial virus in the United States. Jama-J Am Med Assoc 289, 179-186, doi:DOI 10.1001/jama.289.2.179 (2003).

55 Hai, R., Garcia-Sastre, A., Swayne, D. E. & Palese, P. A Reassortment-Incompetent Live Attenuated Influenza Virus Vaccine for Protection against Pandemic Virus Strains. Journal of Virology 85, 6832-6843, doi:10.1128/Jvi.00609-11 (2011).

56 CDC. CDC Smoking & Tobacco Use Factsheet. (2020).

57 Lawrence, H., Hunter, A., Murray, R., Lim, W. S. & McKeever, T. Cigarette smoking and the occurrence of influenza - Systematic review. J Infection 79, 401-406, doi:10.1016/j.jinf.2019.08.014 (2019).

58 Arcavi, L. & Benowitz, N. L. Cigarette smoking and infection. Arch Intern Med 164, 2206-2216, doi:DOI 10.1001/archinte.164.20.2206 (2004).

59 Kark, J. D., Lebiush, M. & Rannon, L. Cigarette-Smoking as a Risk Factor for Epidemic a(H1n1) Influenza in Young Men. New Engl J Med 307, 1042-1046, doi:Doi 10.1056/Nejm198210213071702 (1982).

60 Hanshaoworakul, W. et al. Severe Human Influenza Infections in Thailand: Oseltamivir Treatment and Risk Factors for Fatal Outcome. Plos One 4, doi:ARTN e6051
10.1371/journal.pone.0006051 (2009).

61 Kuschner, W. G., DAlessandro, A., Wong, H. & Blanc, P. D. Dose-dependent cigarette smoking-related inflammatory responses in healthy adults. Eur Respir J 9, 1989-1994, doi:Doi 10.1183/09031936.96.09101989 (1996).

62 Hunninghake, G. W. & Crystal, R. G. Cigarette-Smoking and Lung Destruction - Accumulation of Neutrophils in the Lungs of Cigarette Smokers. Am Rev Respir Dis 128, 833-838 (1983).

63 van Eeden, S. F. & Hogg, J. C. The response of human bone marrow to chronic cigarette smoking. Eur Respir J 15, 915-921, doi:DOI 10.1034/j.1399-3003.2000.15e18.x (2000).

64 Ferrero, M. R. et al. CCR5 Antagonist Maraviroc Inhibits Acute Exacerbation of Lung Inflammation Triggered by Influenza Virus in Cigarette Smoke-Exposed Mice. Pharmaceuticals (Basel) 14, doi:10.3390/ph14070620 (2021).

65 Gualano, R. C. et al. Cigarette smoke worsens lung inflammation and impairs resolution of influenza infection in mice. Resp Res 9, doi:Artn 53 10.1186/1465-9921-9-53 (2008).

66 Feng, Y. et al. Exposure to Cigarette Smoke Inhibits the Pulmonary T-Cell Response to Influenza Virus and Mycobacterium tuberculosis. Infect Immun 79, 229-237, doi:10.1128/Iai.00709-10 (2011).

67 Han, Y. et al. Influenza Virus-Induced Lung Inflammation Was Modulated by Cigarette Smoke Exposure in Mice. Plos One 9, doi:ARTN e86166 10.1371/journal.pone.0086166 (2014).

68 Hong, M. J. et al. Protective role of gamma delta T cells in cigarette smoke and influenza infection. Mucosal Immunol 11, 894-908, doi:10.1038/mi.2017.93 (2018).

69 Lee, S. W. et al. Impact of Cigarette Smoke Exposure on the Lung Fibroblastic Response after Influenza Pneumonia. Am J Resp Cell Mol 59, 770-781, doi:10.1165/rcmb.2018-0004OC (2018).

70 Eddleston, J., Lee, R. U., Doerner, A. M., Herschbach, J. & Zuraw, B. L. Cigarette Smoke Decreases Innate Responses of Epithelial Cells to Rhinovirus Infection. Am J Resp Cell Mol 44, 118-126, doi:10.1165/rcmb.2009-0266OC (2011).

71 Kang, M. J. et al. Cigarette smoke selectively enhances viral PAMP- and virus-induced pulmonary innate immune and remodeling responses in mice. J Clin Invest 118, 2771-2784, doi:10.1172/Jci32709 (2008).

72 Robbins, C. S. et al. Cigarette smoke impacts immune inflammatory responses to influenza in mice. Am J Resp Crit Care 174, 1342-1351, doi:10.1164/rccm.200604-561OC (2006).

73 Finklea, J. F., Sandifer, S. H. & Smith, D. D. Cigarette Smoking and Epidemic Influenza. Am J Epidemiol 90, 390-&, doi:DOI 10.1093/oxfordjournals.aje.a121084 (1969).

74 Aronson, M. D., Weiss, S. T., Ben, R. L. & Komaroff, A. L. Association between cigarette smoking and acute respiratory tract illness in young adults. JAMA 248, 181-183 (1982).

75 Godoy, P. et al. Smoking may increase the risk of influenza hospitalization and reduce influenza vaccine effectiveness in the elderly. Eur J Public Health 28, 150-155, doi:10.1093/eurpub/ckx130 (2018).

76 Nicholson, K. G., Kent, J. & Hammersley, V. Influenza A among community-dwelling elderly persons in Leicestershire during winter 1993-4; cigarette smoking as a risk factor and the efficacy of influenza vaccination. Epidemiol Infect 123, 103-108, doi:Doi 10.1017/S095026889900271x (1999).

77 Thomson, N. C., Chaudhuri, R. & Livingston, E. Asthma and cigarette smoking. Eur Respir J 24, 822-833, doi:10.1183/09031936.04.00039004 (2004).

78 Rosenberg, H. F., Dyer, K. D. & Foster, P. S. Eosinophils: changing perspectives in health and disease. Nature Reviews Immunology 13, 9-22, doi:10.1038/nri3341 (2013).

79 Minty, A. et al. INTERLEUKIN-13 IS A NEW HUMAN LYMPHOKINE REGULATING INFLAMMATORY AND IMMUNE-RESPONSES. Nature 362, 248-250, doi:10.1038/362248a0 (1993).

80 McKenzie, A. N. J. et al. INTERLEUKIN-13, A T-CELL-DERIVED CYTOKINE THAT REGULATES HUMAN MONOCYTE AND B-CELL FUNCTION. Proceedings of the National Academy of Sciences of the United States of America 90, 3735-3739, doi:10.1073/pnas.90.8.3735 (1993).

81 Punnonen, J. et al. INTERLEUKIN-13 INDUCES INTERLEUKIN-4-INDEPENDENT IGG4 AND IGE SYNTHESIS AND CD23 EXPRESSION BY HUMAN B-CELLS. Proceedings of the National Academy of Sciences of the United States of America 90, 3730-3734, doi:10.1073/pnas.90.8.3730 (1993).

82 Zheng, T. et al. Inducible targeting of IL-13 to the adult lung causes matrix metalloproteinase-and cathepsin-dependent emphysema. J Clin Invest 106, 1081-1093, doi:10.1172/jci10458 (2000).

83 Gern, J. E., Lemanske, R. F., Jr. & Busse, W. W. Early life origins of asthma. J Clin Invest 104, 837-843, doi:10.1172/JCI8272 (1999).

84 Moran, T. M., Isobe, H., Fernandez-Sesma, A. & Schulman, J. L. Interleukin-4 causes delayed virus clearance in influenza virus-infected mice. J Virol 70, 5230-5235, doi:10.1128/JVI.70.8.5230-5235.1996 (1996).

85 Wang, J. M., Li, Q. H., Xie, J. G. & Xu, Y. J. Cigarette smoke inhibits BAFF expression and mucosal immunoglobulin A responses in the lung during influenza virus infection. Resp Res 16, doi:ARTN 37 10.1186/s12931-015-0201-y (2015).

86 Duffney, P. F. et al. Cigarette smoke increases susceptibility to infection in lung epithelial cells by upregulating caveolin-dependent endocytosis. Plos One 15, e0232102, doi:10.1371/journal.pone.0232102 (2020).

87 Danov, O. et al. Cigarette Smoke Affects Dendritic Cell Populations, Epithelial Barrier Function, and the Immune Response to Viral Infection With H1N1. Front Med (Lausanne) 7, 571003, doi:10.3389/fmed.2020.571003 (2020).

88 Jaspers, I. et al. Reduced Expression of IRF7 in Nasal Epithelial Cells from Smokers after Infection with Influenza. Am J Resp Cell Mol 43, 368-375, doi:10.1165/rcmb.2009-0254OC (2010).

89 Bauer, C. M. T. et al. Treating Viral Exacerbations of Chronic Obstructive Pulmonary Disease: Insights from a Mouse Model of Cigarette Smoke and H1N1 Influenza Infection. Plos One 5, doi:ARTN e13251 10.1371/journal.pone.0013251 (2010).

90 Boehme, S. A. et al. MAP3K19 Is Overexpressed in COPD and Is a Central Mediator of Cigarette Smoke-Induced Pulmonary Inflammation and Lower Airway Destruction. Plos One 11, e0167169, doi:10.1371/journal.pone.0167169 (2016).

91 Mebratu, Y. A., Smith, K. R., Agga, G. E. & Tesfaigzi, Y. Inflammation and emphysema in cigarette smoke-exposed mice when instilled with poly (I:C) or infected with influenza A or respiratory syncytial viruses. Resp Res 17, doi:ARTN 75 10.1186/s12931-016-0392-x (2016).

92 Wu, W. X. et al. Cigarette smoke attenuates the RIG-I-initiated innate antiviral response to influenza infection in two murine models. Am J Physiol-Lung C 307, L848-L858, doi:10.1152/ajplung.00158.2014 (2014).

93 Duffney, P. F. et al. Cigarette smoke dampens antiviral signaling in small airway epithelial cells by disrupting TLR3 cleavage. Am J Physiol-Lung C 314, L505-L513, doi:10.1152/ajplung.00406.2017 (2018).

94 Hsu, A. C. Y. et al. Targeting PI3K-p110 alpha Suppresses Influenza Virus Infection in Chronic Obstructive Pulmonary Disease. Am J Resp Crit Care 191, 1012-1023, doi:10.1164/rccm.201501-0188OC (2015).

95 Chen, N., Zhang, B. G., Deng, L. L., Liang, B. & Ping, J. H. Virus-host interaction networks as new antiviral drug targets for IAV and SARS-CoV-2. Emerg Microbes Infec 11, 1371-1389, doi:10.1080/22221751.2022.2071175 (2022).

96 de Chassey, B., Meyniel-Schicklin, L., Vonderscher, J., Andre, P. & Lotteau, V. Virus-host interactomics: new insights and opportunities for antiviral drug discovery. Genome Med 6, doi:ARTN 115 10.1186/s13073-014-0115-1 (2014).

97 Shu, L. L., Bean, W. J. & Webster, R. G. Analysis of the evolution and variation of the human influenza A virus nucleoprotein gene from 1933 to 1990. J Virol 67, 2723-2729 (1993).

98 Ortega, J. et al. Ultrastructural and functional analyses of recombinant influenza virus ribonucleoproteins suggest dimerization of nucleoprotein during virus amplification. J Virol 74, 156-163 (2000).

99 Elton, D. et al. Interaction of the influenza virus nucleoprotein with the cellular CRM1-mediated nuclear export pathway. J Virol 75, 408-419, doi:10.1128/JVI.75.1.408-419.2001 (2001).

100 Ma, K., Roy, A. M. M. & Whittaker, G. R. Nuclear export of influenza virus ribonucleoproteins: Identification of an export intermediate at the nuclear periphery. Virology 282, 215-220, doi:DOI 10.1006/viro.2001.0833 (2001).

101 Watanabe, K. et al. Inhibition of nuclear export of ribonucleoprotein complexes of influenza virus by leptomycin B. Virus Res 77, 31-42 (2001).

102 Kakisaka, M., Mano, T. & Aida, Y. A high-throughput screening system targeting the nuclear export pathway via the third nuclear export signal of influenza A virus nucleoprotein. Virus Res 217, 23-31, doi:10.1016/j.virusres.2016.02.007 (2016).

103 Kakisaka, M. et al. A Novel Antiviral Target Structure Involved in the RNA Binding, Dimerization, and Nuclear Export Functions of the Influenza A Virus Nucleoprotein. Plos Pathog 11, doi:ARTN e1005062 10.1371/journal.ppat.1005062 (2015).

104 Tripathi, S. et al. Meta- and Orthogonal Integration of Influenza "OMICs" Data Defines a Role for UBR4 in Virus Budding. Cell Host Microbe 18, 723-735, doi:10.1016/j.chom.2015.11.002 (2015).

105 Sun, N. N. et al. Proteomics Analysis of Cellular Proteins Co-Immunoprecipitated with Nucleoprotein of Influenza A Virus (H7N9). Int J Mol Sci 16, 25982-25998, doi:10.3390/ijms161125934 (2015).

106 Mayer, D. et al. Identification of cellular interaction partners of the influenza virus ribonucleoprotein complex and polymerase complex using proteomic-based approaches. J Proteome Res 6, 672-682, doi:10.1021/pr060432u (2007).

107 Generous, A. et al. Identification of putative interactions between swine and human influenza A virus nucleoprotein and human host proteins. Virol J 11, 228, doi:10.1186/s12985-014-0228-6 (2014).

108 Watanabe, T. et al. Influenza virus-host interactome screen as a platform for antiviral drug development. Cell Host Microbe 16, 795-805, doi:10.1016/j.chom.2014.11.002 (2014).

109 Wanitchang, A., Narkpuk, J. & Jongkaewwattana, A. Nuclear import of influenza B virus nucleoprotein: Involvement of an N-terminal nuclear localization signal and a cleavage-protection motif. Virology 443, 59-68, doi:10.1016/j.virol.2013.04.025 (2013).

110 Sherry, L., Smith, M., Davidson, S. & Jackson, D. The N Terminus of the Influenza B Virus Nucleoprotein Is Essential for Virus Viability, Nuclear Localization, and Optimal Transcription and Replication of the Viral Genome. Journal of Virology 88, 12326-12338, doi:10.1128/Jvi.01542-14 (2014).

111 Stevens, M. P. & Barclay, W. S. The N-terminal extension of the influenza B virus nucleoprotein is not required for nuclear accumulation or the expression and replication of a model RNA. Journal of Virology 72, 5307-5312 (1998).

112 Oka, M. & Yoneda, Y. Importin alpha: functions as a nuclear transport factor and beyond. P Jpn Acad B-Phys 94, 259-274, doi:10.2183/pjab.94.018 (2018).

113 Takeda, S. et al. Isolation and mapping of karyopherin alpha 3 (KPNA3), a human gene that is highly homologous to genes encoding Xenopus importin, yeast SRP1 and human RCH1. Cytogenet Cell Genet 76, 87-93, doi:Doi 10.1159/000134521 (1997).

114 Fagerlund, R., Kinnunen, L., Kohler, M., Julkunen, I. & Melen, K. NF-kappa B is transported into the nucleus by importin alpha 3 and importin alpha 4. Journal of Biological Chemistry 280, 15942-15951, doi:10.1074/jbc.M500814200 (2005)

Figures

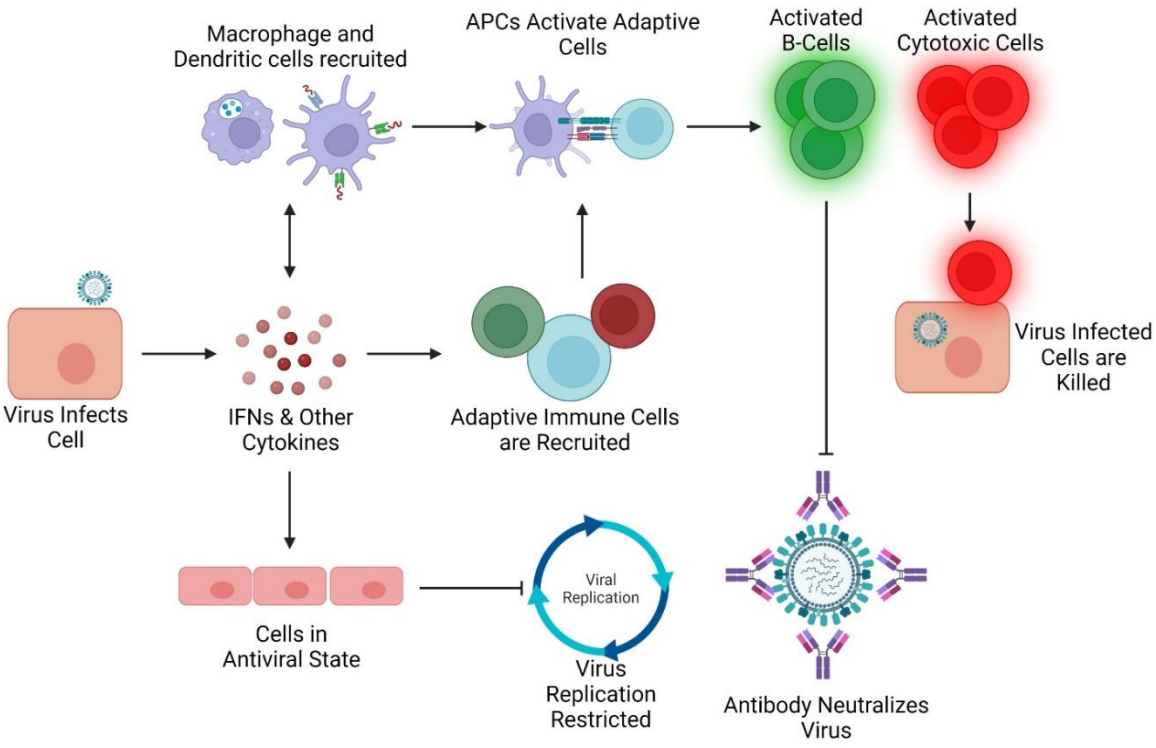

Figure 1.1 Schematic of Basic Host Defenses Against IAV Infection.
Upon infection, infection is detected by intracellular receptors like RIG-I, resulting in IFN and other cytokine production. Secreted pro-inflammatory cytokines like IFNs stimulate ISG transcription resulting in an antiviral state in surrounding cells restricting virus replication. Pro-inflammatory cytokines and chemokines also recruit and activate innate and adaptive cells to the infection. Innate cells slow infection by engulfing and destroying virus particles, and present viral antigens to adaptive immune cells like helper T-cells to trigger activation and proliferation. These T-cells activate both B-cells that produce antiviral antibodies that neutralize virus and Cytotoxic T-cells that kill target and kill virally infected cells, resulting in ultimate clearance of infection. The figure was generated in Biorender and is from my own publication “Effects of Cigarette Smoking on Influenza Virus/Host Interplay” Chavez & Hai 2021. Pathogens 2021, 10, 1636.

Flu Season	A/B Case Ratio	% IAV cases	% IBV Cases
2000-2001	5337/4625	54	46.0
2001-2002	13706/1965	87.5	12.5
2002-2003	6180/4768	56.4	43.6
2003-2004	24400/249	99	1.0
2004-2005	17750/5799	75.4	24.6
2005-2006	14355/3642	79.7	20.3
2006-2007	18817/4936	79.2	20.8
2007-2008	28263/11564	71	29.0
2008-2009	18175/9507	66	34.0
2009-2010	155591/2273	99	1.0
2010-2011	40282/13994	74	26.0
2011-2012	19285/3132	86	14.0
2012-2013	51675/21455	71	29.0
2013-2014	46727/6743	87.4	12.6
2014-2015	104,822/20,640	83.5	16.5
2015-2016	62982/28477	68.9	31.1
2016-2017	116590/45361	72	28.0
2017-2018	189716/88187	68.3	31.7
2018-2019	208153/11189	94.9	5.1
2019-2020	27617/19357	58.8	41.2

Table 1.1 Yearly IAV to IBV Infection cases in the United States as reported in the CDC

Chapter 1: Interrogating the Interaction Between IMPα4 and Influenza B Virus Nucleoprotein and its Role in Virus Replication

Jerald Chavez, Duo Xu, Young kin Sang, Phang-Lang Chen, Rong Hai

Abstract

IMPα proteins are a family of 7 conserved proteins that act as adapters for cytoplasmic cargo to bind with IMPβ, which facilitates nuclear Import. Influenza A virus utilizes this IMPα/β system to facilitate NP and vRNA nuclear import. We recently found through yeast-two-hybrid analysis that IMPα4 interacted with Influenza B virus NP (BNP). Co-localization of both proteins in human cells indicates both proteins localize in the nucleus. We used Co-IP and mutational analysis of BNP and IMPα4 to further explore the nature of this interaction. We found BNP and IMPα4 do interact in 293T cells by Co-IP, and that Armadillo repeats 6-10 of IMPα4 were sufficient for this interaction, but amino acids 44-47 of BNP are necessary for interaction. Finally, knockout of IMPα4 protein expression did statistically lower IBV viral replication ex vivo, but not by more than two-fold. Together, this suggests that while BNP interacts with IMPα4, the interaction is not necessary for viral replication, and likely suggests that other proteins factors could also facilitate nuclear entry for IBV proteins and the vRNAs.

Introduction

For influenza viruses, replication, and transcription of the viral RNAs (vRNAs) occurs in the nucleus of infected cells (1-3). Previous reports have shown that independent of viral entry, the viral ribonucleoprotein (vRNP) is imported into the nucleus upon injection into the cytoplasm (4). The vRNP is composed of a heterotrimeric viral polymerase, 1 of 8 vRNA genomic segments, and multiple copies of the viral nucleoprotein (NP). The NP protein is necessary to mediate the import of the vRNA into the nucleus (5). Amino acids 1-20 of NP are sufficient to mediate NP nuclear import (6).

Cellular nuclear import is the process of cytoplasmic proteins passing through the nuclear membrane, either by passive diffusion or via a facilitated active process. The nuclear membrane maintains separation of cellular contents between the nucleus and the cytoplasm, allowing for specialized function of each area. Processes such as transcription, DNA repair, and splicing that occur only in the nucleus rely on effector proteins translocating from their sites of translation to the interior of the nucleus. The nuclear membrane contains multiple nuclear pore complexes (NPCs) that act as gateways for nuclear entry of proteins and other molecules (7). The NPCs are comprised of approximately 30 different types of nucleoporins (Nups) (8). These subunits Nups form a channel structure, with specific Nups carrying out distinct functions. Phe-Gly nucleoporins (FG Nups) form the inner channel of the NPC and are attached to a protein scaffold comprised of conserved Nups that make up the outwards surface of the channel (9, 10). This channel allows for passive transport of molecules/proteins up to 40-60 kDa across the nuclear membrane, though more recent analysis suggests this passive barrier size limit is flexible (11, 12). Active transport through the NPC requires interaction

with a nuclear import pathway, dubbed the importin pathway, based on our current understanding (13-15). This system is comprised of two proteins, Importin α and Importin β. In this system, cytoplasmic protein cargo encoding a nuclear localization signal (NLS) (16) interact first with Importin α (IMPα). IMPα proteins act as adapters, linking the cargo protein to an Importin β protein (IMPβ), forming a heterotrimeric complex in the cytoplasm. Subsequently, IMPβ facilitates nuclear entry by interaction with the FG-Nups in the NPC (17), including Nup 62, 153, 214 (18-20). In the nucleus, Ran-GTP interacts with IMPα releasing the cargo and allowing for IMPα and IMPβ proteins to be recycled back to the cytoplasm for continued use. In humans, IMPα and IMPβ are part of families, with 7 IMPα and 20 IMPβ proteins, respectively (21). This diversity in α□and β□ proteins grants the cell granular import regulation of cargo. Besides this common pathway, certain nuclear proteins, such as CaMKIV, achieve their nuclear translocation with only IMPα or β (22, 23).

Influenza viruses have evolved to utilize the IMPα/β pathway to facilitate nuclear import of viral proteins during replication. There are 4 types of Influenza viruses: Influenza A virus (IAV), Influenza B virus (IBV), Influenza C virus (ICV), and Influenza D virus (IDV). These are negative sense, RNA, enveloped viruses and part of the orthomyxovirus family. Seasonal epidemics of IAV and IBV cause 290,000 to 650,000 deaths globally each year (24). Upon infection, the viral ribonucleoprotein complexes (vRNPs) are released into the cytoplasm. The vRNPs are comprised of three components, including the viral heterotrimeric polymerase (PB1/PB2/PA) and multiple copies of the viral nucleoprotein (NP) encapsulated with a segment of the viral RNA genome (vRNA). The expression of the IBV NEP protein requires alternative splicing of the viral NS RNA segment. This protein mediates the nuclear export of vRNPs once

assembled to the cytoplasm for translation and packaging. Thus, nuclear import of the vRNPs is necessary for the alternative splicing of the NS segment. IBV NP (BNP) has been co-crystalized with IMPα7 (25). Previous reports indicate that BNP does localize to the nucleus, and has a putative nuclear localization signal (26, 27). Similarly, IAV NP (ANP) has been shown to interact with multiple members of the IMPα family, Including IMPα1, α3, α5, and nuclear import of ANP and the vRNA have been shown in vitro to be dependent on the IMP α/β system (5). Thus, it is likely that BNP will interact with other IMPα's besides IMPα7.

We recently conducted a Y2H library screen against BNP to determine potential host protein interactions, and we found that mouse and human IMPα4 interacted with BNP. Here, we further confirmed this interaction by Co-IP analysis, and explored the amino acids involved in the interaction, and how IMPα4 impacts IBV infection. Our Co-IP results indicated that the Armadillo repeats (ARMs) 6-10 of IMPα4 and BNP amino acids 44-47 are required for this interaction. IBV replicated less efficiently in cells lacking IMPα4. These results indicated IMPα4 is one of the IMPα factors involved in IBV infection through its interaction with the BNP protein. Together, our findings warrant new studies to further understand the likelihood of other IMPα's involved in IBV nuclear entry to enable us to develop antivirals targeting this nuclear entry pathway.

Results

Host Interaction partners for BNP protein. To generate a potential list of host proteins and pathways BNP may interact with, we conducted a Yeast-two-hybrid (Y2H) cDNA library screen using BNP as the “bait” for potential interactions. We utilized a human B cells library, which is shown to have the maximal coverage of human genomic coding sequences. This library was constructed by digesting the cDNA and adding universal adapters to the cDNA for cloning into the library vector. We initially found upon sequencing a list of 134 potential interacting partners for BNP. Clones were removed from this list based on 4 criteria: a) if the gene was an obvious false positive such as rRNA which does not make a known protein; b) if the cDNA region was from outside the genes known protein coding sequence (ex: UTR); c) if the genes natural coding sequence was not in frame with the GAL4 binding domain of the library vector backbone; and d) if the gene’s cDNA was cloned in the “antisense” direction. After removing clones based on these criteria, we were left with 13 remaining possible BNP interacting proteins (Table 2.1). To confirm these interactions, we also performed the same Y2H analysis using a mouse library against BNP for comparison (Table 2.2). KPNA3 was the only interaction partner revealed in both the human and mouse library screens.

In humans, KPNA3 codes for the IMPα4 protein, a nuclear import adapter protein. To confirm that BNP interacts with KPNA3, we conducted a co-immunoprecipitation in HEK293T cells. We fused a 3x flag-tag to the N-terminus of BNP in a human expression vector, p3xFLAG_CMV10. IMPα4 is part of the 7 member gene family. These proteins all share similar secondary and tertiary structures, comprised of 10 repeating alpha helixes termed armadillo repeats (ARMs). The cDNA sequence for

IMPα4 isolated from our Y2H clone contained ARM 6-10 of the full-length IMPα4. This sequence was cloned into pCAGGS vector with a N myc tag, annotated as IMPα4_Y2H. We additionally cloned ARM 1-10 (all ARMS) into the same Myc tagged vector to create IMPα4_FL (Figure 2.1A). We noted that both the IMPα4_Y2H and IMPα4_FL were both co-precipitated with BNP-Flag, but not in its absence (Figure 2.1B). Additionally, we conducted GST pulldown experiments to determine if BNP_Flag and IMPα4_FL_Myc interactions were specific. In samples transfected either with GST_Flag or GST_Myc constructs, GST specific beads did not pull down Impα4_FL_Myc or BNP_Flag, respectively (Figure 2.1C). Together, this suggests that BNP does specifically interact with IMPα4 in cell lysates

Determining molecular mechanism of the BNP-IMPα4 interaction. To define the amino acids involved in the interaction between BNP and IMPα4, we deleted or mutated specific regions of each protein. IMPα proteins generally interact with nuclear localization signals, or “NLS” sequences in cargo proteins to facilitate nuclear import. Since it is still disputable about the location of the NLS in BNP proteins, we utilized NLS Mapper, SeqNLS, and NLStradamus (28-30) to identify broad areas of the BNP coding sequence that could serve as NLS’s (Figure 2.3A Top). In conjunction with previous reported putative NLSs, such as BNP amino acids 44-47 (26), we generated a panel of constructs to delete these putative NLS regions. Their involvement in BNP/IMPα4 interactions were examined by Co-IP analysis. We found that relative to WT BNP, most regions deleted did not impact the relative ratio of IMPα4 to BNP in our Co-IPs, which suggest that they are not required for IMPα4/BNP interaction (Figure 2.3B). Interestingly however, mutation of amino acids 44-47 to alanine or deletion of this same region resulted in

almost full loss of immunoprecipitation to IMPα4. This suggests that the BNP amino acids 44-47 are necessary for interaction with IMPα4.

IMPα proteins interact with cargo proteins NLS via ARMs. Yeast clone VB224 contained the coding sequences for IMPα4 ARMs 6-10. This suggests that these ARM segments are sufficient for interaction with BNP. To further narrow down the specific ARM segment among 6-10 required for the interaction, we generated a group of mutants, in which we deleted ARMs 6-10 one by one incrementally. All of these mutants can be expressed relatively equally to WT IMPα4 (Figure 2.3C). Their roles in interaction with BNP was examined via Co-IP. Interestingly, we found that WT BNP was unable to co-immunoprecipitated any of the IMPα4 ARM mutants (Figure 2.3C). This suggests that all ARMs 6-10 are required for the IMPα4/BNP interaction, which is likely due to the loss of any of the ARM regions destabilizing the overall tertiary structure of IMPα4.

The impact of IMPα4 in IBV infection. To further dissect the potential role of IMPα4 in IBV infection, we first tested its impact on IBV replication. We generated IMPα4 knock out A549 cells through CRISPR-Cas9. To minimize the impact of potential off-target effects associated with the CRISPR-Cas9 system, we selected two independent IMPα4 deficient cell lines, dubbed clone #6 and clone #12. These two cell lines contain different mutations that result in a pre-mature stop codon in exon 3 and exon 2, respectively (Figure 2.4A). The loss of IMPα4 expression in these cells was confirmed by western blot analysis using an IMPα4 specific antibody (Santa Cruz Biotech, # sc-514101) (Figure 2.4B). Subsequently, we performed a multistep replication curve analysis on #6 and #12 cells with B/Victoria/2/87 WT virus at a MOI of 0.05. We found that IBV

replication in #6 was significantly lower compared to WT at 36 hours post infection and IBV replication in #12 was significantly lower at 10 and 24 hours post infection.

Discussion

In order to better understand the potential proteins and pathways BNP interacts with, we conducted a unbiassed whole genome screen using Y2H libraries including both human and mouse cDNAs using BNP as the bait. We found that Victoria and Yamagata BNP interacted with a combined potential total of 13 different human genes and 5 mouse genes. Interestingly, KPNA3 was found on both lists. We proceeded to confirm that IMPα4 and Victoria BNP interacted by Co-IP. Further interrogation of the specifics of this interaction yielded that amino acids 44-47 of BNP are necessary for interaction with IMPα4 in cell lysates, while deletion of any ARM from 6-10 of IMPα4 results in total loss of binding to BNP. Finally, loss of IMPα4 expression in A549 cells did statistically reduce IBV replication, but biologically was less than two-fold.

ANP has been shown to be necessary and sufficient for the import of viral RNAs into the nucleus in-vitro, and that this entry is facilitated by Importin α□β (5). It would be of interest to determine if BNP similarly facilitates vRNA nuclear import. Additionally, it would be of interest to determine the potential redundancy of the 7 known IMPα proteins in terms of their interaction with BNP. It has been previously shown that IMPα7 could be co-crystalized with BNP (25). We speculate it's unlikely that IMPα4 and IMPα7 are the only members of the family that interact with BNP given ANP's known interactions with IMPα1, α3, and α5 (31). Reliance on a single or small number of host proteins for replication would make IBV evolutionarily vulnerable to host specific expression of a small number of factors like IMPα. Indeed, Xie et al., showed that KO of KPNA3 gene resulted in early reduced viral replication of serotype 4 fowl adenovirus (FAdV-4) in LMH cells, while KPNA4 KO resulted in reduced replication at all timepoints

(32). This would likely suggest that IMPα4 is only one of many factors utilized by viruses during replication, especially considering the conservation in relative structure and function of the IMPα family. If these IMPα family members are important to virus replication, we speculate that their levels of expression may increase upon infection to ensure delivery of viral NP and RNA to the nucleus. This could be measured easily by infection of cells in culture and monitoring of KPNA gene expression over time via qPCR. Multiple studies have shown that members of the IMPα protein family interact with ANP. For example, ANP has been shown to interact with IMPα1 (5, 31, 33), IMPα3 (31), IMPα5(31), and IMPα7 (34). BNP in contrast has only been shown to interact with IMPα7 (25). To our knowledge, this is the first time IMPα4 has been shown to interact with any influenza NP protein. Of the family members, IMPα4 has not been extensively studied. However, a few interactions have been discovered. For example, IMPα4 has been shown to interact with and implicated in the nuclear import of methyl-CpG binding protein 2 (MeCP2) (35), a protein involved in reading of DNA methylation and the neurodevelopmental disorder termed Rett Syndrome (36). Additionally, IMPα4 has been shown to interact with and facilitate the nuclear import of NF-Kβ (37). NF-Kβ is critical for facilitating pro-inflammatory cytokine responses in multiple immune cell types, including macrophages, T-Cells, and B-Cells. Upon activation of cellular receptors, like T-cell receptors, IκBα is degraded and releases NF-kβ, which can then be imported into the nucleus by IMPα3 & IMPα4, where it acts as a transcription factor to activate pro-inflammatory gene responses (38). Ye et al., showed that Japanese Encephalitis Virus (JEV) NS5 protein blocks antiviral defenses by competitively binding to IMPα1, IMPα3, and IMPα4, thereby blocking these proteins from importing their normal cargo to the nucleus during infection, including NF-kβ, resulting in reduced IFN-β production (39). It is

possible that in addition to possibly facilitating import of NP and the vRNA, BNP binding to IMPα4 could similarly be a viral defensive mechanism against IFN or similar responses. If this was the case, we would have expected that KO of IMPα4 would result in higher viral loads during infection, however, it was not. However, Ye et al noted that JEV NS5 interacted with multiple IMPα family members to achieve this suppression. It has already been shown that IMPα7 also interacts with BNP. We speculate that if BNP is facilitating a defense against antiviral programs, it likely does so as a multi-pronged approach, interacting with multiple IMPα proteins rather than a single IMPα. As such, the loss of IMPα4 alone is likely to not result in total loss of nuclear import associated with antiviral defense. To test this, it would be interesting to determine how IFN-β expression changes in response to Poly IC stimulation in the presence and absence of BNP.

The nuclear localization signal normally facilitates interaction between the cargo protein and an IMPα protein to increase transport. There have been potentially conflicting reports regarding which regions of BNP are required for nuclear localization. Using Xenopus oocytes, Davey et al first identified BNP amino acids 327 to 345 as necessary for nuclear import (40). Stevens and Barclay would go on to show that deletion of BNP N-terminal amino acids 1-69 resulted in no change to nuclear localization of BNP in MDCK cells (27), suggesting that the N-terminus of BNP is not involved in nuclear localization and does not contain an NLS. In contrast, Wang et al showed that deletion of amino acids 1-70 of BNP resulted in cytoplasmic retention of BNP and deletion of BNP amino acids 254 to 356 did not alter nuclear localization compared to WT BNP in hela cells (6). Wanitchang et al noted that BNP amino acids 1-15 are necessary for efficient nuclear import of this fragment, but this peptide alone could not facilitate nuclear import of a GFP protein in HEK293T cells. Additionally,

alanine mutations of BNP amino acids 44 and 45 ablated BNP-GFP nuclear import, suggesting these amino acids may serve in the NLS (26). Finally, Wang et al., noted BNP amino acids 1-20 were sufficient to facilitate nuclear import of an unrelated measles p protein, but Wanitchang found that while BNP amino acids 1-15 were critical for BNP nuclear import, amino acids 1-45 were not sufficient to mediate GFP nuclear import, but BNP amino acids 1-60 could. Wanitchang speculated that amino acids 44-47, representing a well conserved KRXR motif, serves as a nuclear localization signal based on their mutational data. Importin α proteins are composed of 10 repeating alpha helices called Armadillo repeats, or ARMS. The ARMs act as Importin α's interface to the NLS, and is divided into major (ARM 2-4) and minor (ARM 6-10) NLS binding sites. The NLS serves as the cargos interface for binding to the importin α subunit. There are multiple types of NLSs, including classical monopartite and bipartite signals. The consensus monopartite signal is K (K/R) X (K/R) (41), which resembles the proposed BNP putative NLS. Our mutational data on Wanitchang's putative NLS is congruent with these amino acids serving as an NLS, as deletion or alanine substitutions in BNP amino acids 44-47 resulted in loss of binding to IMPα4. While this result supports a model where the NLS of BNP resides in the N-terminal, it is possible that these differences in results could be at least partially due to experimental system differences, including various cell types used to measure BNP nuclear imports. The above studies utilize Xenopus, canine, human cancer, and immortalized human embryonic kidney cells. This difference in species and cells types likely plays a role in variance of results.

Along with Importin α4, our Y2H screen also revealed other host factors putatively associated with BNP. Some of these factors are known to play a role in transcription and translation. For example, SYF2 is a splicing factor and part of the

spliceosome in yeast (42). This interaction could represent BNP serving in a role to attract necessary splicing factors required for the expression of such genes like NEP. IAV NP has been reported to interact with splicing factors such as RAF-2p48, which increases viral RNA synthesis (43). It would be of interest not only to first confirm SYF2 interaction by Co-IP or other means, but it would be interesting to determine if splicing is affected by its absence or overexpression, which would suggest a more direct role in viral replication. Another example is eEF1A1, or Eukaryotic Translation Elongation Factor 1 Alpha 1, which is normally responsible for enzymatic delivery of aminoacyl tRNAs to ribosomes. Interestingly, multiple reports have indicated that eEF1A1 is recruited to the virions of many viruses, including HIV-1, DENV, and WNV. In DENV and WNV, eEF1A1 facilitates assembly of the replication complex and is necessary for maximal viral replication. While there is no previous report of eEF1A1 having a role in Influenza virus replication, eEF1D has been previously reported not only to interact with IAV PA/PB1/PB2/NP, but inhibits the nuclear import of NP and inhibits viral replication (44). For IBV, it would be of interest to not only confirm eEF1A1 interaction with BNP, but to determine if overexpression has a negative impact on replication and BNP nuclear import.

Much of our data on interaction relies on Co-IP to confirm the interactions of IMPα4 and BNP from our Y2H screen. It should be recognized that while the proteins studied were made in cells that were transfected with plasmids, interaction between said proteins could have occurred either in the cell prior to lysis, or post lysis in solution. To further confirm if this interaction occurs in living cells, it could be best achieved through the use of FRET. Finally, while we hypothesized that loss of IMPα4 expression would result in reduced virus replication, the opposite should be testable, were overexpression

should increase virus replication resulting from increased import of viral RNP complex mediated by NP into the nucleus. Collectively however, we have shown for the first time that BNP interacts with the nuclear import adapter IMPα4 through Y2H and Co-IP, and that this interaction so far in the literature is not tested with IAV. Additionally, specific regions relating to the NLS of BNP are necessary for this interaction, and these amino acids represent tantalizing targets for future analysis, possibly as targets for drug inhibition as this would not likely affect host protein function.

Material and Methods

Virus and cells. Influenza B/Victoria/2/87 and B/Yamagata/16/88 viruses were propagated in pathogen free eggs purchased from Charles River Laboratories Inc. and stored at -80°C. HEK293T/A549 and Madin-Darby canine kidney (MDCK) cells were cultured at 37°C in DMEM medium supplemented with 10% FBS, or MEM medium supplemented with 10% FBS, respectively.

Multi-step growth curve. 3x105 A549 cells per well were transfected with 0.5µg of pCANMyc_Impα4_FL using Lipofectamine 2000 (Invitrogen) in DMEM supplemented with 10% FBS for 48 hours (hrs) in 6-well plates in triplicate. Subsequently, media was removed, and cells were infected with a multiplicity of infection (MOI) of 0.05 of Influenza B/Victoria/2/87 or B/Yamagata/16/88 virus diluted in PBS/BSA/PS (1x PBS, 0.42% BSA, 100ug/ml Pen-strep, 0.8mM CaCl2-2*H2O, 1mM MgCl2-6H2O) and incubated at 33°C for one hour. Then, virus solutions were aspirated and replaced with 1ml of post infection media (1x DMEM, 0.35% BSA, 100U/ml Pen-strep, 2mM L-glutamine, 0.15% sodium bicarbonate, 20mM HEPES pH 7.0, 0.25ug/ml TPCK). Infection samples were collected at 24 and 48 hours post infection. The virus concentrations were evaluated by standard plaque assays.

Plasmids. To construct “bait” plasmids for Y2H experiments, we fused BNP coding sequences with the GAL4 binding domain. B/Victoria/2/1987 or

B/Yamagata/16/88 NP coding sequence (amino acids 2-560) was PCR amplified with primers containing homologous ends to pGBKT7. PCR inserts were cloned into pGBKT7 (Clontech #630489) by In-Fusion reaction according to the manufacturer's protocols (Takara Bio, USA), fusing the GAL4 binding domain to the N-terminus of NP to construct pGBKT7_VicNP or pGBKT7_YaNP.

To express the KPNA3 cDNA sequence in human cells with a N-terminal myc tag, we PCR amplified the KPNA3 cDNA from the library plasmid isolated by yeast mini-prep (see Y2H section below) with primers containing homologous ends to pCAGGS_NMyc. The PCR insert was cloned into XhoI/EcoR1 digested pCAGGS_Nmyc via In-Fusion reaction to construct (pCANMyc_IMPα4_Y2H). Full length KPNA3 coding sequence was similarly cloned into pCAGGS_Nmyc. HsCD00334711 plasmid containing the KPNA3 coding sequences was purchased from the Harvard Plasma Database and used as template for PCR. Inserts were cloned into pCAGGS_Nmyc to construct pCANMyc_IMPα4_FL (Full Length).

For expression of the BNP gene in human cells for Co-IP experiments, the B/Victoria/2/1987 NP sequence was PCR amplified with homologous ends to Hind III/EcoR1 digested p3XFLAG-CMV-10 (Sigma-Aldrich, # E7658). PCR inserts were cloned into Hind III/EcoR1 digested p3XFLAG-CMV-10 plasmid by In-Fusion reaction.

To construct myc and flag-tagged version of GST for expression in human cells, we cloned the full length coding sequence of Schistosoma japonicum GST

into either pCAGGS_NMyc or p3XFLAG-CMV-10. PCR was used to amplify the GST sequence with homologous ends to either XhoI/EcoR1 digested pCAGGS_Nmyc or p3XFLAG-CMV-10, and were cloned into the multiple cloning sites of each plasmid by In-Fusion reaction.

CRISPR-CAS9 gene editing was used to introduce knockout mutations through non-homologous end joining (NHEJ) to exon coding regions of the KPNA3 gene. Guide RNAs (gRNAs) targeting exon 2 (5'-ACATAGAAATGAAGTGACAG-3') and exon 5 (5'-CAGCACTCAATTGGACCACT-3') of the KNPA3 genes were used. The sense and antisense version of each gRNA were synthesized with Bbs I sticky ends and cloned into pX549 (containing the CRISPR CAS9 system) by oligo annealing to construct pX549Ex2 (exon 2) and pX549Ex5 (exon 5).

mCherry tagged IMPα4 and GFP tagged BNP were expressed in 293T cells to determine if they co-localized in the nucleus. Amino acids 1-560 of B/Victoria/2/87 were PCR amplified and cloned into EcoR1/Kpn1 digested pCAGGS_eGFP via In-Fusion reaction to construct pCAGFP_BNP, expressing a C-terminal enhanced GFP tag. The full length KPNA3 coding sequence was PCR amplified from HsCD00334711 and cloned into EcoR1/BamH1 digested pmCherry-c1 by In-Fusion reaction. 1 ug of each plasmid were co-transfected with each other or with empty GFP/mCherry plasmids as controls into 1 x 106 293Tcells via PEI.

Yeast-2-Hybrid. We cloned the B/Victoria/2/1987 NP coding sequence (amino acids 2-560) into pGBKT7, fusing the GAL4 binding domain to the N-terminus of NP to create pGBKT7_VicNP. pGBKT7_VicNP was transformed into competent empty yeast cells to serve as “bait” against a library screen. A single colony of pGBKT7_VicNP yeast was used to inoculate 50ml of growth medium for 48 hours (hrs) at 30°C. This was used to inoculate 1 liter of growth medium and grown to between 0.8-1.0 OD600 (equating to 1.26-1.85 $x10^7$ haploid yeast cells). Cells were centrifuged at 3000G at room temperature and resuspended in 200ml of sterile H2O to wash. Cells were centrifuged then resuspended in 100ml LiSORB (100mM Lithium Acetate, 1M Sorbitol in 1X TE). Cells were centrifuged at 3000G. Yeast cells were resuspended in 10ml LiSORB. 100µg of Library DNA was prepared by adding 80mg of carrier ssDNA (Salmon sperm, SIGMA, sheared to average size of 1-2KB, Phenol/CHCl3 extracted, and ethanol precipitated) and boiled for 10min. DNA Library mixture was cooled to handle, then added to 5ml of competent pGBKT7_VicNP yeast cells. 30ml of LiPEG (40% PEG3350, 100mM LiAc in 1XTE) was mixed with cells and incubated for 30min at 30°C. 350µl of 100% DMSO was added, then cells were heat shocked at 42°C for 15 min. Cells were added to 200ml sterile selection medium and shaken at low RPM for 1hr at 30°C for recovery. Cells were centrifuged at 3000G for 10min at room temperature, washed with 20ml of selection media, centrifuged, and finally resuspended in 10ml selection media. 1ml of cells was

plated per 100mm plate with selection agar medium, then grown at 30°C for 2-3 days. Single colonies were picked and spotted onto separate plates.

Individual yeast clones were grown in 2ml of selection medium for 48hrs at 30°C. cells were washed with 1ml of sterile H2O and centrifuged at 3200G for 2min. Cells were resuspended in 50µl H2O with RNAse (100ug/ml). 50ul of 2x Lyticase was mixed with cells, then incubated at 37°C for 1hr. Plasmid DNA from yeast was then purified using the OMEGA miniprep kit (D6942-00S, OMEGA bio-tek, Norcross, Georgia) according to supplied protocol. Plasmids were sequenced with standard sanger sequencing.

Co-immunoprecipitation. We conducted co-immunoprecipitation to verify the interaction of VicNP with IMPα4. We fused amino acid 2-560 of VicNP to a N-terminus 3x Flag tag in p3xFLAG-CMV to make pCMVVic87NP_NFLG. Amino acid 2-591 of the IMPα4 coding sequence (NM_002267.3) was fused to a N-terminus Myc tag in pCAGGS to make pCANMyc_Impα4. 1µg of each plasmid (or control PUC19 plasmid) were transfected into 1x106 HEK293T cells by suspension PEI transfection, and plated in DMEM supplemented with 5% FBS in 6 well plates at 37°C for 48hrs. Cells were scrapped off plates and washed with 1x PBS, then lysed with 600ul of NP 40 lysis buffer (50mM Tris HCL, pH 8, 150mM NaCl, 1% NP40, 1mM PMSF, 1mM DTT) for 30min on ice. Cell debris was removed by centrifugation at 20,000G for 5min.

Recombinant protein G sepharose G4 beads (# 101243, Invitrogen) were blocked with 10% BSA in 1x PBS for 1hr at room temperature, then stored in 1x PBS at 4°C until use. 15µl of bead slurry/sample was washed with 1ml of ice-cold NP-40 lysis buffer three times. Beads were resuspended in 1ml of ice-cold NP 40 lysis buffer, and 0.3µg of Anti flag antibody (#F3165, SIGMA) was conjugated to the beads by rocking at room temperature for 1hr. Beads were washed three times with ice-cold NP-40 lysis buffer and resuspended in 15µl of ice-cold NP-40 lysis buffer. Beads were then added to cell lysates, and rocked at room temperature for 1hr. Beads were washed three times with ice-cold NP 40 lysis buffer, all liquid was removed by syringe, boiled in 30µl of 2x SDS dye for 10min, and frozen at -80°C until western blots were performed.

Co-localization. Amino acids 1-560 of B/Victoria/2/1987 NP coding sequence was cloned into pCAGGS_GFP to create pCA_VicNP_GFP. pCA_VicNP_GFP expresses eGFP fused to the C-terminus of B/Victoria/2/1987 NP. Amino acids 2-521 of IMPα4 coding sequence were cloned into pmCherry_C1, resulting in the fusion of mCherry to the N-terminus of IMPα4. 1µg of each plasmid were co-transfected (or with empty puc19 vector) into $1x10^6$ HEK293T cells via polyethylenimine (PEI) in a 6 well plate. 24 hrs later, cells were imaged via fluorescent microscopy.

Knockout of IMPα4 gene and viral kinetic assays. IMPα4_A549 KO cells loss of IMPα4 protein expression was confirmed by western blot. For kinetic analysis, $1x10^6$ of either WT or IMPα4_A549 KO cells were plated in 6 well plates and placed at 37°C. 24hrs later, cells were infected for 1hr at 33°C with B/Victoria/2/1987 at an MOI of 0.05 with virus diluted in virus dilution buffer (1x PBS supplemented with 0.4% BSA, 100µg/ml Penn/Strep, 0.8mM $CaCl_2$, 1mM MgCl2). Virus solution was replaced with 1ml of post infection media, and cells were incubated at 33°C for 72hrs. 200ul samples were collected at the specified timepoints and 200ul fresh post infection media was added to replace the lost volume. Samples were clarified by centrifugation at 1000G for 5 min, and stored at -80°C until analysis. Viral titers were measured by standard plaque assays using MDCK cells.

References

1 Herz, C., Stavnezer, E., Krug, R. & Gurney, T., Jr. Influenza virus, an RNA virus, synthesizes its messenger RNA in the nucleus of infected cells. Cell 26, 391-400 (1981). https://doi.org:10.1016/0092-8674(81)90208-7

2 Jackson, D. A., Caton, A. J., Mccready, S. J. & Cook, P. R. Influenza-Virus Rna Is Synthesized at Fixed Sites in the Nucleus. Nature 296, 366-368 (1982). https://doi.org:DOI 10.1038/296366a0

3 Shapiro, G. I., Gurney, T. & Krug, R. M. Influenza-Virus Gene-Expression - Control Mechanisms at Early and Late Times of Infection and Nuclear-Cytoplasmic Transport of Virus-Specific Rnas. Journal of Virology 61, 764-773 (1987). https://doi.org:Doi 10.1128/Jvi.61.3.764-773.1987

4 Kemler, I., Whittaker, G. & Helenius, A. Nuclear import of microinjected influenza virus ribonucleoproteins. Virology 202, 1028-1033 (1994). https://doi.org:10.1006/viro.1994.1432

5 Oneill, R. E., Jaskunas, R., Blobel, G., Palese, P. & Moroianu, J. Nuclear Import of Influenza-Virus Rna Can Be Mediated by Viral Nucleoprotein and Transport Factors Required for Protein Import. J Biol Chem 270, 22701-22704 (1995). https://doi.org:DOI 10.1074/jbc.270.39.22701

6 Wang, P., Palese, P. & ONeill, R. E. The NPI-1/NPI-3 (Karyopherin alpha) binding site on the influenza A virus nucleoprotein NP is a nonconventional nuclear localization signal. Journal of Virology 71, 1850-1856 (1997). https://doi.org:Doi 10.1128/Jvi.71.3.1850-1856.1997

7 Hampoelz, B., Andres-Pons, A., Kastritis, P. & Beck, M. Structure and Assembly of the Nuclear Pore Complex. Annu Rev Biophys 48, 515-536 (2019). https://doi.org:10.1146/annurev-biophys-052118-115308

8 Ibarra, A. & Hetzer, M. W. Nuclear pore proteins and the control of genome functions. Genes Dev 29, 337-349 (2015). https://doi.org:10.1101/gad.256495.114

9 Aitchison, J. D. & Rout, M. P. The Yeast Nuclear Pore Complex and Transport Through It. Genetics 190, 855-883 (2012). https://doi.org:10.1534/genetics.111.127803

10 Makio, T. & Wozniak, R. W. Passive diffusion through nuclear pore complexes regulates levels of the yeast SAGA and SLIK coactivator complexes. Journal of Cell Science 133 (2020). https://doi.org:10.1242/jcs.237156

11 Wang, R. W. & Brattain, M. G. The maximal size of protein to diffuse through the nuclear pore is larger than 60 kDa. Febs Letters 581, 3164-3170 (2007). https://doi.org:10.1016/j.febslet.2007.05.082

12 Popken, P., Ghavami, A., Onck, P. R., Poolman, B. & Veenhoff, L. M. Size-dependent leak of soluble and membrane proteins through the yeast nuclear pore complex. Molecular Biology of the Cell 26, 1386-1394 (2015). https://doi.org:10.1091/mbc.E14-07-1175

13 Gorlich, D. Nuclear protein import. Curr Opin Cell Biol 9, 412-419 (1997). https://doi.org:10.1016/s0955-0674(97)80015-4

14 Nigg, E. A. Nucleocytoplasmic transport: signals, mechanisms and regulation. Nature 386, 779-787 (1997). https://doi.org:10.1038/386779a0

15 Weis, K. Importins and exportins: how to get in and out of the nucleus. Trends Biochem Sci 23, 185-189 (1998). https://doi.org:Doi 10.1016/S0968-0004(98)01204-3

16 Kalderon, D., Roberts, B. L., Richardson, W. D. & Smith, A. E. A Short Amino-Acid Sequence Able to Specify Nuclear Location. Cell 39, 499-509 (1984). https://doi.org:Doi 10.1016/0092-8674(84)90457-4

17 Gorlich, D., Vogel, F., Mills, A. D., Hartmann, E. & Laskey, R. A. Distinct Functions for the 2 Importin Subunits in Nuclear-Protein Import. Nature 377, 246-248 (1995). https://doi.org:DOI 10.1038/377246a0

18 Kapinos, L. E., Schoch, R. L., Wagner, R. S., Schleicher, K. D. & Lim, R. Y. H. Karyopherin-Centric Control of Nuclear Pores Based on Molecular Occupancy and Kinetic Analysis of Multivalent Binding with FG Nucleoporins. Biophys J 115, 2512 (2018). https://doi.org:10.1016/j.bpj.2018.11.3125

19 Shah, S., Tugendreich, S. & Forbes, D. Major binding sites for the nuclear import receptor are the internal nucleoporin Nup153 and the adjacent nuclear filament protein Tpr. J Cell Biol 141, 31-49 (1998). https://doi.org:DOI 10.1083/jcb.141.1.31

20 Gorlich, D. et al. Two different subunits of importin cooperate to recognize nuclear localization signals and bind them to the nuclear envelope. Curr Biol 5, 383-392 (1995). https://doi.org:10.1016/s0960-9822(95)00079-0

21 Kimura, M. & Imamoto, N. Biological Significance of the Importin-beta Family-Dependent Nucleocytoplasmic Transport Pathways. Traffic 15, 727-748 (2014). https://doi.org:10.1111/tra.12174

22 Cingolani, G., Bednenko, J., Gillespie, M. T. & Gerace, L. Molecular basis for the recognition of a nonclassical nuclear localization signal by importin beta. Molecular Cell 10, 1345-1353 (2002). https://doi.org:10.1016/s1097-2765(02)00727-x

23 Kotera, I. et al. Importin alpha transports CaMKIV to the nucleus without utilizing importin beta. Embo Journal 24, 942-951 (2005). https://doi.org:10.1038/sj.emboj.7600587

24 Organization, W. H. WHO Influenza Seasonal Factsheet 2020. (2020).

25 Labaronne, A. et al. Structural analysis of the complex between influenza B nucleoprotein and human importin-alpha. Sci Rep-Uk 7 (2017). https://doi.org:ARTN 1716410.1038/s41598-017-17458-z

26 Wanitchang, A., Narkpuk, J. & Jongkaewwattana, A. Nuclear import of influenza B virus nucleoprotein: Involvement of an N-terminal nuclear localization signal and a cleavage-protection motif. Virology 443, 59-68 (2013). https://doi.org:10.1016/j.virol.2013.04.025

27 Stevens, M. P. & Barclay, W. S. The N-terminal extension of the influenza B virus nucleoprotein is not required for nuclear accumulation or the expression and replication of a model RNA. Journal of Virology 72, 5307-5312 (1998).

28 Ba, A. N. N., Pogoutse, A., Provart, N. & Moses, A. M. NLStradamus: a simple Hidden Markov Model for nuclear localization signal prediction. Bmc Bioinformatics 10 (2009). https://doi.org:Artn 20210.1186/1471-2105-10-202

29 Lin, J. R. & Hu, J. J. SeqNLS: Nuclear Localization Signal Prediction Based on Frequent Pattern Mining and Linear Motif Scoring. Plos One 8 (2013). https://doi.org:ARTN e7686410.1371/journal.pone.0076864

30 Kosugi, S., Hasebe, M., Tomita, M. & Yanagawa, H. Systematic identification of cell cycle-dependent yeast nucleocytoplasmic shuttling proteins by prediction of composite motifs. P Natl Acad Sci USA 106, 10171-10176 (2009). https://doi.org:10.1073/pnas.0900604106

31 Melen, K. et al. Importin alpha nuclear localization signal binding sites for STAT1, STAT2, and influenza A virus nucleoprotein. J Biol Chem 278, 28193-28200 (2003). https://doi.org:10.1074/jbc.M303571200

32 Xie, Q. et al. Domain in Fiber-2 interacted with KPNA3/4 significantly affects the replication and pathogenicity of the highly pathogenic FAdV-4. Virulence 12, 754-765 (2021). https://doi.org:10.1080/21505594.2021.1888458

33 Cros, J. F., Garcia-Sastre, A. & Palese, P. An unconventional NLS is critical for the nuclear import of the influenza A virus nucleoprotein and ribonucleoprotein. Traffic 6, 205-213 (2005). https://doi.org:10.1111/j.1600-0854.2005.00263.x

34 Shapira, S. D. et al. A physical and regulatory map of host-influenza interactions reveals pathways in H1N1 infection. Cell 139, 1255-1267 (2009). https://doi.org:10.1016/j.cell.2009.12.018

35 Baker, S. A., Lombardi, L. M. & Zoghbi, H. Y. Karyopherin alpha 3 and Karyopherin alpha 4 Proteins Mediate the Nuclear Import of Methyl-CpG Binding Protein 2. Journal of Biological Chemistry 290, 22485-22493 (2015). https://doi.org:10.1074/jbc.M115.658104

36 Good, K. V., Vincent, J. B. & Ausio, J. MeCP2: The Genetic Driver of Rett Syndrome Epigenetics. Front Genet 12 (2021). https://doi.org:ARTN 620859 10.3389/fgene.2021.620859

37 Fagerlund, R., Kinnunen, L., Kohler, M., Julkunen, I. & Melen, K. NF-kappa B is transported into the nucleus by importin alpha 3 and importin alpha 4. J Biol Chem 280, 15942-15951 (2005). https://doi.org:10.1074/jbc.M500814200

38 Liu, T., Zhang, L., Joo, D. & Sun, S. C. NF-kappaB signaling in inflammation. Signal Transduct Target Ther 2 (2017). https://doi.org:10.1038/sigtrans.2017.23
39 Ye, J. et al. Japanese Encephalitis Virus NS5 Inhibits Type I Interferon (IFN) Production by Blocking the Nuclear Translocation of IFN Regulatory Factor 3 and NF-kappaB. J Virol 91 (2017). https://doi.org:10.1128/JVI.00039-17

40 Davey, J., Dimmock, N. J. & Colman, A. Identification of the sequence responsible for the nuclear accumulation of the influenza virus nucleoprotein in Xenopus oocytes. Cell 40, 667-675 (1985). https://doi.org:10.1016/0092-8674(85)90215-6
41 Lu, J. N. et al. Types of nuclear localization signals and mechanisms of protein import into the nucleus. Cell Commun Signal 19 (2021). https://doi.org:ARTN 60 10.1186/s12964-021-00741-y

42 Ben-Yehuda, S. et al. Genetic and physical interactions between factors involved in both cell cycle progression and pre-mRNA splicing in Saccharomyces cerevisiae. Genetics 156, 1503-1517 (2000).

43 Momose, F. et al. Cellular splicing factor RAF-2p48/NPI-5/BAT1/UAP56 interacts with the influenza virus nucleoprotein and enhances viral RNA synthesis. J Virol 75, 1899-1908 (2001). https://doi.org:10.1128/JVI.75.4.1899-1908.2001

44 Gao, Q. X. et al. Eukaryotic Translation Elongation Factor 1 Delta Inhibits the Nuclear Import of the Nucleoprotein and PA-PB1 Heterodimer of Influenza A Virus (vol 95, e01391-20, 2021). Journal of Virology 95 (2021). https://doi.org:ARTN e01413-21 10.1128/JVI.01413-21
.

Figures and Tables

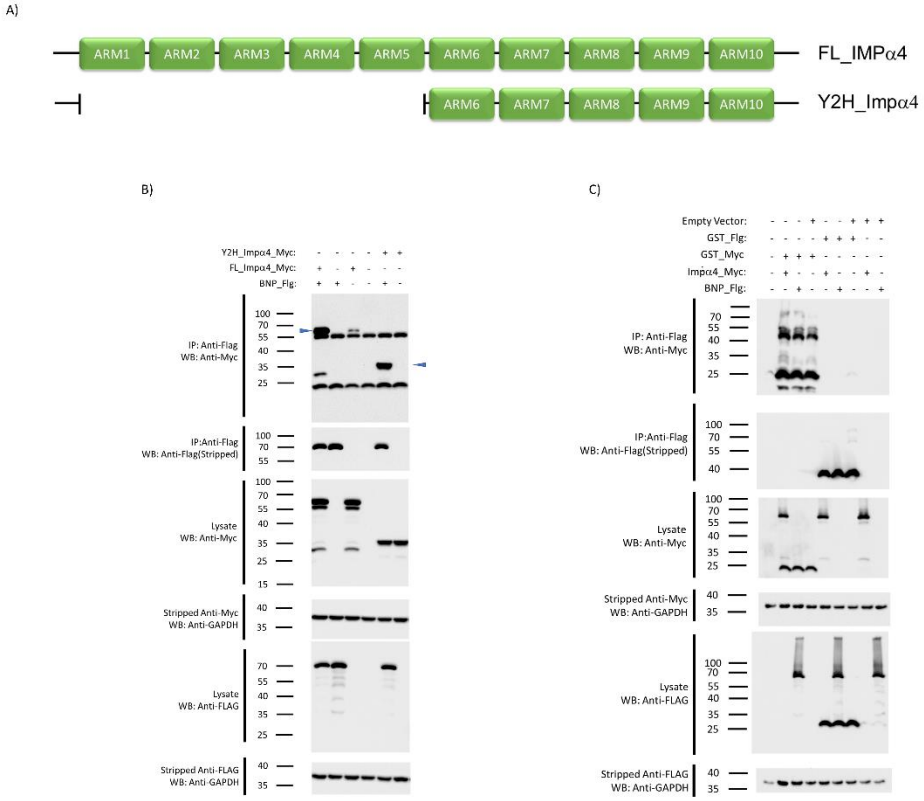

Figure 2.1 BNP does Co-Immunoprecipitate with IMPα4 protein.
A) schematic of ARM Repeats present in prey plasmids containing IMPα4. B) Western blots of 293T cells were transfected with 1ug indicated plasmids and harvested, lysed and IP'ed 48 hours post transfection. Top blue arrow indicates full length IMPα4 band, with lower blue arrow indicating Y2H Impα4 band. C) Western blots of 293T cells transfected with 1ug indicated plasmids and harvested, lysed and GST pulled down 48 hours post transfection.

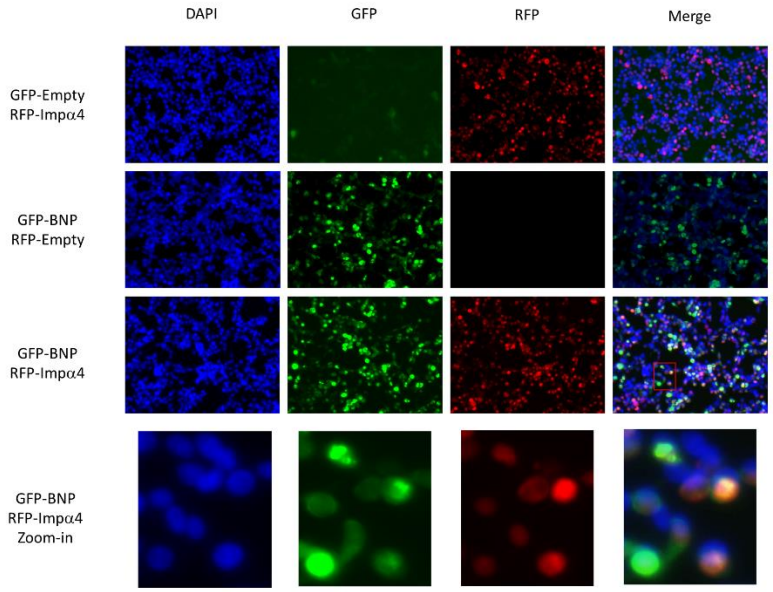

Figure 2.2 BNP and IMPα4 Co-localize in 293T cells.
0.5 ug of each indicated plasmid were co-transfected into 293T cells in 12 well plates on glass cover slips. Cells were fixed and DAPI stained 24 hours post transfection, and fluorescence was visualized by 10X microscopy

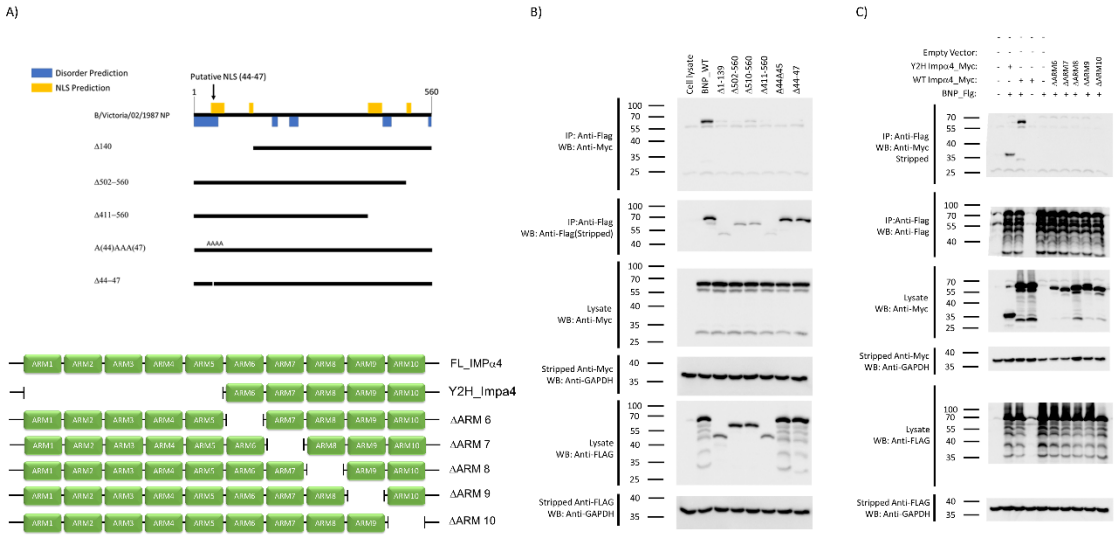

Figure 2.3 BNP amino acids 44-47 and ARM 6-10 of IMPα4 are necessary for BNP-IMPα4 interaction.

A) Schematic indicating (top) predicted NLS and disordered regions of BNP along with regions of BNP deleted or mutated for analysis (bottom) panel of incremental deletion of ARMs mutants from Impa4. B) 293T cells were co-transfected with WT IMPα4 and WT BNP or a BNP deletion mutant. Cells were harvested 48hrs later then BNP was used as bait for Co-IP and analyzed by western blot. C) 293T cells were co-transfected with WT BNP and WT IMPα4 or an ARM deletion mutant. Cells were harvested 48 hrs later then BNP was used as bait for Co-IP and analyzed by western blot.

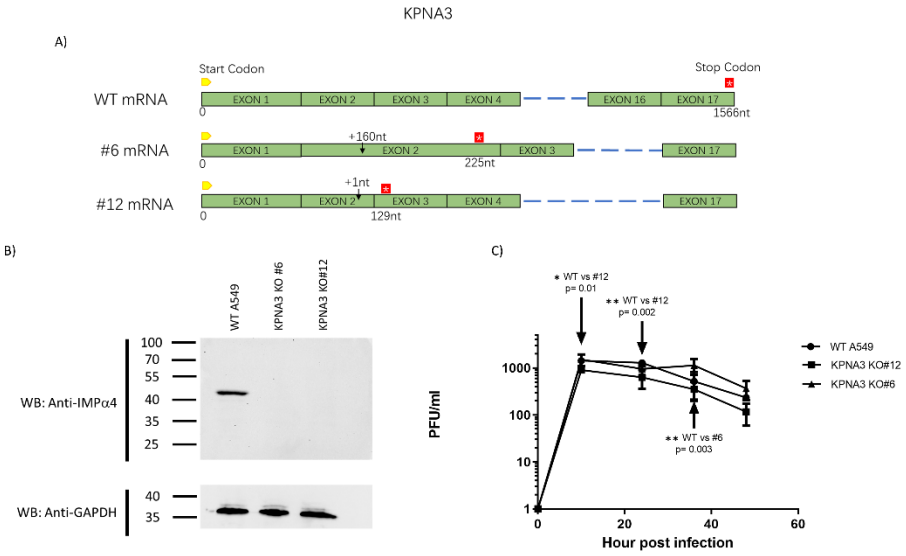

Figure 2.4. IBV replication is reduced in KPNA3 knockout cells.
A) Schematic showing mutations introduced into clone #6 and #12 A549 KPNA2 knockout cells by CRISPR-Cas9 mutations. B) A549 WT or KPNA3 KO cells were grown to full confluency in 6 wells plates for 24 hours, then lysed for western blot analysis for IMPa4 expression. C) A549 WT or KO cells were infected with IBV at an MOI of 0.05 and multi-step growth assays was used to measure replication. Cell supernatant samples were tittered by standard plaque assay

Gene ID	Gene Name	Uniprot ID	IBV NP Interactor
DBR1	Debranching RNA lariats 1	Q9UK59	Victoria
GAPDH	Glyceraldehyde-3-phosphate dehydrogenase	P04406	Victoria & Yamagata
EEF1A1	Eukaryotic translation elongation factor 1 alpha 1	P68104	Victoria
ERGIC3	ERGIC and golgi 3	Q9Y282	Yamagata
RPL10	Ribosomal protein L10	P27635	Yamagata
SYF2	SYF2 pre-mRNA splicing factor	O95926	Yamagata
MIF	Macrophage migration inhibitory factor	P14174	Victoria
KPNA3	Importin subunit alpha-4	O00505	Victoria
RPS13	Ribosomal protein S13	P62277	Victoria
IGLL5	Immunoglobulin lambda like polypeptide 5	B9A064	Victoria
PCBP1	Poly(rC) binding protein 1	Q15365	Victoria & Yamagata
METAP2	Methionyl aminopeptidase 2	P50579	Yamagata

Table 2.1 Human host proteins that interact with BNP via yeast-two-hybrid

Gene ID	Gene Name	Uniprot ID	IBV NP Interactor
Grrp1	Glycine/arginine rich protein 1	Q80X91	Yamagata
Faf1	Fas-associated factor 1	P54731	Yamagata
Kpna3	Karyopherin (importin) alpha 3	O35344	Yamagata
Mpp6	Membrane protein, palmitoylated 6	Q9JLB0	Victoria
Snf8	ESCRT-II complex subunit	Q9CZ28	Victoria
Zfp451	zinc finger protein 451	Q8C0P7	Yamagata

Table 2.2 Mouse host proteins that interact with BNP via yeast-two-hybrid

Chapter 2: Attenuation of a Reassortment-Incompetent Live Virus Vaccine Through Incremental Mutation of the HA Membrane Proximal Region

Authors: Jerald Chavez, Samantha Cordingley, Christine Light, Rong Hai.

Abstract

Influenza A virus and Influenza B virus are negative sense, segmented RNA viruses whom are part of the Orthomyxoviridae family. These viruses are responsible for yearly seasonal epidemics that result in 3-5 million cases of severe respiratory illness and between 290,000-650,000 deaths globally every year. In addition to yearly epidemics, Influenza A Virus (IAV) is a consistent pandemic threat since it zoonotically transmits between its host reservoir, avian waterfowl, and terrestrial species. Vaccination is the most cost-effective means of combating infections and reducing disease burden. While current live attenuated influenza virus (LAIV) vaccines are safe and effective, concerns regarding reassortment with circulating IAV restoring pathogenicity limit their use during pandemic situations. Hai et al., had previously developed a reassortment incompetent recombinant IBV expressing IAV HA which was attenuated through NS1 truncation. To improve upon this design, attenuation was achieved via progressive replacement of the IAV HA C-terminus with IBV HA sequence. This simultaneously attenuated these viruses and prevents restoration of pathogenicity in the event of reassortment with circulating IBV. In mice, these candidate viruses do not cause weight loss post immunization, elicit neutralizing antibodies against their homologous IAVs, and protect mice from lethal IAV challenge. However, vaccine lung replication was similar to WT IBV. Together, this data indicates that our recombinant viruses can illicit protective immune responses necessary

to serve as a live virus vaccine, but require further analysis of lung pathology to ensure they are safe for further testing.

Introduction

Influenza viruses are negative sense segmented RNA enveloped viruses and part of the Orthomyxoviridae family. In humans, these viruses are normally transmitted by aerosol particles (such as saliva from coughs or sneezing) from one individual to the next, causing local infection of the upper respiratory tract. Influenza A Virus (IAV) and Influenza B Virus (IBV) can cause severe respiratory illness, including primary viral pneumonia (1-3) and secondary bacterial pneumonia (4, 5) especially in the elderly (65+) and immune compromised (6). Together, these viruses are globally responsible for 3-5 million cases of severe respiratory disease and between 290,000—650,000 deaths annually (7). Besides seasonal epidemics, IAV has resulted in four major pandemics, most recently with swine-origin H1N1 IAV in 2009. This persistent pandemic threat stems from IAV's ability to zoonotically transmit from avian waterfowl (its known animal reservoir) to that of land terrestrial species including livestock animals such as pigs, chickens and turkeys. Contact with these infected animals can result in highly pathogenic infections in humans and is believed to be the pathogenesis of the 1918 H1N1 pandemic which killed an estimated 50 million globally (8).

Avian H9N2 and H7N9 have been regularly found in waterfowl and poultry species during standard influenza surveillance. H9N2, originally first isolated from humans in Hong Kong in 1999, has since gone on to cause sporadic infections in human individuals to date (9-18). While not yet causing severe disease, H9N2 appears to have contributed internal genes to avian subtype H7N9 strains through reassortment (19) that resulted in 5 epidemic waves in China, resulting in more than 600 deaths (20). While both avian H9N2 and H7N9 subtypes have limited airborne transmissibility in ferrets (21-28) their rapid ability to genetically shift make both viruses a significant future pandemic

threat. Given this, preventative measures to combat these viruses are critical steps in the prevention of future pandemics.

Prophylactic vaccination is still the most cost-effective means to prevent influenza virus infection and reduce disease burden across multiple age, health related, and regional demographics (29-39). There are two broad categories of vaccines available for influenza viruses: subunit/killed virus vaccines and live attenuated influenza vaccines (LAIVs). Unlike subunit/killed virus vaccines, LAIVs mimic actual IAV infection of the upper respiratory tract, and were shown to stimulate both mucosal (40-42) and cellular immune responses (43-45). The current US LAIVs are produced by multiple serial passages at lower temperatures that results in the accumulation of temperature sensitive mutations in the PB1, PB2, and NP viral segments (46), allowing the virus to replicate in the cooler upper respiratory tract, but prevent them from replicating in the warmer lower respiratory tract (attenuation), reducing the risk for development of severe disease. However, safety concerns regarding their use during these situations prevents their wider adoption during pandemics. Specifically, should these LAIVs reassort with a circulating IAV, the segments harboring temperature sensitive mutations could be replaced with circulating versions of these genes, potentially resulting in restoration of virulence, exposing a totally naive population to a highly pathogenic virus.

To address this, a previous study expressed IAV HA ectodomain in the IBV backbone and attenuated the virus by NS1 truncation (47). The resulting virus could protect mice from lethal challenge, was incapable of reassortment with circulating IAV, had lower potential for genetic drift due to IBVs lower mutation rate, and was less likely to zoonotically transmit since IBV has no known animal reservoir. However, in that design, its attenuation marker was located in the IBV NS segment, which has the potential to

reassort with circulating IBV to restore the WT NS segment. To improve upon this design, we created a panel of recombinant IBVs expressing the IAV ectodomain in which we incrementally introduced IBV HA coding sequence into the C-terminus of the IAV HA ectodomain and selected for the most attenuated of the panel (Fig 1A). This method simultaneously attenuates these viruses and locks the attenuation to the HA segment, meaning even in the event of reassortment with circulating IBV, attenuation would be passed to all progeny viruses. To this end, we chose to generate a panel of attenuated recombinant IBV (rIBV) H9 and H7 subtype viruses. rIBV-H9HA with 9 and 8 amino acids from IBV in the attenuation region resulted in significant reduction in viral replication compared to WT IBV. These candidates were able to stimulate significant IgG responses specific for IAV H9 vaccinated mice. These H9HA specific IgGs neutralized IAV significantly well, and did not cause weight loss after infection. Vaccinated mice were protected from lethal IAV H9 challenge and had significantly lower viral lung replication compared to unvaccinated controls. However, vaccine virus lung replication was similar to WT IBV. Together, this data suggests that we successfully developed an IAV reassortment-incompetent vaccine that does not cause severe disease, but further analysis of lung pathology to ensure safety post vaccination is warranted.

Results

Generation of attenuated recombinant influenza B virus expressing H7 or H9 Hemagglutinins. We generated a panel of recombinant IBV HA segment expressing H7 or H9 IAV ectodomain in which we progressively introduced increasing numbers of IBV stalk amino acids into the C-terminus MAR (membrane anchor region) region of the IAV ectodomain (Figure 3.1). These segments retain the signal peptide sequence, transmembrane domain, cytoplasmic domain and packaging signals from B/Yamagata/16/88. We rescued replication competent IBV virus using our recombinant HA segments. The resulting viruses possess 7 B/Yamagata/16/88 segments in addition to one of our A/B chimeric segments encoding the IAV hemagglutinin segment. After transfection in 293T cells, we were able to successfully rescue and expand all but the rIBV-9aa-H7HA virus (Figure 3.2A), suggesting this virus may be too attenuated to rescue.

rIBV-9aa-H9HA/rIBV-8aa-H9HA are attenuated in vitro and in vivo. We first selected the most attenuated of our viruses in culture by evaluating the growth kinetics of our panel of chimeric H7 and H9 viruses in a multi-step growth curve analysis in MDCK cells. Cells were infected with a MOI of 0.05, and virus in the culture supernatants was measured at the indicated time points post infection on MDCK cells by plaque assay. From the chimeric H7 panel, none of the rIBVs have significantly lower replication compared to the Ya88 vector control, indicating we were unable to attenuate these viruses (Figure 3.2B left). As such, we chose not to proceed to vaccination in animal models with any of the rIBV H7 variants. However, from the H9 panel, rIBV-8aa-H9HA & rIBV-9aa-H9HA had significantly lower titers compared to the vector control at 72hpi (Fig

2B right). Specifically, both rIBV-8aa-H9HA and rIBV-9aa-H9HA were ~2 logs lower (or more) than the WT control. These observations are similar to previous studies utilizing NS-1 truncation to achieve attenuation in A/B chimeric viruses (47). We chose rIBV-8aa-H9HA and rIBV-9aa-H9HA viruses to continue further studies with due to these viruses having the lowest peak titers compared to the rest of their respective panel and Ya88 vector control. We confirmed IAV H9 HA expression in our rIBVs via infection in MDCK cells and subsequent western blot (Figure 3.2C).

Weight loss is an important in vivo measure of viral pathogenicity. We investigated the attenuation of rIBV-8aa-H9HA and rIBV-9aa-H9HA viruses in vivo by measuring weight loss and survival rates in mice vaccinated with our rIBVs. We infected C57BL/6J mice (n=5) intranasally with 10-fold serial dilutions of either recombinant virus (1×10^5 to 1×10^3 PFU) and measured body weights 14 days post infection. Similar to mock PBS and infected Ya88 controls, none of the doses of recombinant viruses reduced body weights below 90% and all mice hovered at or near their initial body weight for the duration of the experiment (Figure 3.3A). To evaluate pulmonary replication, mice were infected with 1×10^5 PFU of either rIBV-8aa-H9HA and rIBV-9aa-H9HA (n=3). Both 3 and 6 dpi rIBV-8aa-H9HA and rIBV-9aa-H9HA replication are not statistically different from the WT Ya88 level (Figure 3.3B), however total replication levels are below the initial dose level, and weight loss data suggests both rIBV-8aa-H9HA and rIBV-9aa-H9HA viruses have an attenuated phenotype in vivo.

rIBV-9aa-H9HA & rIBV-8aa-H9HA elicit neutralizing antibodies to H9 IAV in C57BL/6J Mice. Antibody response to infection represents a primary means of defense against influenza virus and therefor is a necessary step to achieve in successful

vaccination. To evaluate the protective humoral response to rIBV-8aa-H9HA and rIBV-9aa-H9HA, we examined the antibody response post vaccination. Mice were vaccinated with rIBV-8aa-H9HA, rIBV-9aa-H9HA, or rWT/Ya88 B virus and serum IAV H9 IgG specific antibody levels were analyzed by ELISA 21 days post vaccination (Figure 3.4A & B). rIBV-8aa-H9HA and rIBV-9aa-H9HA at all doses, both induced significant levels of IAV H9 IgG-specific antibodies in the sera of vaccinated mice compared to the PBS mock or Ya88 IBV controls up to 900-fold dilutions. This indicates vaccination with our H9 rIBVs are successfully eliciting IAV H9 specific IgGs as intended from vaccination.

Vaccine induced antibodies should be both specific to a virus and capable of preventing said virus infection. Subsequently, we evaluated if these HA-specific antibodies can prevent H9 IAV infection of MDCK cells by microneutralization assay. Sera from mice that were vaccinated with rIBV-8aa-H9HA, rIBV-9aa-H9HA, rWT B virus, or PBS were combined with cH9/1 PR8 IAV and used to infect MDCK cells. Infection levels were detected by ELISA for the IAV M2 viral protein. rIBV-8aa-H9HA and rIBV-9aa-H9HA both had significantly higher microneutralization titers than the PBS or rWT B/Ya88 virus controls over multiple serial dilution ranges (Figure 3.4C & D). Together, these data indicate that our rIBVs can elicit IAV specific and potent IgGs, which are classical correlates of protection.

rIBV-9aa-H9HA & rIBV-8aa-H9HA protect C57BL/6J mice from lethal influenza A virus challenge. Efficacious vaccines should protect from infection and/or onset of severe disease. To evaluate if our rIVBs could protect mice from infection, rIBV-8aa-H9HA & rIBV-9aa-H9HA vaccinated mice were challenged with cH9/1 PR8 IAV. We evaluated these mice for pulmonary virus replication (Figure 3.5A) and weight loss post

challenge (Figure 3.5B & C). All vaccinated mice, from all doses and rIBV groups had significantly lower replication at 3 and 6 days post infection compared to the IBV-Ya88 control. It should also be noted that while the low dose 9aa vaccination group was the only vaccine group to have detectable IAV replication, replication was approximately three logs lower than the Ya88 control vaccine group. The high dose 9aa vaccine group had no detectable replication in comparison at either time point. This suggest vaccination with our rIBV panel is significantly reducing infection in-vivo.

To evaluate if vaccination could fully protect animals from lethal viral infection, rIBV-8aa-H9HA & rIBV-9aa-H9HA vaccinated mice were challenged with a lethal dose of cH9/1 PR8. All mice immunized with either rIBV-8aa-H9HA (Fig 3.5B left) or rIBV-9aa-H9HA survived lethal challenge 14 days post challenge and did not exhibit weight loss or any other clinical signs of disease (Fig 3.5B & C). In comparison, mice vaccinated with Ya88 WT B virus or PBS mock vaccinated showed significant weight loss almost immediately, became lethargic, and were sacrificed at 7 days post challenge per IACUC regulations regarding weight loss. Taken together, these data suggest our approach to achieving attenuation through progressive introduction of IBV amino acids into IAV HA can produce recombinant IBVs capable of protecting mice from onset of disease and lethal challenge.

Discussion

We developed a panel of recombinant IBVs which expressed the ectodomain of IAV (either H7 or H9) HA and progressively introduced IBV HA N-terminal amino acids into the linker region of the IAV HA TM region (Figure 3.1). Against the WT Ya88 controls, we achieved significantly reduced peak and endpoint titers for rIBV-H9HA-9aa & 8aa equal to or exceeding 1 log in vitro. rIBV H7 5aa-8aa virus replication was similar Ya88 control virus replication. We were unable to rescue rIBV H7 9aa viruses. Vaccination of mice with any dose of rIBV-H9HA-9aa & 8aa did not have significant weight loss effects on the mice, though pulmonary replication with the highest dose was not statistically different at 3 or 6 dpi. 3 weeks post vaccination, mice exhibited statistically higher IAV H9HA specific antibody titers when vaccinated with rIBVs vs IBV controls, and these antibodies could neutralize cH9/PR8 IAV infection in vitro. Finally, vaccination with rIBV-H9HA-9aa & 8aa were able to fully protect mice from lethal challenge with cH9/PR8 IAV and eliminated day 6 lung cH9/PR8 IAV replication.

In the United States, current generation LAIVs are generated via co-infection and reassortment of internal gene segments from a master donor virus (MDV), A/Ann Arbor/6/60, and seed virus harboring HA & NA segments based on recommendations from the CDC and other global surveillance agencies' annual influenza surveillance. Current evidence suggests the majority of theoretical reassorted vaccine viruses do not achieve wild type replication levels (51), nonetheless the possibility that reassortment could restore or exacerbate virulence of vaccine viruses and result in exposure of a naive population to a pathogenic virus possess a consistent safety challenge in the design of future live virus vaccines. Interestingly, IAV HA can functionally substitute for IBV HA, however no reassortments between IAV or IBV have ever been detected in

nature or laboratory conditions, in part because IAV and IBV packaging sequences appear incompatible (52). Utilizing this observation, introducing the IAV HA ectodomain into the Ya88 genetic background led to the development of candidate vaccine viruses that were incapable of reassortment with circulating IAVs as was done with previous approaches (47). To improve upon previous LAIV designs and negate potential effects on virulence from reassortment with circulating IBVs, we attenuated these viruses by progressive introduction of IBV C-terminal amino acids into the putative transmembrane (TM) linker region of H7 and H9 HA coding regions and selecting for the most attenuated of a panel of candidates. Thus, because the attenuation is built into HA segment, reassortment with 7 other segments would most likely not increase the virulence of our viruses. In additional to reassortment with circulating strains, interference between A and B viruses also possess a potential concern to the efficacy and effectiveness of current generation vaccines. IAV and IBV are known to interfere with each other's replication (53, 54), which has spurred concerns that because both the trivalent and quadrivalent formulations contain both types of seasonal influenza virus, interference could result in decreased vaccine effectiveness, even though available evidence has yet to support this (reviewed in (55)). Because our LAIV design utilizes IBV as its genetic background, our design could be introduced with current IBV vaccine formulations without the concern that intertypic interference would occur. Finally, current generation LAIVs produced in mass via chicken egg propagation require multiple passages at specific temperatures to adapt them for large scale growth and to attenuate them for safety purposes. Growth under these conditions therefore limits the speed of production and additionally can introduce mutations required for egg growth into HA that alters its antigenic properties (56, 57), making it potentially less effective in eliciting the proper immune response

against the circulating strain. Our attenuation method would not require cold adaptation and would also be less likely to introduce mutations into any segment in general as IBV overall has a lower mutation rate than IAV (58).

While sequencing of the virally infected cells (data not shown) confirmed our mutations were present and maintained during replication, plaque sizes in vitro for both H7 and H9 rIBVs were both inconsistent in contrasts to previous studies (47). One possible explanation for this is that mutations outside of HA were potentially introduced. If so, further analysis of mutations in other viral segments may be warranted. We also noted that while pulmonary replication of the challenging IAV was significantly reduced compared to mock controls, vaccine rIBV H9HA pulmonary replication was similar to the Ya88 IBV control replication. The previous study which utilized a chimeric IAV/IBV HA segment similar to ours showed lower pulmonary replication of the vaccine strain compared to the IBV control. It should be noted that the replication level seen in our study did not exceed the total PFU dose administered during vaccination, suggesting these viruses were still attenuated and did not exceed WT Ya88 IBV replication. There are at least three potential different and possibly compounding explanations for this level of pulmonary replication. First, these results could reflect mouse genetic background response differences between the two studies, as Hai et al. utilized BALB/c mice while we utilized C57BL/6J mice. Second Hai et al used NS1 truncation to attenuate their virus candidates. Because NS1 acts as an interferon antagonist, complete loss of functional NS1 could result in more severe in vivo attenuation then our system, as our chimeric viruses still possess a fully functional NS1coding sequence. While NS1 could be truncated to match the original studies In-vivo attenuation, reassortment with circulating IBV would negate this potential benefit thus justifying the consolidation of attenuation

into the HA segment. Third, Hai et al originally used H5HA for its study design while we focused on H7 and H9 variants. While from the same type of influenza virus, these two HA protein sequences share only 50% sequence identity, and this variability in protein sequence could lead to dramatically different structure and tolerance to introduction of foreign IBV sequence. As a result, further analysis of structural changes made to HA in response to mutations in the transmembrane anchor region could lead to further insight that would direct subsequent HA attenuations approaches.

In summary, we have successfully developed a methodology to attenuate reassortment incompetent rIBVs though incremental, progressive introduction of IBV coding sequences into the IAV ectodomain. These viruses could elicit specific neutralizing antibodies against their target IAV virus, and could protect mice from lethal challenge. While these results are promising as a proof of concept for our attenuation technique, vaccine virus replication in the lungs demands further analysis of pulmonary pathology to ensure full safety requirements are met prior to proceeding to higher level vaccine trials.

Materials and Methods

Cells and viruses. Human embryonic kidney 293T (HEK293T) and Madin-Darby canine kidney (MDCK) cells were maintained in Dulbecco's modified Eagle's medium (DMED, Genesee Scientific, San Diego, Ca) and minimal essential media (MEM, GE Healthcare Life Sciences, Logan, Utah) respectively, supplemented with 10% fetal bovine serum (Gibco, Carlsbad, CA) and 1% penicillin-streptomycin (Hyclone, Logan, Utah), 0.35% bovine serum albumin (BSA, Proliant Biologicals, Boone, IA), 2mM L-glutamine (Genesee Scientific, San Diego, Ca), 0.15% $NaHCO_3$, and 2 mM HEPES.
All viruses used in these experiments were propagated in pathogen free embryonated chicken eggs (Charles River Laboratories Inc). 10-day-old embryonated chicken eggs were inoculated with IBV or IAV for 3 days at 33°C or 2 days at 37°C respectively (48).

Construction of plasmids. The reverse genetics plasmids used for generating rIBVs were constructed as previously described (48). The plasmids encoding the chimeric A/B HAs were derivatives of the corresponding wild-type (WT) A/HA segment. Briefly, the chimeric pDZ-B/VN HA was constructed by swapping the A/H7N9 or A/H9N2/WF10/99 hemagglutinin (without a polybasic cleavage site) into the B/HA sequence using site directed mutagenesis (47). Progressive single amino acid additions from B/HA were introduced by overlapping PCR into the membrane anchor region (MAR) of the A/HA ectodomain (Figure 3.1A).

Rescue of recombinant chimeric IBV. Rescue of influenza B viruses from plasmid DNA was performed as previously described (48, 49). Briefly, 293T cells were co-

cultured with MDCK cells and transfected with 1ug of each of the eight plasmids using Lipofectamine 2000 (Invitrogen, Carlsbad, CA). At 12h post transfection, cell media was replaced with DMEM containing 0.35% bovine serum albumin, 10mM HEPES, and 1ug/ml TPCK (L-1-tosylamide-2-phenylethyl chloromethyl ketone) – treated trypsin. At three days post transfection, virus containing cell culture supernatants were collected and inoculated into 10-day-old pathogen free embryonated chicken eggs. Allantoic fluid was harvested after 3 days of incubation at 33°C and assayed for the presence of virus by plaque formation in MDCK cells by standard plaque assay.

Multi-step virus replication assay. To analyze viral replication, confluent MDCK cells were grown in MEM supplemented with 10% FBS. Cells were infected the next day at a multiplicity of infection (MOI) of 0.05 and incubated at 33°C in minimal essential medium (MEM) containing 0.3% BSA and 1.0-µg/ml TPCK-treated trypsin. Supernatants were taken at 10, 36, 48, and 72 hours post infection (hpi). Viral titers in supernatants were determined by standard plaque assay on MDCK cells.

Mouse immunizations and challenge. Six-eight-week-old female C57BL/6J mice (Jackson Laboratory) were anesthetized with Isoflurane administered by inhalation and infected intranasally (IN) with 10-fold serial dilutions of different rIBVs (in 50-ul volumes) diluted in PBS/BSA/PS. Survival and body weight loss were monitored for 14 days post-vaccination or challenge. Blood samples were taken via retro-orbital bleeding at 21 days post vaccination (dpv) to monitor for IgG responses. Blood samples were centrifuged and seras were frozen at -80°C until use. Mice were subsequently challenged 21 days post vaccination with $5x10^6$ PFU/mouse of influenza A/cH9/1 PR8 virus.

To determine pulmonary virus titers, mice were vaccinated as above and were euthanized at 3 or 6 days post vaccination or challenge with various concentration of rIBVs or $5x10^5$ PFU of influenza A/cH9/1 PR8 virus respectively. Mice were euthanized by CO2 and lungs extracted and homogenized in 1 ml sterile PBS containing 0.35% BSA. Samples were centrifuged, and lysates were stored at -80°C until use. Viral titers from lung lysates were evaluated on MDCK cells.

All animal procedures performed in this study were in accordance with Institutional Animal Care and Use Committee (IACUC) guidelines and have been approved by the IACUC of the University of California, Riverside.

Enzyme linked immunosorbent assays (ELISA) and Microneutralization Assays. To assess the levels of virus-specific antibodies present in immunized mice, ELISAs were performed on diluted serum samples as described (48). In brief, serum samples were obtained directly before viral challenge 21 days post vaccination and stored at -80°C. 96 well MaxiSorp ELISA plates (Thermo Fisher Scientific, #442404, Rochester, NY) were coated with 50ul of 10ug/ml purified A/cH9/1 PR8 virions. After virus treatment, wells were blocked at room-temp with PBS containing 1% dried milk and 0.1% Tween 20 (blocking buffer) for 2hrs, washed with PBS/0.1% Tween 20, and subsequently incubated with serum samples diluted in blocking buffer. After 2hr room-temp incubations, plates were washes with PBS containing 0.1% Tween 20 (wash buffer) and incubated with secondary anti-mouse horse radish peroxidase conjugated (Millipore, AP503P, Temecula, Ca) IgGγ for 30min at room-temp. Plates were washed and incubated with colorimetric substrate (o-phenylenediamine dihydrochloride, Invitrogen,

Carlsbad, CA) for 30min and read with plate reader measuring optical density at 450 nm (OD450).

To assess levels of neutralizing antibody against the challenge virus, we performed microneutralization assays as described (50). Briefly, $6x10^4$ MDCK cells were plated in 96well plates in MEM supplemented with 10% FBS. 24hrs after plating, 2000 PFU of cH9/1 N1 PR8 virus was incubated with serum samples diluted in PBS containing 0.35% BSA for 1hr at 37°C. Virus-serum mixtures (100ul) were added to MDCK cells (MOI=0.003) and incubated at 37°C for 1hr, then washed with PBS. Cells were then incubated overnight at 37°C in MEM containing 0.35% BSA, 2mM L-glutamine, 0.15% $NaHCO_3$, and 2 mM Hepes. 24 hours post infection (hpi), cells were fixed with 20% Methanol for 20min at 4°C and washed with PBS. Cells were blocked at room-temp with PBS containing 1% dried milk and 0.1% Tween 20 (blocking buffer) for 1hr and subsequently incubated with Pan IAV M2 antibody diluted in blocking buffer. After 1hr room-temp incubations, plates were washes with wash buffer and incubated with secondary anti-mouse horse radish peroxidase conjugated antibody (Millipore, Temecula, CA) IgGγ for 30min at room-temp. Plates were washed and then incubated with colorimetric substrate (o-phenylenediamine dihydrochloride, Invitrogen, Carlsbad, CA) for 30min and read with plate reader measuring optical density at 450 nm (OD450). Statistical Analysis. Statistics were calculated using Graphpad Prism 9.0.

Reference

1 Jain, S. et al. Hospitalized Patients with 2009 H1N1 Influenza in the United States, April-June 2009. New Engl J Med 361, 1935-1944, doi:10.1056/NEJMoa0906695 (2009).

2 Thompson, W. W. et al. Influenza-associated hospitalizations in the United States. Jama-J Am Med Assoc 292, 1333-1340, doi:DOI 10.1001/jama.292.11.1333 (2004).

3 Simonsen, L., Fukuda, K., Schonberger, L. B. & Cox, N. J. The impact of influenza epidemics on hospitalizations. J Infect Dis 181, 831-837, doi:Doi 10.1086/315320 (2000).

4 Morens, D. M., Taubenberger, J. K. & Fauci, A. S. Predominant role of bacterial pneumonia as a cause of death in pandemic influenza: Implications for pandemic influenza preparedness. J Infect Dis 198, 962-970, doi:10.1086/591708 (2008).

5 Gill, J. R. et al. Pulmonary Pathologic Findings of Fatal 2009 Pandemic Influenza A/H1N1 Viral Infections. Arch Pathol Lab Med 134, 235-243 (2010).

6 Kalil, A. C. & Thomas, P. G. Influenza virus-related critical illness: pathophysiology and epidemiology. Crit Care 23, doi:ARTN 258 10.1186/s13054-019-2539-x (2019).

7 World Health Organization Influenza Seasonal Factsheet 2018. (2018).

8 Johnson, N. P. A. S. & Mueller, J. Updating the accounts: global mortality of the 1918-1920 "Spanish" influenza pandemic. B Hist Med 76, 105-115, doi:DOI 10.1353/bhm.2002.0022 (2002).

9 Huang, Y. W. et al. Human infection with an avian influenza A (H9N2) virus in the middle region of China. J Med Virol 87, 1641-1648, doi:10.1002/jmv.24231 (2015).

10 Liu, R. C. et al. Clinical and epidemiological characteristics of a young child infected with avian influenza A (H9N2) virus in China. J Int Med Res 46, 3462-3467, doi:10.1177/0300060518779959 (2018).

11 Guo, Y., Li, J. & Cheng, X. [Discovery of men infected by avian influenza A (H9N2) virus]. Zhonghua Shi Yan He Lin Chuang Bing Du Xue Za Zhi 13, 105-108 (1999).

12 Ali, M. et al. Avian Influenza A(H9N2) Virus in Poultry Worker, Pakistan, 2015. Emerg Infect Dis 25, 136-139, doi:10.3201/eid2501.180618 (2019).

13 Gou, Y., Xie, J. & Wang, M. [A strain of influenza A H9N2 virus repeatedly isolated from human population in China]. Zhonghua Shi Yan He Lin Chuang Bing Du Xue Za Zhi 14, 209-212 (2000).

14 Xu, J. N. et al. Human infection with a further evolved avian H9N2 influenza A virus in Sichuan, China. Sci China Life Sci 61, 604-606, doi:10.1007/s11427-017-9150-8 (2018).

15 Yuan, J. et al. Full-length genome analysis of an avian influenza A virus (H9N2) from a human infection in Changsha City. Future Virol 13, 323-330, doi:10.2217/fvl-2017-0151 (2018).

16 Yuan, R. Y. et al. Human infection with an avian influenza A/H9N2 virus in Guangdong in 2016. J Infection 74, 422-425, doi:10.1016/j.jinf.2017.01.003 (2017).

17 Pan, Y. et al. Human infection with H9N2 avian influenza in northern China. Clin Microbiol Infec 24, 321-323, doi:10.1016/j.cmi.2017.10.026 (2018).

18 Peacock, T. H. P., James, J., Sealy, J. E. & Iqbal, M. A Global Perspective on H9N2 Avian Influenza Virus. Viruses 11, doi:10.3390/v11070620 (2019).

19 J. He, L. N. a. Y. T. Origins and evolutionary genomics of the novel 2013 avian-origin H7N9 influenza A virus in China: early findings. ArXiv 1304 (2013).

20 H7N9 Situation Update. Food and Agriculture Organization of the United Nations. (2019).

21 Shanmuganatham, K. K. et al. The replication of Bangladeshi H9N2 avian influenza viruses carrying genes from H7N3 in mammals. Emerg Microbes Infect 5, e35, doi:10.1038/emi.2016.29 (2016).

22 Wan, H. et al. Replication and transmission of H9N2 influenza viruses in ferrets: evaluation of pandemic potential. Plos One 3, e2923, doi:10.1371/journal.pone.0002923 (2008).

23 Group, S. H. W. Assessing the fitness of distinct clades of influenza A (H9N2) viruses. Emerg Microbes Infect 2, e75, doi:10.1038/emi.2013.75 (2013).

24 Belser, J. A. et al. Pathogenesis and transmission of avian influenza A (H7N9) virus in ferrets and mice. Nature 501, 556-559, doi:10.1038/nature12391 (2013).

25 Richard, M. et al. Limited airborne transmission of H7N9 influenza A virus between ferrets. Nature 501, 560-+, doi:10.1038/nature12476 (2013).

26 Watanabe, T. et al. Characterization of H7N9 influenza A viruses isolated from humans. Nature 501, 551-+, doi:10.1038/nature12392 (2013).

27 Xu, L. L. et al. Novel Avian-Origin Human Influenza A(H7N9) Can Be Transmitted Between Ferrets via Respiratory Droplets. J Infect Dis 209, 551-556, doi:10.1093/infdis/jit474 (2014).

28 Zhang, Q. Y. et al. H7N9 Influenza Viruses Are Transmissible in Ferrets by Respiratory Droplet. Science 341, 410-414, doi:10.1126/science.1240532 (2013).

29 Nichol, K. L. The efficacy, effectiveness and cost-effectiveness of inactivated influenza virus vaccines. Vaccine 21, 1769-1775, doi:10.1016/S0264-410x(03)00070-7 (2003).

30 Weycker, D. et al. Population-wide benefits of routine vaccination of children against influenza. Vaccine 23, 1284-1293, doi:10.1016/j.vaccine.2004.08.044 (2005).

31 Nichol, K. L. Cost-benefit analysis of a strategy to vaccinate healthy working adults against influenza. Arch Intern Med 161, 749-759, doi:DOI 10.1001/archinte.161.5.749 (2001).

32 Cohen, G. M. & Nettleman, M. D. Economic impact of influenza vaccination in preschool children. Pediatrics 106, 973-976, doi:DOI 10.1542/peds.106.5.973 (2000).

33 Thommes, E. W., Ismaila, A., Chit, A., Meier, G. & Bauch, C. T. Cost-effectiveness evaluation of quadrivalent influenza vaccines for seasonal influenza prevention: a dynamic modeling study of Canada and the United Kingdom. Bmc Infect Dis 15, doi:ARTN 46510.1186/s12879-015-1193-4 (2015).

34 Ting, E. E. K., Sander, B. & Ungar, W. J. Systematic review of the cost-effectiveness of influenza immunization programs. Vaccine 35, 1828-1843, doi:10.1016/j.vaccine.2017.02.044 (2017).

35 Hodgson, D. et al. Effect of mass paediatric influenza vaccination on existing influenza vaccination programmes in England and Wales: a modelling and cost-effectiveness analysis. Lancet Public Health 2, E74-E81, doi:10.1016/S2468-2667(16)30044-5 (2017).

36 Imai, C. et al. A systematic review and meta-analysis of the direct epidemiological and economic effects of seasonal influenza vaccination on healthcare workers. Plos One 13, doi:ARTN e019868510.1371/journal.pone.0198685 (2018).

37 Xu, J. et al. Cost-effectiveness of seasonal inactivated influenza vaccination among pregnant women. Vaccine 34, 3149-3155, doi:10.1016/j.vaccine.2016.04.057 (2016).

38 O'Reilly, D. J. et al. Economic analysis of pharmacist-administered influenza vaccines in Ontario, Canada. Clinicoeconomic Outc 10, 655-663, doi:10.2147/Ceor.S167500 (2018).

39 D'Angiolella, L. S. et al. Costs and effectiveness of influenza vaccination: a systematic review. Ann I Super Sanita 54, 49-57, doi:10.4415/Ann_18_01_10 (2018).

40 Ambrose, C. S., Wu, X., Jones, T. & Mallory, R. M. The role of nasal IgA in children vaccinated with live attenuated influenza vaccine. Vaccine 30, 6794-6801, doi:10.1016/j.vaccine.2012.09.018 (2012).

41 Barria, M. I. et al. Localized mucosal response to intranasal live attenuated influenza vaccine in adults. J Infect Dis 207, 115-124, doi:10.1093/infdis/jis641 (2013).

42 Lewis, K. D. C. et al. Immunogenicity and Viral Shedding of Russian-Backbone, Seasonal, Trivalent, Live, Attenuated Influenza Vaccine in a Phase II, Randomized, Placebo-Controlled Trial Among Preschool-Aged Children in Urban Bangladesh. Clin Infect Dis 69, 777-785, doi:10.1093/cid/ciy1003 (2019).

43 Aljurayyan, A. et al. Activation and Induction of Antigen-Specific T Follicular Helper Cells Play a Critical Role in Live-Attenuated Influenza Vaccine-Induced Human Mucosal Anti-influenza Antibody Response. J Virol 92, doi:10.1128/JVI.00114-18 (2018).

44 Petukhova, G. et al. B- and T-cell memory elicited by a seasonal live attenuated reassortant influenza vaccine: assessment of local antibody avidity and virus-specific memory T-cells using trogocytosis-based method. Influenza Other Respir Viruses 6, 119-126, doi:10.1111/j.1750-2659.2011.00279.x (2012).

45 Pizzolla, A. et al. Nasal-associated lymphoid tissues (NALTs) support the recall but not priming of influenza virus-specific cytotoxic T cells. P Natl Acad Sci USA 114, 5225-5230, doi:10.1073/pnas.1620194114 (2017).

46 Maassab, H. F. Adaptation and Growth Characteristics of Influenza Virus at 25 Degrees C. Nature 213, 612-&, doi:DOI 10.1038/213612a0 (1967).

47 Hai, R., Garcia-Sastre, A., Swayne, D. E. & Palese, P. A Reassortment-Incompetent Live Attenuated Influenza Virus Vaccine for Protection against Pandemic Virus Strains. Journal of Virology 85, 6832-6843, doi:10.1128/Jvi.00609-11 (2011).

48 Hai, R. et al. Influenza B Virus NS1-Truncated Mutants: Live-Attenuated Vaccine Approach. Journal of Virology 82, 10580-10590, doi:10.1128/Jvi.01213-08 (2008).

49 Fodor, E. et al. Rescue of influenza A virus from recombinant DNA. Journal of Virology 73, 9679-9682 (1999).

50 Tan, G. S. et al. Characterization of a Broadly Neutralizing Monoclonal Antibody That Targets the Fusion Domain of Group 2 Influenza A Virus Hemagglutinin. Journal of Virology 88, 13580-13592, doi:10.1128/Jvi.02289-14 (2014).

51 Parks, C. L. et al. Phenotypic properties resulting from directed gene segment reassortment between wild-type A/Sydney/5/97 influenza virus and the live attenuated vaccine strain. Virology 367, 275-287, doi:10.1016/j.virol.2007.05.004 (2007).

52 Baker, S. F. et al. Influenza A and B Virus Intertypic Reassortment through Compatible Viral Packaging Signals. Journal of Virology 88, 10778-10791, doi:10.1128/Jvi.01440-14 (2014).

53 Mikheeva, A. & Ghendon, Y. Z. Intrinsic Interference between Influenza a-Virus and B-Virus. Arch Virol 73, 287-294, doi:Doi 10.1007/Bf01318082 (1982).

54 Kaverin, N. V. et al. Studies on Heterotypic Interference between Influenza-a and Influenza-B Viruses - a Differential Inhibition of the Synthesis of Viral-Proteins and Rnas. Journal of General Virology 64, 2139-2146, doi:Doi 10.1099/0022-1317-64-10-2139 (1983).

55 Bandell, A., Woo, J. & Coelingh, K. Protective efficacy of live-attenuated influenza vaccine (multivalent, Ann Arbor strain): a literature review addressing interference. Expert Rev Vaccines 10, 1131-1141, doi:10.1586/Erv.11.73 (2011).

56 Skowronski, D. M. et al. Low 2012-13 Influenza Vaccine Effectiveness Associated with Mutation in the Egg-Adapted H3N2 Vaccine Strain Not Antigenic Drift in Circulating Viruses. Plos One 9, doi:ARTN e9215310.1371/journal.pone.0092153 (2014).

57 Zost, S. J. et al. Contemporary H3N2 influenza viruses have a glycosylation site that alters binding of antibodies elicited by egg-adapted vaccine strains. P Natl Acad Sci USA 114, 12578-12583, doi:10.1073/pnas.1712377114 (2017).

58 Nobusawa, E. & Sato, K. Comparison of the mutation rates of human influenza A and B viruses. Journal of Virology 80, 3675-3678, doi:10.1128/Jvi.80.7.3675-3678.2006 (2006).

Figures and Tables

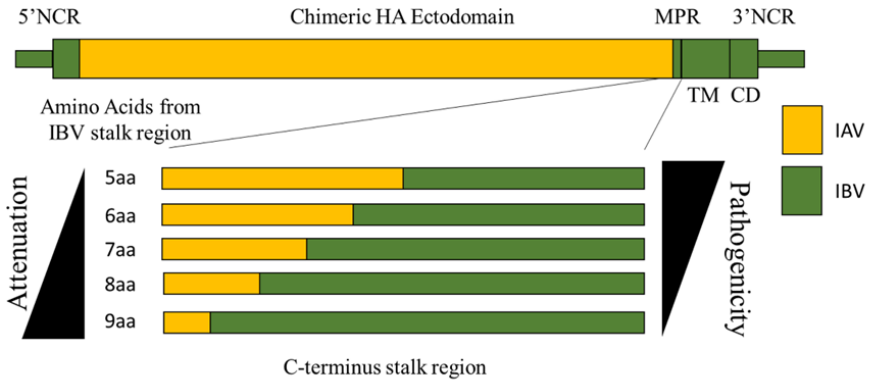

MPR = Membrane Proximal Region, NCR = Non-Coding Region, TM = Transmembrane Region, CD = Cytoplasmic Domain

Figure 3.1 Schematic design of HA gene attenuation by progressive introduction of IBV HA stalk amino acids into the IAV H9 ectodomain

MAR = Membrane anchor region, NCR = Non-coding region. Yellow is IAV sequence, green is IBV sequence

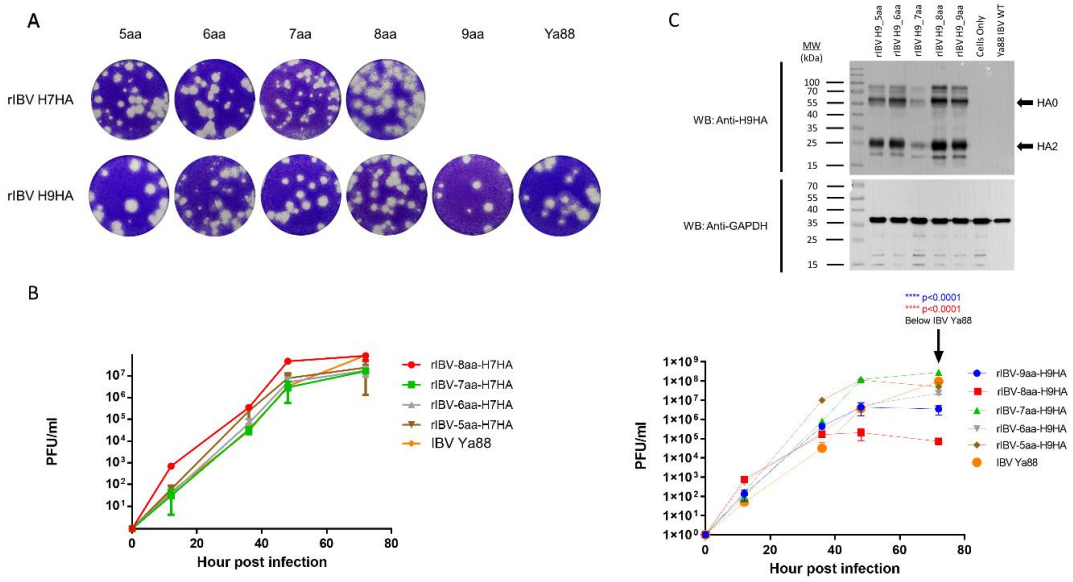

Figure 3.2 Characterization of recombinant chimeric influenza B/Yamagata/88 ex vivo. (A) Plaque size phenotype of the chimeric B viruses on MDCK cells (B) Multicycle growth curves of recombinant H7 (left) & H9 (right) viruses in MDCK cells infected at a MOI of 0.05 in triplicate and titrated by plaque assay on MDCK cells. The limit of detection was 50 PFU. (C) MDCK cells were infected with rIBVs or Ya88 WT IBV at an MOI of 0.1. Cells were harvested and lysed with SDS loading dye 24hr post infection and western blot for H9HA was performed.

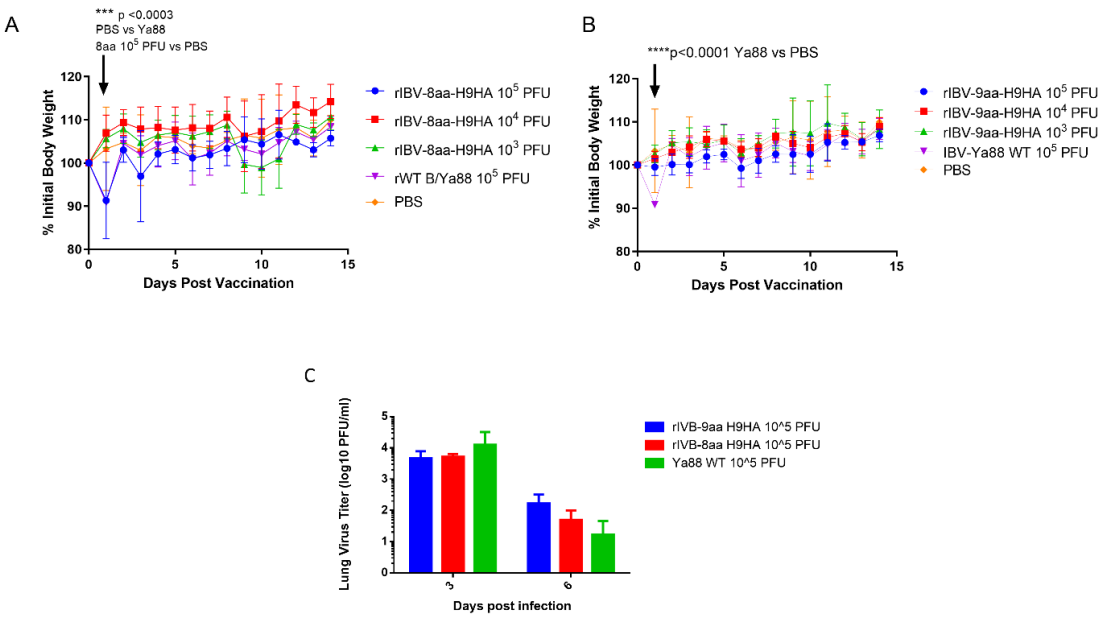

Figure 3.3 Characterization and pathogenicity of recombinant chimeric influenza B/Yamagata/88 in vivo.

Percent weight change following intranasal vaccination with 10-fold serial dilution of rIBV-8aa-H9HA (left)(A) or rIBV-9aa-H9HA (right)(B). (C) Pulmonary replication of recombinant viruses in mice. Average Lung titers and standard deviations are depicted. The limit of detection was 50 PFU.

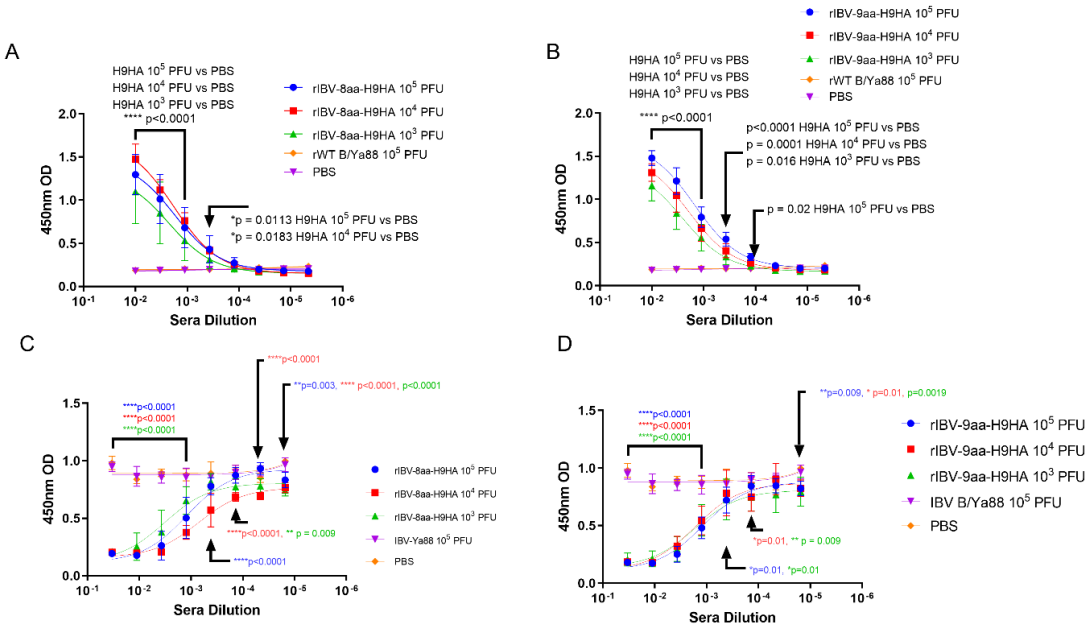

Figure 3.4 Mice immunized with chimeric viruses generate neutralizing influenza A virus specific antibodies.

Six-eight-week-old female C57BL/6J mice (n=5) were immunized with indicated viruses doses or PBS as negative controls. Serum samples were collected 21 days post vaccination. Serum IgG antibodies against A/H9 HA were detected by ELISA for rIBV-H9HA-8aa (A) or rIBV-H9HA-9aa (B) vaccinated groups. Significance was evaluated by two-way ANOVA using multiple comparisons. (B) Neutralization of A/H9/1 PR8 by serum IgG antibodies was detected by microneutralization assay and ELISA for rIBV-H9HA-8aa (C) or rIBV-H9HA-9aa (D) vaccinated groups. Significance was evaluated by two-way ANOVA using multiple comparisons. Indicated p-values represent comparisons to PBS control mice.

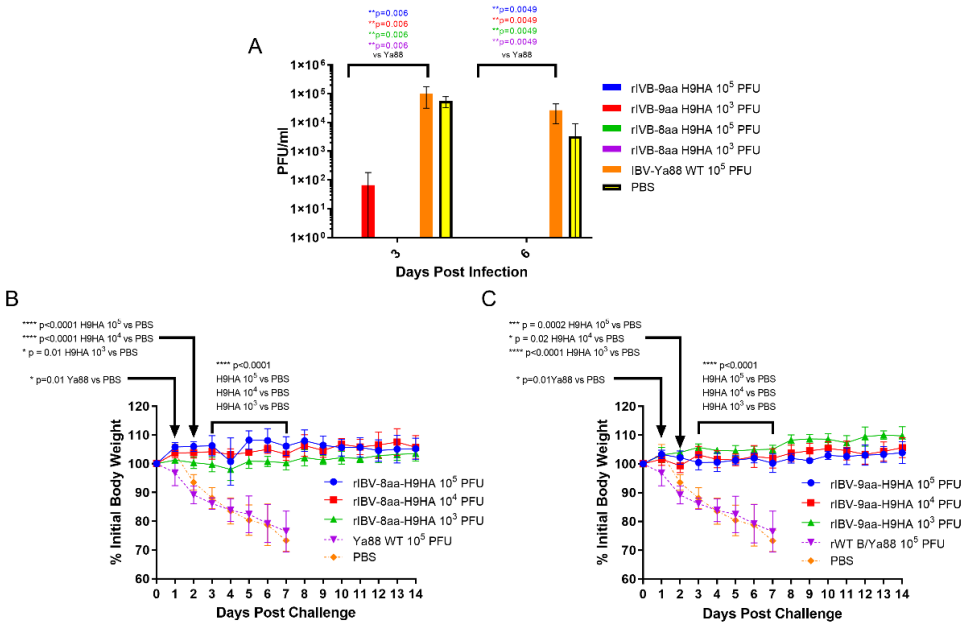

Figure 3.5 Vaccination with chimeric viruses protects c57BL/6J mice against lethal infection with influenza A virus cH9/1 PR8.

Six-eight-week-old female C57BL/6J mice (n=5) were immunized with indicated virus doses or PBS as negative controls. Mice were subsequently challenged with cH9/1 PR8 virus A) Infected mice were sacrificed and 3 & 6 days post challenge and whole lungs were extracted, homogenized, and tittered with standard plaque assays. Significant differences were determined by one-way ANOVA for each day, and p-values indicate differences to the Ya88 control group. (B&C) Six-eight-week-old female C57BL/6J mice (n=5) were immunized with indicated virus doses of rIBV-H9HA-8aa (B) and rIBV-H9HA-9aa (C) or PBS as negative controls. Mice were subsequently challenged with a lethal dose of cH9/1 PR8 virus and were monitored for body weight changes and survival 14 days post challenge. Significant differences were calculated by two-way ANOVA.

Chapter 3: Modeling the Effects of Cigarette Smoke Extract on Influenza B Virus Infections in Mice

Jerald Chavez, Wangyuan Yao, Harrison Dulin, Rong Hai.

Abstract

Influenza B virus (IBV) is a major respiratory viral pathogen. Due to a lack of pandemic potential for IBV, there is a lag in research on IBV pathology and immunological responses compared to IAV, including how certain environmental and lifestyle factors effect infection. Among them, cigarette smoking (CS) increases the risk and likelihood of worse disease outcomes caused by IAV infections. However, there is little to no information on how CS affects IBV infections, particularly in animal models. To this end, we developed an animal model system by pre-treating mice for two weeks with cigarette smoke extract (CSE), then infected them with IBV and monitored the resulting pathological, immunological, and virological effects. Our results reveal that the CSE treatment decreased IBV specific IgG levels yet did not change viral replication in the upper airway/the lung, and weight recovery post infection. However, higher concentrations of CSE did result in higher mortality post infection. Together, this suggests that CS induced inflammation coupled with IBV infection resulted in exacerbated disease outcome.

Introduction

Influenza virus infections cause seasonal epidemics that result in significant disease and economic burden (1). Between 2010-2020, estimated yearly symptomatic infections caused by Influenza viruses' range between 9-45 million cases, 140,000-710,000 hospitalizations, and between 12,000-52,000 deaths in the United States (2). Extending out to the global population, 290,000-650,000 die worldwide annually as a result of Influenza virus infections (3). Economically, these infections result in an estimated 2.8-5.0 billion dollars in medical costs in the United States alone as of 2017 (4), representing 0.014-0.03% of the US national GDP for that year (5). Therefore, to better prevent and treat influenza viral infection, it is imperative that we further examine any factors that could exacerbate disease outcomes.

Influenza viruses are negative sense, segmented, RNA enveloped viruses belonging to the Orthomyxoviridae family. There are 4 types: Influenza A virus (IAV), Influenza B virus (IBV), Influenza C virus (ICV), and Influenza D virus (IDV). Type A-C all infect humans, however IAV and IBV are primarily responsible for seasonal epidemics. Between 2000-2020, IAV remained the dominant seasonal influenza virus type in the United States (Table 4.1) (6-24). Historically, IAV has dominated research efforts and understanding of IBV has lagged behind. This stagnation in research likely stems from IBV not having caused a known human pandemic and being less immune divergent, with only two lineages rather than multiple subtypes like IAVs, and therefore not assessed as a priority. However, this gap in IBV research should be filled since IBV is also a known public health concern. For example, IBV accounted for significant percentages of known cases in the United States, as high as 45% in certain years (Table 4.1). Of the

aforementioned 2.8-5 billion dollar medical cost estimate in 2017, IBV infections accounted for 37% of that total (4). Outside of the United States, IBV has achieved dominant status over IAV in Europe in some years (25). Additionally, IBV can adversely affect specific vulnerable populations. In pediatric cases for example, IBV infection can be more virulent compared to adult cases (26). Despite these sizable economic and disease burdens, IBV remains relatively understudied compared to IAV. With awareness of the impact of IBV, the field has begun to increase efforts for IBV. As evidence, both lineages of IBV have been included in seasonal Flu vaccines, dubbed the quadrivalent Flu vaccine, since 2012 in US. However, it remains largely unknown what is the impact of respiratory related lifestyle factors, such as cigarette smoking, on IBV infection, and its associated co-morbidities.

Cigarette smoking also represents a medical and environmental factor known to damage respiratory tissues. Thus, it is likely to exacerbate IBV infection and disease outcomes. Cigarette smoking (CS) results in an estimated 480,000 deaths in the United States each year, representing approximately 6.8% of the annual cigarette related deaths worldwide (27). CS is known to increase the risk and/or be causative of a number of chronic diseases, including, but not limited to: heart disease, multiple types of cancer, diabetes, and chronic obstructive pulmonary disease (COPD) (28). Smoking is also an established risk factor for infectious disease, including pulmonary bacterial infections like pneumonia (29, 30), Tuberculosis (31-34), acute respiratory tract infections in children exposed to environmental cigarette smoke (dubbed secondhand smoke) (35), and viral infections like Human papillomavirus (HPV) infections (36) and Influenza A virus infection (37-39).

Besides the risk, CS is also known to increase the severity of IAV disease in patients (37). Similarly, cigarette smoke has been shown to decrease weight gain (slow recovery) (40-43) and increase both lung remodeling (44) and mortality in animal models of IAV infection (41-43, 45, 46). Interestingly, multiple studies have reported that animal models of cigarette smoking do not exhibit higher viral titers than non-smoking controls post infection (41, 45-47), suggesting that worse disease outcomes are likely not due to changes in the viral replication. However, CS does appear to alter pro-inflammatory cytokine profile responses to IAV infection. Specifically, CS exposure in mice greater than two weeks appears to result in higher levels of pulmonary pro-inflammatory cytokines including (but not limited to) TNF-α, IFN-γ, IL-6, IL-12, IL-23, IL-1, IL-5, IL-10, KC, MIP-1a, IL-17, and IL-1B (42-44, 46, 48). The favorable explanation is that this increased pro-inflammatory response could give rise to exacerbation of pulmonary inflammation post infection, resulting in greater damage and slower recovery (40, 43, 44, 46, 47, 49).

Surprisingly however, to our knowledge, there is very little information regarding how cigarette smoking affects IBV infections and disease outcomes specifically. Lacking pathological, virological, and immunological profiling of smoking effects on IBV infection could result in severe lag-time between treatment, development and deployment, especially in sever epidemics or situations when IBV is of particular concern. To this point, we know secondhand smoke has been shown to result in not only higher incidents of infection, but also hospitalization in infants and children (50-52), and because IBV infection can be severe in children, it is critical we further investigate the role of CS in IBV infection. To this end, it is critical to establish an experimental model of how

cigarette smoke affects the pathology, virology, immunology, and disease outcomes from IBV infection in mice.

Here, we developed an animal model system to better understand how aspects of CS may affect IBV infections by treating mice for two weeks with liquid cigarette smoke extract, then infecting them with IBV. Our results showed that exposure to cigarette smoke extract (CSE) decreased IBV specific antibodies but oddly did not compromise their neutralization potency for IBV. Similar to previous studies in IAV, we also did not observe an impact of CSE on virus replication, and associated disease. Intriguingly, we observed about a 2-fold increase in IBV specific activated splenocytes from animal exposed to CSE versus the control animals. Additionally, we observed a dose dependent effect of increasing concentrations of CSE on mortality in mice. These data represent the first information regarding the pathological and immunological effects of water-soluble components of CS on IBV infection in vivo and suggested that there is a negative impact on IBV disease outcome. Our studies provide an experimental platform to further dissect the impact of CSE on IBV infection. The results support the guiding of better administrative policy making.

Results

CSE did not affect IBV replication in A549 cells. Duffney et al. has previously shown that there was more WSN (A/WS/1933 H1N1) IAV infectivity in human airway epithelial cells exposed to cigarette smoke compared to the control cells (55). To evaluate whether there is a similar impact in human lung cells exposed to the water-soluble components of CS on IBV infection, we treated A549 cells with either PBS (mock), 1x CSE, or 2.5x CSE for 24hr, then infected with Influenza B/Victoria/2/87. We noted that 24 hours post CSE treatment, 1x CSE and mock control cells appeared to have similar morphology (Figure 1A). However, 2.5x CSE treated cells appeared to cease proliferation, likely due to toxicity from high dose CSE. Yet, these cells were still attached to the plate (Figure 4.1A). Post infection, 1x CSE did not appear to increase or decrease virus replication, but 2.5x CSE did appear to significantly decrease viral titers 24 hours post infection (hpi) (Figure 4.1B). However, it is likely that lower viral titers were due to either a cessation of proliferation or cell death due to CSE toxicity.

Low dose of CSE did not exacerbate IBV infection. To examine the pathological effects of cigarette smoke on IBV infection in vivo, we intranasally inoculated 6-8 week old female BALB/cJ mice with 1x CSE for two weeks, 6 days/week (Figure 4.2A). For this period of treatment, 1x CSE exposure did not affect the weights over a two-week period (Figure 4.2B). Furthermore, 1x CSE exposure did not substantially increase pathological damage in the lungs of mice compared to PBS control mice (Figure 1G, Top). Subsequently, we infected these mice with $1X10^3$, $1X10^4$, or $1X10^5$ PFU/mouse of IBV (Influenza B/Victoria/2/87). We observed mice body weight changes for 14 days

post infection. We found that 1x CSE exposure did not increase weight loss during this two-week period post infection, regardless of the dose of IBV compared to PBS control mice (Figure 4.2C & 2E), nor did 1x CSE exposure have any effect on mortality among different groups of mice (Figure 4.2D & 2F). Finally, lung histology on tissue from three days post infection indicated immunocyte infiltration only in infected samples with or without CSE treatment. However, the phenomenon was not observed in samples from CSE treatment alone (Figure 4.2G, Bottom). This suggests that our current CSE dose is not high enough to mimic the natural smoking conditions.

We next assessed the potential impact of CSE on the viral pulmonary replication and immunological responses post IBV infection. We treated mice with 1x CSE and infected as described in earlier sections (Figure 4.3A). We observed that with both low and high doses of IBV, 1x CSE exposure did not affect the amount of virus detected in the lungs from mice at 3 & 6 days post infection (dpi) (Figure 4.3B & 3C) compared to control PBS groups. Similarly, we did not find any difference between 1x CSE and PBS viral titers in the upper respiratory fluid 3 or 6 dpi (Figure 4.2D). Also, we found that 1x CSE treatment did not have a significant impact on pro-inflammatory cytokine gene expression 3 dpi (Figure 4.2H).

Because smoking has been shown to alter innate and adaptive immune responses post IAV infection in some reports (42-44, 56), we went further to determine whether CSE exposure influences the host immune responses after IBV infection. Here, we examined both cellular and humoral responses through evaluating IFN-γ production from the IBV specific splenocytes, IBV specific IgA level from nasal lavage samples, and IBV specific IgG levels from sera samples (Figure 4.4A). Even though we observed significantly higher IFN-γ production from splenocytes of CSE mice versus those of PBS

control animals (Figure 4.4B), we did not observe a discernable difference in PBS vs CSE treated animal in their IgA (Figure 4.4C) or IgG (Figure 4.4D) titers at 21dpi. Furthermore, we evaluated the potency of those IBV specific IgGs by microneutralization assays. Similarly, we did not detect significant difference between CSE or PBS treatment groups (Figure 4.4E). To evaluate whether our observation is independent of IBV dose usage, we repeated the experiments with a higher dose infection at 1x105 PFU/mouse. Similarly, we found that neither IgG (Figure 4.5A) nor neutralization titers (Figure 4.5B) differed between CSE or PBS groups. Collectively, our results suggest that early cellular immune responses are elevated in CSE mice, but mucosal and humoral immunity by later stages post infection have equalized. However, this is likely due to the low dose of CSE used here in these studies. At three days post infection, lung histology indicated cell infiltration only in infected samples regardless of CSE treatment, which was not observed in samples from CSE treatment alone (Figure 2G, Bottom). This suggests a likely caveat that our current CSE dose is not high enough to mimic the natural smoking conditions.

Increasing concentration of CSE reduces survival of mice post IBV infection. Smoking commonly varies among people, typically between 1 cigarette to multiple packs a day (https://www.lung.org/research/trends-in-lung-disease/tobacco-trends-brief/overall-tobacco-trends). To better mimic the physiologic condition, but more importantly to mimic the heavy smoking conditions, we further tested higher dose of CSE on IBV pathology, disease outcome, and immune responses. To this end, we first treated mice as described in Figure 6A with increasing amount of CSE. We observed that mice exhibited similar weight changes among different groups during the two-week CSE treatment

period. The result suggested that increasing concentrations of CSE did not have an overwhelming impact on mice with up to 14 days treatment resulting in no significant effect of weight changes (Figure 4.6B). Following the same amount (10^5 PFU) of IBV infection, based on the weight records for surviving animals, we did not find significant differences in weight between our CSE treatment groups and the PBS mock treatment group (Figure 4.6C). However, from our survival data, we observed that the survival rate was inversely correlated with the amount of CSE used (Figure 4.6D). To further assess impact of high dose CSE on humoral responses, we tested IgA levels of nasal wash samples (mucosal) and IgG level of sera samples (systematic). Intriguingly, we observed a significant decrease in IBV specific IgA titers only for the undiluted samples (Figure 4.6E) and a more profound significant decrease in IBV specific IgG titers up to around 900-fold of dilutions of original sera (Figure 4.6F). On the contrary, we did not observe a difference in IgG neutralizing titers for IBV (Figure 4.6G) between CSE treated animals and PBS controlled animals. Furthermore, with increasing amounts of CSE used, we observed a decrease in survival following the subsequent IBV infection. This fact revealed the direct negative impact of CSE on the following influenza B infection. Overall, we established a smoking model system for IBV using water-soluble components of CS. We found that the treatment negatively affected IBV infection outcomes and dampened host immune responses. The results validate that our smoking system mimics natural smoking behavior. Together, we provided a valuable resource to further understand the impact of CS on IBV vaccination and even the co-infection of IBV and IAV.

Discussion

Cigarette smoking increases the risk of IAV infection and exacerbates negative health outcomes, increasing both time to recover and mortality. However, there is very little data on how cigarette smoking affects IBV infection, disease and to what degree. To this end, we developed a in vivo smoking model to study the pathological, immunological, and viral effects cigarette smoking may have on IBV infections. This was accomplished by pre-treating mice for two weeks with various concentrations of CSE, then infecting them with IBV and monitoring morbidity, mortality, lung inflammation, viral pulmonary and upper airway replication, and IBV specific serum and mucosal antibody levels. Ex vivo, IBV viral replication is not altered by 1x CSE treatment in A549 cells. In vivo, weight loss and mortality post IBV infection were not affected by 1x CSE regardless of the IBV dose compared to PBS control mice. Similarly, IgA, IgG, and neutralizing IgG levels were all similar in 1x CSE and PBS mock controls. However, 1x CSE induced a roughly 2-fold increase in IBV specific spleenocyte IFN-γ levels compared to PBS controls. Finally, increasing concentrations of CSE resulted in increased mortality compared to PBS controls after subsequent IBV infection, a significant decrease in IBV specific IgA or IgG levels but did not impact weight loss. Together, our system established a platform for further study of CS on IBV and provided first in vivo data on impact of CS on IBV infection in model systems.

Studying cigarette smoking and determining the specific chemical or compound in CS responsible for certain pathological or immunological responses is difficult for many reasons. Noah et al. measured live IBV vaccine RNA and specific cytokine levels post vaccination in nasal lavage fluid from active young smokers, secondhand smoke

exposed, and never smoker groups (57). They noted that smokers had higher levels of IBV vaccine RNA and lower IL-6/IFN-γ levels compared to never smoker controls. Noteworthy, their conclusions were heavily influenced by variation in daily cigarettes consumed, type of cigarettes smoked, age, genetic background, unknown co-morbidities, and other environmental factors, and use of attenuated vaccine virus. To minimize the impact from those factors, it is necessary to perform a similar evaluation in a better control experimental system. Traditionally, the experimental system is built on the usage of a smoking chamber. Even though it can better mimic natural respiratory conditions, it suffers from the imprecise inoculation amount, let alone the financial requirements necessary for purchase. Here, we established a system based on the usage of water-soluble components from CS. Cigarette smoke is comprised of over 7000 chemicals and compounds. Our system will allow us to quickly distinguish water soluble component effects of cigarette smoke on IBV infection from the non-water soluble effects with fewer confounding factors. Additionally, it is superior in financial cost and prevents research personnel from handling mice that otherwise may be covered in toxic or carcinogenic components of cigarette smoke collected on their fur from side-stream smoke exposure. All these factors make this system a simple yet robust platform for evaluating CSE on respiratory viral infection.

We found that CSE treatment did not affect weight loss at any concentration from 1x to 20x. This is curious as smoking has been shown to result in weight loss in mice (58, 59). At least three factors could partially explain this lack of weight loss: a) the CSE we made contains only the water-soluble components of cigarette smoke, b) the mice were not exposed to CSE long enough to induce physical changes, or c) there were chemical variation in the cigarettes we used compared to previous studies. During the

actual act of smoking cigarettes, there would be constant exposure of the lungs to water soluble and insoluble components of CS. To make our CSE, we bubble CS through PBS to capture the water soluble components, but allow the rest of the smoke to escape through the pump. Subsequently, any water insoluble particles that are trapped on the liquid surface are mostly removed by filter sterilization. As such, it's possible the water insoluble particles or the combination with soluble components are necessary to induce weight loss. For CSE exposure length, previous studies have shown that there is a difference in pro-inflammatory cytokine response profiles depending on CS exposure of less than or greater than 2 weeks (60). It is possible that CSE exposure more than 2 weeks could have yielded a more significant effect on morbidity and mortality. Animal model studies with IAV range from as few as 3 days (61) to as long as 6 months (48). Given that there is huge variation in treatment period and amount of cigarettes used, it is not surprising to observe no significant weight loss from CSE treatment alone. Additionally, the brand of cigarette used in a study may have potential consequences on disease outcomes, including damage to the lungs. For example, Goel et al. found that among 27 brands of US commercially available cigarettes, there was as much as a 12-fold variation in free radicals in the gas phase of the CS (62). These free radicals can cause damage to cellular membranes and DNA (63), resulting in tissue damage to exposed organs. Because cigarette smoke contains over 7000 different chemicals and compounds (64), variation in which cigarettes are used in academic studies are likely going to lead to phenotypic variation post infection. Nevertheless, our CSE treatment did exhibit negative impacts on experimental animals, which resulted in decreased survival after subsequent IBV infection in a CSE dose dependent manner. The difference in

weight loss warrants necessity for future studies to further titrate the specific amount, treatment time and types of CS or CSE.

Our data indicates that 1x CSE treatment did not impact IBV viral loads at 3 or 6 dpi with high or low doses of IBV. Gualano et al. has reported that cigarette smoke exposure in mice can lead to a moderate increase to viral loads (40). However, more reports indicate CS exposure does not impact viral loads of IAV infections, which is in line with our findings (41, 45-47). This would suggest that worse disease outcomes in our smoking model is likely not due to increased viral burden. Our speculation is in line with previous reports, which have correlated the final severity of disease outcome with the elevated inflammatory responses post IAV infection in smoking conditions, rather than with viral replication.

We noted interestingly that 1x CSE treatment resulted in increased IFN-□ production in spleenocytes compared to the PBS controls. IFN-γ promotes differentiation and proliferation of $CD8^+$ T-cells and upregulates antigen presenting cell MHC II expression, aiding in $CD4^+$ T-cell activation (65, 66). Only a specific set of immune cells produce IFN-γ including $CD8^+$ cytotoxic T-cells, B cells, and antigen presenting cells (APCs)(67). Our data suggests that post infection, CSE treatment may have resulted in either an expansion of IBV specific immune cells or the spleenocyte immune cells are producing more IFN-γ than none CSE treatment under the same IBV specific stimulation. This was also mentioned earlier that there was a time dependent effect of CS on immune cytokine responses to infection (60). It is possible that elevated IFN-γ responses post infection could reflect higher inflammatory responses (attracting more cells) post IBV infection in 1x CSE treated mice. Interestingly, this differs from IAV data, as Feng et al. has shown that there was reduced IFN-γ from the lungs of CS mice, as well as

reduced numbers of IFN-γ+ cells from lungs and spleens of CS treated mice compared to control mice (41). It is possible this represents a potential pathological difference between IAV and IBV models of smoking, but it also may likely reflect experimental parameter differences including 1) exposure time, 6 weeks CS exposure vs 2 weeks CSE exposure and 2) exposure materials, CS versus CSE. Additionally, treatments with higher concentrations of CSE led to higher mortality after IBV infection. This suggests that higher concentrations of CSE are resulting in higher levels of inflammation post infection and could be responsible for exacerbating disease outcomes. Indeed, a number of IAV/CS studies have found higher lung and upper airway cell infiltration in CS mice compared to control groups (44, 46, 47).

Together, our results show that our system is a valid, rapid, and safer method to explore the effects of CS on IBV pathology and immune response compared to traditional experimental chamber models. We used the system to provide evidence to validate the negative impact of smoking on IBV infection. Our system could be used to extend our understanding of other respiratory microbes in the smoking condition or other co-morbidities, such as diabetes, to help guide clinicians to better treatment outcomes.

Materials and Methods

Virus and cells: Influenza B/Victoria/2/87 virus was propagated in pathogen free eggs purchased from Charles River laboratories Inc and stored at -80°C. A549 and Madin-Darby canine kidney (MDCK) cells were cultured at 37°C in DMEM medium supplemented with 10% FBS, or MEM medium supplemented with 10% FBS, respectively.

Multi-step growth curve. To evaluate viral replication under the influence of CSE, A549 cells were plated at 3x105 cells per well in 6 well plates in DMEM supplemented with 10% FBS for 24 hours (hrs). Cells were aspirated, then treated overnight with either PBS, 1x CSE, or 2.5x CSE diluted in DMEM with 10% FBS. The following day, media with CSE or PBS was removed, and cells were infected with a multiplicity of infection (MOI) of 0.05 of Influenza B/Victoria/2/87 virus diluted in PBS/BSA/PS (1x PBS, 0.42% BSA, 100ug/ml Pen-strep, 0.8mM $CaCl_2$-2*H_2O, 1mM $MgCl_2$-6H_2O) and incubated at 33°C for one hour. Then, virus solutions were aspirated and replaced with 1ml of post infection media (1x DMEM, 0.35% BSA, 100U/ml Pen-strep, 2mM L-glutamine, 0.15% sodium bicarbonate, 20mM HEPES pH 7.0, 0.25ug/ml TPCK). Infection samples were collected at 24 and 48 hours post infection. The virus concentrations were evaluated by standard plaque assays.

Plaque Assay. MDCK cells were plated in 12 well plates at 5x105 cells/well the night before in MEM supplemented with 10% FBS. Virus was serially diluted in PBS/BSA/PS. MEM media from cells was aspirated and replaced with 200µl of virus dilution for 1hr at

33°C. Plates were rocked every 15 min. Virus was aspirated and replaced with plaque overlay (1x EMEM, 0.21% BSA, 100µg/ml Pen/Strep, 2mM L-Glutamine, 0.22% Sodium Bicarbonate, 10mM HEPEs pH 7.0, 0.1% D-dextrose, 0.7% Avicel, 1µg/ml TPCK). Plates were incubated at 33°C for 72hrs. Cells were fixed with 3.7% Formaldehyde in 1x PBS for 1hr, then stained with 0.08% Crystal Violet.

Mice. 6-8 weeks old Female BALB/cJ mice were purchased from the Jackson Laboratory and housed in a pathogen free vivarium facility at the University of California, Riverside. Food and water were available ad libitum.

Cigarette Smoke Extract (CSE) Exposure. Cigarette smoke extract was prepared as previously described (53, 54). Briefly, cigarette smoke from 40 commercially available Marlboro Class A Cigarettes were filtered through 12.5ml of sterile 1xPBS at a rate of 1 cigarette every 1 minutes in a chemical hood. Cigarettes were smoked until they reached the filter, then replaced. The resulting liquid was filter sterilized through a 0.22uM filter and classified as “40X cigarette smoke extract (CSE)”. 40x CSE was aliquoted and frozen at -80°C until use.

6 to 8-week-old BALB/cJ female mice were anesthetized with isoflurane, then intranasally inoculated with 50µl of specified concentration of CSE (diluted in sterile PBS) or PBS as a mock control. Mice were daily treated in the same manner, 6-days per week for two weeks.

Influenza Virus infections. After two weeks of CSE exposure, mice were isoflurane anesthetized and intranasally inoculated with 50µl of Influenza B/Victoria/2/87 WT virus

diluted in PBS/BSA/PS. Total PFU per mouse given were as specified in figures. Mice were sacrificed on day 0, 3, 6, or 21 post infection depending on the experiment.
Lung Pathology. After two weeks of CSE or PBS treatments, mice were infected with 105 PFU B/Victoria/2/87 WT virus per mouse. Mice were sacrificed 0 and 3 days post infection, and lungs were extracted, washed in 1x PBS, then fixed in 4% formaldehyde at room temperature. Lungs were dehydrated, embedded in paraffin, and lung sections were subjected to Hematoxylin and Eosin (H&E) staining.

Hematoxylin and Eosin (H&E) staining. Mice were euthanized with CO2, and lungs were extracted and washed with PBS, the fixed it with 4% formaldehyde for 72 hrs at room temperature. Lungs were subsequently dehydrated with 70%, 80%, 90%, and 95% ethanol for 2, 2, 1, and 1hr respectively, then dehydrated again with 100% ethanol for 1 hr. After xylene treatment, lungs were immersed in liquid paraffin wax. Lungs were sectioned using microtome (Lecia Microsystems, Leica RM2235,) at approximately 4µm thickness per slice. The slices were then attached to a glass slide and dried at 45°C for 12 hrs. Last, slides were Hematoxylin-Eosin stained, dried, fixed with neutral resin, then covered with cover slips.

BAL fluid Collection. 21 days post IBV infection, mice were sacrificed. Tracheas were exposed and incisions were made above the manubrium. One ml of sterile PBS was pushed through the incision and out the nasal cavity for collection. BAL fluid was clarified by centrifugation, aliquoted, and frozen at -80°C until analysis.

Enzyme-linked immunosorbent assay (ELISA) for IgG and IgA. To assess the levels of virus-specific IgG and IgA antibodies present in samples from IBV infected mice, ELISAs were performed on blood sera (for IgG) or lavage fluid (for IgA) samples. In brief, 96 well MaxiSorp ELISA plates (Thermo Fisher Scientific, #442404, Rochester, NY) were coated with 50µl of 10µg/ml purified B/Victoria/2/87 WT virions. Wells were blocked at room temperature with PBS containing 1% dried milk and 0.1% Tween 20 (blocking buffer) for 2hrs, washed with PBS containing 0.1% Tween 20 (wash buffer), and subsequently incubated with blood sera or lavage samples serially diluted in blocking buffer. After 2hr room-temp incubations, plates were washes with wash buffer and incubated with secondary horse radish peroxidase conjugated antibody (Southern Biotech #1040-05 for IgA; Millipore, CAT# AP503P, Temecula, Ca for IgGγ for 30min at room temperature. Plates were washed with wash buffer and incubated with colorimetric substrate (o-phenylenediamine dihydrochloride, Invitrogen, Carlsbad, CA) for 30min at room temperature, then read with a plate reader measuring optical density at 450 nm (OD450).

IFN-γ evaluation. Mice were sacrificed 6 days post IBV infection. Spleens were removed and washed in 5ml of R10 media (RPMI media supplemented with 2mM L-glutamine, 100ug/ml Pen-strep, 100mM Hepes pH 7.0, and 10% FBS). Spleens were homogenized through a 40 µM cell strainer, washed with 5 ml of R10 media, centrifuged at 1000g for 5 min, then aspirated. Homogenates were treated with 3ml of Ammonium-Chloride-Potassium (ACK) lysis buffer (NH_4Cl 150mM, $KHCO_3$ 10mM, EDTA 0.1mM, pH to 7.2) for 10min and neutralized with 10ml of R10 media. Homogenates were centrifuged, aspirated, resuspended in 4ml R10 media, then counted. 3x105 cells/well were plated in

triplicate per spleen in 96 well plates in R10 media. Boiled B/Victoria/2/87 WT virus was added to a final concentration of 30ug/ml for stimulation, and plates were placed at 37°C for 72 hours. Anti CD3/CD28 antibody at 20ug/ml and R10 media was used as positive and negative controls respectively. Supernatants were harvested, clarified by centrifugation, then frozen at -80°C until ELISA analysis.

We used ELISAs to evaluate IFN-γ content in the supernatant samples. Specifically, nunc Maxisorp plates were coated with 50µl of 0.5ng/µl Anti-mouse IFN-□ purified antibody (Invitrogen eBioscience #14-7313-85) overnight at 4°C. Wells were washed 3x with wash buffer (PBS with 0.05% Tween 20). 50 µl of supernatant samples were diluted 1:10 in dilutant buffer (PBS with 1% BSA and 0.05% tween 20) and added to wells for 2 hours at 37°C. Wells were washed, then treated with 50µl (0.5 µg/ml) of biotin conjugated anti-mouse IFN-γ antibody (Invitrogen ebioscience #13-7312-85) for 1hr at 37°C. Wells were washed, then treated with 100 µl (0.5µg/ml) of HRP conjugated streptavidin (Jackson Immunoresearch #016-030-084) for 30min at 37°C. Wells were washed, then incubated with colorimetric substrate (o-phenylenediamine dihydrochloride, Invitrogen, Carlsbad, CA) for 30min and read with plate reader measuring optical density at 450 nm (OD450).

Microneutralization Assay. To assess neutralizing potency of antibodies against the challenge virus, we performed microneutralization assays. Briefly, $6x10^4$ MDCK cells were plated in 96well plates. 24hr after plating, 2000 PFU of B/Victoria/2/87 WT virus was incubated with serum samples serially diluted in PBS containing 0.35% BSA for 1hr at 33°C. Virus-serum mixtures (100µl) were added to MDCK cells (MOI=0.003) and incubated at 33°C for 1hr, then washed with PBS. Cells were then incubated overnight at

33°C in MEM media containing 0.35% BSA, 2mM L-glutamine, 0.15% $NaHCO_3$, and 2 mM HEPES pH 7.0, and 1µg/ml TPCK. 24 hours post infection (hpi), cells were fixed with 100% methanol for 20min at -20°C and washed with PBS. Cells were blocked at room-temp with PBS containing 1% dried milk and 0.1% Tween 20 (blocking buffer) for 1hr, and then incubated with sera from B/Victoria/2/87 virus infected mice diluted in blocking buffer. After 1hr room-temp incubations, plates were washes with wash buffer and incubated with secondary anti-mouse horse radish peroxidase conjugated antibody HRP (Millipore, Temecula, CA) IgGγ for 30min at room-temp. Plates were washed and then incubated with colorimetric substrate (o-phenylenediamine dihydrochloride, Invitrogen, Carlsbad, CA) for 30min and read with plate reader measuring optical density at 450 nm (OD450).

RNA Extraction and qRT-PCR. Mice were euthanized 3 days post infection by CO2 and lungs were immediately extracted and placed in 1ml of Trizol reagent. Samples were homogenized, then frozen at -80°C until time of RNA extraction. 250µl of Chloroform was added. Samples were vortexed and centrifuged at 20,000g for 15min at 4°C. The RNA from the aqueous phase was precipitated with isopropyl alcohol at a ratio of 1:1.1 using glycogen as a carrier. The resulting RNA pellet was washed with 70% ethanol, air dried, and resuspended in nuclease-free water.

To remove contaminating genomic DNA, RNA was treated with DNAse I (Ambion #2222, Austin, TX). DNAse was removed by phenol/chloroform extraction and RNA was resuspended in nuclease free water. cDNA was synthesized from 1ug of RNA per sample using Superscript II in 20µl reactions (18064-022, Invitrogen, Carlsbad CA). qRT-PCR reactions used 2µl of a 1:10 dilution of cDNA, 400 nM of each primer, and

10µl of 2x Radiant Green Lo-Rox qPCR mix (QS1005, Alkali Scientific, Fort Lauderdale FL). β-Actin internal control was used to normalize results.

Statistical Analysis. The experimental data were analyzed by the student t-test or the two-way ANOVA depending on the specific setting using the GraphPad Prism V. 9.0. Ethics and biosafety statement. Animal studies were approved by University of California, Riverside Institutional Animal Care and Use Committee (IACUC) and performed in the biosafety level 2 facility. All animals were cared for in the Animal Resources Facility under specific-pathogen-free conditions in appliance with the Institute for Laboratory Animal Research Guide for the Care and Use of Laboratory Animals, 8th edition.

References

1 Lee, V. J. et al. Advances in measuring influenza burden of disease. Influenza Other Respir Viruses 12, 3-9, doi:10.1111/irv.12533 (2018).

2 CDC Factsheet: Influenza Disease Burden

3 Organization, W. H. WHO Influenza Seasonal Factsheet 2020. (2020).

4 Yan, S. K., Weycker, D. & Sokolowski, S. US healthcare costs attributable to type A and type B influenza. Human Vaccines & Immunotherapeutics 13, 2041-2047, doi:10.1080/21645515.2017.1345400 (2017).

5 Bank, W. GDP (current US$), <https://data.worldbank.org/indicator/NY.GDP.MKTP.CD>

6 CDC. 2000-2001 INFLUENZA SEASON SUMMARY, <https://www.cdc.gov/flu/weekly/weeklyarchives2000-2001/00-01summary.htm> (2001).

7 CDC. 2001-02 INFLUENZA SEASON SUMMARY, <https://www.cdc.gov/flu/weekly/weeklyarchives2001-2002/01-02summary.htm> (2002).

8 CDC. 2002 - 03 U.S. INFLUENZA SEASON SUMMARY, <https://www.cdc.gov/flu/weekly/weeklyarchives2002-2003/02-03summary.htm>

9 CDC. 2003 - 04 U.S. INFLUENZA SEASON SUMMARY, <https://www.cdc.gov/flu/weekly/weeklyarchives2003-2004/03-04summary.htm> (2004).

10 CDC. 2004-05 U.S. INFLUENZA SEASON SUMMARY, <https://www.cdc.gov/flu/weekly/weeklyarchives2004-2005/04-05summary.htm> (2005).

11 CDC. 2005-06 U.S. INFLUENZA SEASON SUMMARY, <https://www.cdc.gov/flu/weekly/weeklyarchives2005-2006/05-06summary.htm> (2006).

12 CDC. 2006-07 U.S. INFLUENZA SEASON SUMMARY, <https://www.cdc.gov/flu/weekly/weeklyarchives2006-2007/06-07summary.htm> (2007).

13 CDC. 2007-08 U.S. INFLUENZA SEASON SUMMARY, <https://www.cdc.gov/flu/weekly/weeklyarchives2007-2008/07-08summary.htm> (2008).

14 CDC. 2008-2009 Influenza Season Summary, <https://www.cdc.gov/flu/weekly/weeklyarchives2008-2009/08-09summary.htm> (2009).

15 CDC. 2009-2010 Influenza Season Summary, <https://www.cdc.gov/flu/weekly/weeklyarchives2009-2010/09-10Summary.htm> (2010).

16 CDC. Update: Influenza Activity - United States, 2010-11 Season, and Composition of the 2011-12 Influenza Vaccine, <https://www.cdc.gov/mmwr/preview/mmwrhtml/mm6021a5.htm> (2011).

17 CDC. Update: Influenza Activity - United States, 2011-12 Season and Composition of the 2012-13 Influenza Vaccine, <https://www.cdc.gov/mmwr/preview/mmwrhtml/mm6122a4.htm> (2012).

18 CDC. Influenza Activity - United States, 2012-13 Season and Composition of the 2013-14 Influenza Vaccine, <https://www.cdc.gov/mmwr/preview/mmwrhtml/mm6223a5.htm?s_cid=mm6223a5_e> (2013).

19 CDC. Influenza Activity - United States, 2013-14 Season and Composition of the 2014-15 Influenza Vaccines, <https://www.cdc.gov/mmwr/preview/mmwrhtml/mm6322a2.htm> (2014).

20 CDC. Influenza Activity - United States, 2014-15 Season and Composition of the 2015-16 Influenza Vaccine, <https://www.cdc.gov/mmwr/preview/mmwrhtml/mm6421a5.htm> (2015).

21 CDC. Influenza Activity - United States, 2015-16 Season and Composition of the 2016-17 Influenza Vaccine, <https://www.cdc.gov/mmwr/volumes/65/wr/mm6522a3.htm> (2016).

22 CDC. Update: Influenza Activity in the United States During the 2016–17 Season and Composition of the 2017–18 Influenza Vaccine, <https://www.cdc.gov/mmwr/volumes/66/wr/mm6625a3.htm> (2017).

23 CDC. Update: Influenza Activity in the United States During the 2017–18 Season and Composition of the 2018–19 Influenza Vaccine, <https://www.cdc.gov/mmwr/volumes/67/wr/mm6722a4.htm?s_cid=mm6722a4_w> (2018).

24 CDC. FluView Interactive Map (2019-2020, weeks 40-26), <https://gis.cdc.gov/grasp/fluview/fluportaldashboard.html>

25

26 Bhat, Y. R. Influenza B infections in children: A review. World J Clin Pediatr 9, 44-52, doi:10.5409/wjcp.v9.i3.44 (2020).

27 CDC Smoking & Tobacco Use Factsheet. (2020).

28 Control, C. f. D. CDC Smoking & Tobacco Use: Health Effects Factsheet.

29 Almirall, J., Gonzalez, C. A., Balanzo, X. & Bolibar, I. Proportion of community-acquired pneumonia cases attributable to tobacco smoking. Chest 116, 375-379, doi:10.1378/chest.116.2.375 (1999).

30 Almirall, J., Bolibar, I., Balanzo, X. & Gonzalez, C. A. Risk factors for community-acquired pneumonia in adults: a population-based case-control study. European Respiratory Journal 13, 349-355, doi:10.1183/09031936.99.13234999 (1999).

31 Aryanpur, M. et al. Cigarette smoking in patients newly diagnosed with pulmonary tuberculosis in Iran. International Journal of Tuberculosis and Lung Disease 20, 679-684, doi:10.5588/ijtld.15.0662 (2016).

32 Alcaide, J. et al. Cigarette smoking as a risk factor for tuberculosis in young adults: A case-control study. Tubercle and Lung Disease 77, 112-116, doi:10.1016/s0962-8479(96)90024-6 (1996).

33 Smith, G. S. et al. Cigarette smoking and pulmonary tuberculosis in northern California. Journal of Epidemiology and Community Health 69, 568-573, doi:10.1136/jech-2014-204292 (2015).

34 Bonacci, R. A. et al. Impact of cigarette smoking on rates and clinical prognosis of pulmonary tuberculosis in Southern Mexico. Journal of Infection 66, 303-312, doi:10.1016/j.jinf.2012.09.005 (2013).

35 Pavic, I., Jurkovic, M. & Pastar, Z. Risk Factors for Acute Respiratory Tract Infections in Children. Collegium Antropologicum 36, 539-542 (2012).

36 Mazarico, E., Gomez-Roig, M. D., Guirado, L., Lorente, N. & Gonzalez-Bosquet, E. Relationship between smoking, HPV infection, and risk of cervical cancer. European Journal of Gynaecological Oncology 36, 677-680 (2015).

37 Kark, J. D., Lebiush, M. & Rannon, L. Cigarette-Smoking as a Risk Factor for Epidemic a(H1n1) Influenza in Young Men. New Engl J Med 307, 1042-1046, doi:Doi 10.1056/Nejm198210213071702 (1982).

38 Finklea, J. F., Sandifer, S. H. & Smith, D. D. Cigarette Smoking and Epidemic Influenza. Am J Epidemiol 90, 390-&, doi:DOI 10.1093/oxfordjournals.aje.a121084 (1969).

39 Aronson, M. D., Weiss, S. T., Ben, R. L. & Komaroff, A. L. Association between cigarette smoking and acute respiratory tract illness in young adults. JAMA 248, 181-183 (1982).

40 Gualano, R. C. et al. Cigarette smoke worsens lung inflammation and impairs resolution of influenza infection in mice. Resp Res 9, doi:Artn 53 10.1186/1465-9921-9-53 (2008).

41 Feng, Y. et al. Exposure to Cigarette Smoke Inhibits the Pulmonary T-Cell Response to Influenza Virus and Mycobacterium tuberculosis. Infect Immun 79, 229-237, doi:10.1128/Iai.00709-10 (2011).

42 Han, Y. et al. Influenza Virus-Induced Lung Inflammation Was Modulated by Cigarette Smoke Exposure in Mice. Plos One 9, doi:ARTN e86166 10.1371/journal.pone.0086166 (2014).

43 Hong, M. J. et al. Protective role of gamma delta T cells in cigarette smoke and influenza infection. Mucosal Immunol 11, 894-908, doi:10.1038/mi.2017.93 (2018).
44 Kang, M. J. et al. Cigarette smoke selectively enhances viral PAMP- and virus-induced pulmonary innate immune and remodeling responses in mice. J Clin Invest 118, 2771-2784, doi:10.1172/Jci32709 (2008).

45 Ferrero, M. R. et al. CCR5 Antagonist Maraviroc Inhibits Acute Exacerbation of Lung Inflammation Triggered by Influenza Virus in Cigarette Smoke-Exposed Mice. Pharmaceuticals (Basel) 14, doi:10.3390/ph14070620 (2021).

46 Robbins, C. S. et al. Cigarette smoke impacts immune inflammatory responses to influenza in mice. Am J Resp Crit Care 174, 1342-1351, doi:10.1164/rccm.200604-561OC (2006).
47 Bauer, C. M. T. et al. Treating Viral Exacerbations of Chronic Obstructive Pulmonary Disease: Insights from a Mouse Model of Cigarette Smoke and H1N1 Influenza Infection. Plos One 5, doi:ARTN e1325110.1371/journal.pone.0013251 (2010).

48 Wang, J. M., Li, Q. H., Xie, J. G. & Xu, Y. J. Cigarette smoke inhibits BAFF expression and mucosal immunoglobulin A responses in the lung during influenza virus infection. Resp Res 16, doi:ARTN 3710.1186/s12931-015-0201-y (2015).

49 Mebratu, Y. A., Smith, K. R., Agga, G. E. & Tesfaigzi, Y. Inflammation and emphysema in cigarette smoke-exposed mice when instilled with poly (I:C) or infected with influenza A or respiratory syncytial viruses. Resp Res 17, doi:ARTN 75 10.1186/s12931-016-0392-x (2016).

50 Ladomenou, F., Kafatos, A. & Galanakis, E. Environmental tobacco smoke exposure as a risk factor for infections in infancy. Acta Paediatrica 98, 1137-1141, doi:10.1111/j.1651-2227.2009.01276.x (2009).

51 Jedrychowski, W. & Flak, E. Maternal smoking during pregnancy and postnatal exposure to environmental tobacco smoke as predisposition factors to acute respiratory infections. Environmental Health Perspectives 105, 302-306, doi:10.1289/ehp.97105302 (1997).

52 Miyahara, R. et al. Exposure to paternal tobacco smoking increased child hospitalization for lower respiratory infections but not for other diseases in Vietnam. Scientific Reports 7, doi:10.1038/srep45481 (2017).

53 Aedo, G., Miranda, M., Chavez, M. N., Allende, M. L. & Egana, J. T. A Reliable Preclinical Model to Study the Impact of Cigarette Smoke in Development and Disease. Curr Protoc Toxicol 80, e78, doi:10.1002/cptx.78 (2019).

54 Elliott, M. K., Sisson, J. H., West, W. W. & Wyatt, T. A. Differential in vivo effects of whole cigarette smoke exposure versus cigarette smoke extract on mouse ciliated tracheal epithelium. Experimental Lung Research 32, 99-118, doi:10.1080/01902140600710546 (2006).

55 Duffney, P. F. et al. Cigarette smoke increases susceptibility to infection in lung epithelial cells by upregulating caveolin-dependent endocytosis. Plos One 15, e0232102, doi:10.1371/journal.pone.0232102 (2020).

56 Jaspers, I. et al. Reduced Expression of IRF7 in Nasal Epithelial Cells from Smokers after Infection with Influenza. Am J Resp Cell Mol 43, 368-375, doi:10.1165/rcmb.2009-0254OC (2010).

57 Noah, T. L. et al. Tobacco Smoke Exposure and Altered Nasal Responses to Live Attenuated Influenza Virus. Environ Health Persp 119, 78-83, doi:10.1289/ehp.1002258 (2011).

58 Chen, H. et al. Effect of short-term cigarette smoke exposure on body weight, appetite and brain neuropeptide Y in mice. Neuropsychopharmacology 30, 713-719, doi:10.1038/sj.npp.1300597 (2005).

59 Chen, H. et al. Cigarette smoke exposure reprograms the hypothalamic neuropeptide Y axis to promote weight loss. Am J Respir Crit Care Med 173, 1248-1254, doi:10.1164/rccm.200506-977OC (2006).

60 Chavez, J. & Hai, R. Effects of Cigarette Smoking on Influenza Virus/Host Interplay. Pathogens 10, doi:10.3390/pathogens10121636 (2021).

61 Boehme, S. A. et al. MAP3K19 Is Overexpressed in COPD and Is a Central Mediator of Cigarette Smoke-Induced Pulmonary Inflammation and Lower Airway Destruction. Plos One 11, e0167169, doi:10.1371/journal.pone.0167169 (2016).

62 Goel, R. et al. Variation in Free Radical Yields from US Marketed Cigarettes. Chemical Research in Toxicology 30, 1038-1045, doi:10.1021/acs.chemrestox.6b00359 (2017).

63 Machlin, L. J. & Bendich, A. Free-radical tissue-damage - protective role of antioxidant nutrients. Faseb Journal 1, 441-445, doi:10.1096/fasebj.1.6.3315807 (1987).

64 National Cancer Institute: Harms of Cigarette Smoking and Health Benefits of Quitting Factsheet, <https://www.cancer.gov/about-cancer/causes-prevention/risk/tobacco/cessation-fact-sheet#:~:text=Of%20the%20more%20than%207%2C000,least%2069%20can%20cause%20cancer.>

65 Maraskovsky, E., Chen, W. F. & Shortman, K. IL-2 AND IFN-GAMMA ARE 2 NECESSARY LYMPHOKINES IN THE DEVELOPMENT OF CYTOLYTIC T-CELLS. Journal of Immunology 143, 1210-1214 (1989).

66 Curtsinger, J. M., Agarwal, P., Lins, D. C. & Mescher, M. F. Autocrine IFN-gamma Promotes Naive CD8 T Cell Differentiation and Synergizes with IFN-alpha To Stimulate Strong Function. Journal of Immunology 189, 659-668, doi:10.4049/jimmunol.1102727 (2012).

67 Castro, F., Cardoso, A. P., Goncalves, R. M., Serre, K. & Oliveira, M. J. Interferon-Gamma at the Crossroads of Tumor Immune Surveillance or Evasion. Frontiers in Immunology 9, doi:10.3389/fimmu.2018.00847 (2018).

Figures and Tables

Flu Season	A/B Case Ratio	% IAV cases	% IBV Cases
2000-2001	5337/4625	54	46.0
2001-2002	13706/1965	87.5	12.5
2002-2003	6180/4768	56.4	43.6
2003-2004	24400/249	99	1.0
2004-2005	17750/5799	75.4	24.6
2005-2006	14355/3642	79.7	20.3
2006-2007	18817/4936	79.2	20.8
2007-2008	28263/11564	71	29.0
2008-2009	18175/9507	66	34.0
2009-2010	155591/2273	99	1.0
2010-2011	40282/13994	74	26.0
2011-2012	19285/3132	86	14.0
2012-2013	51675/21455	71	29.0
2013-2014	46727/6743	87.4	12.6
2014-2015	104,822/20,640	83.5	16.5
2015-2016	62982/28477	68.9	31.1
2016-2017	116590/45361	72	28.0
2017-2018	189716/88187	68.3	31.7
2018-2019	208153/11189	94.9	5.1
2019-2020	27617/19357	58.8	41.2

Table 4.1 Yearly IAV to IBV Infections in the United States as Reported by the CDC

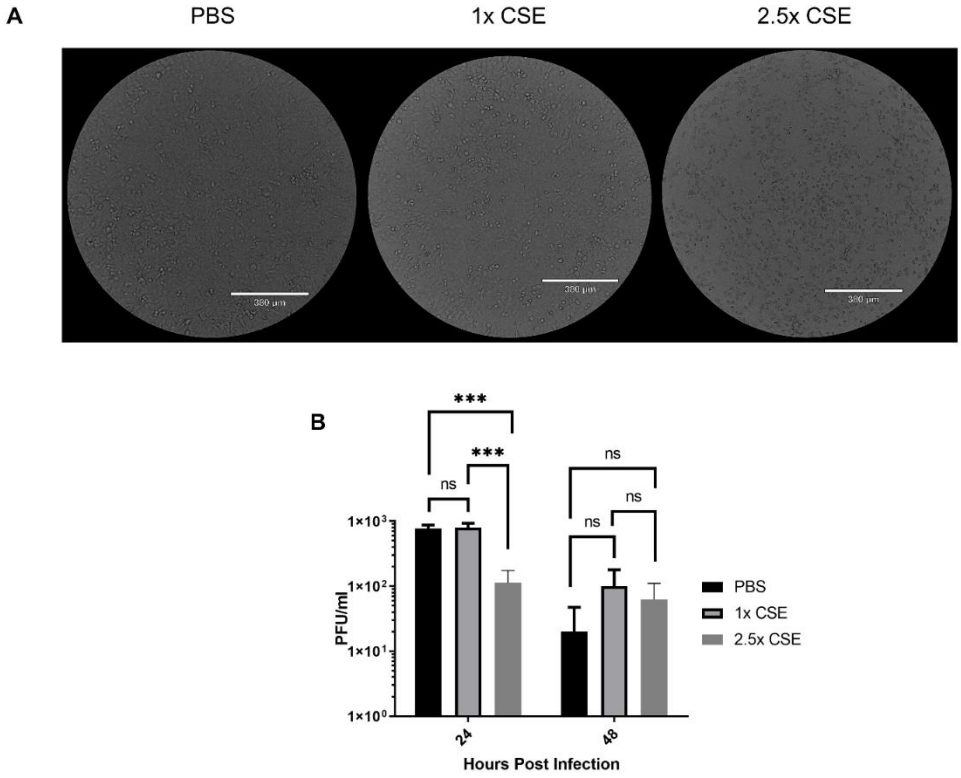

Figure 4.1 CSE does not affect viral replication ex vivo

A) 10X magnification of A549 cells treated for 24hrs with either PBS (mock), 1x CSE, or 2.5x CSE. B) Treated cells were infected with Influenza B/Victoria/2/87 at an MOI = 0.05. Supernatant samples were taken at 24 and 48 hpi and tittered by standard plaque assay. A standard 2-way ANOVA with multiple comparisons was used for statistical analysis in PRISM software 9.0, *** = $p<0.0001$. N=4 per treatment group.

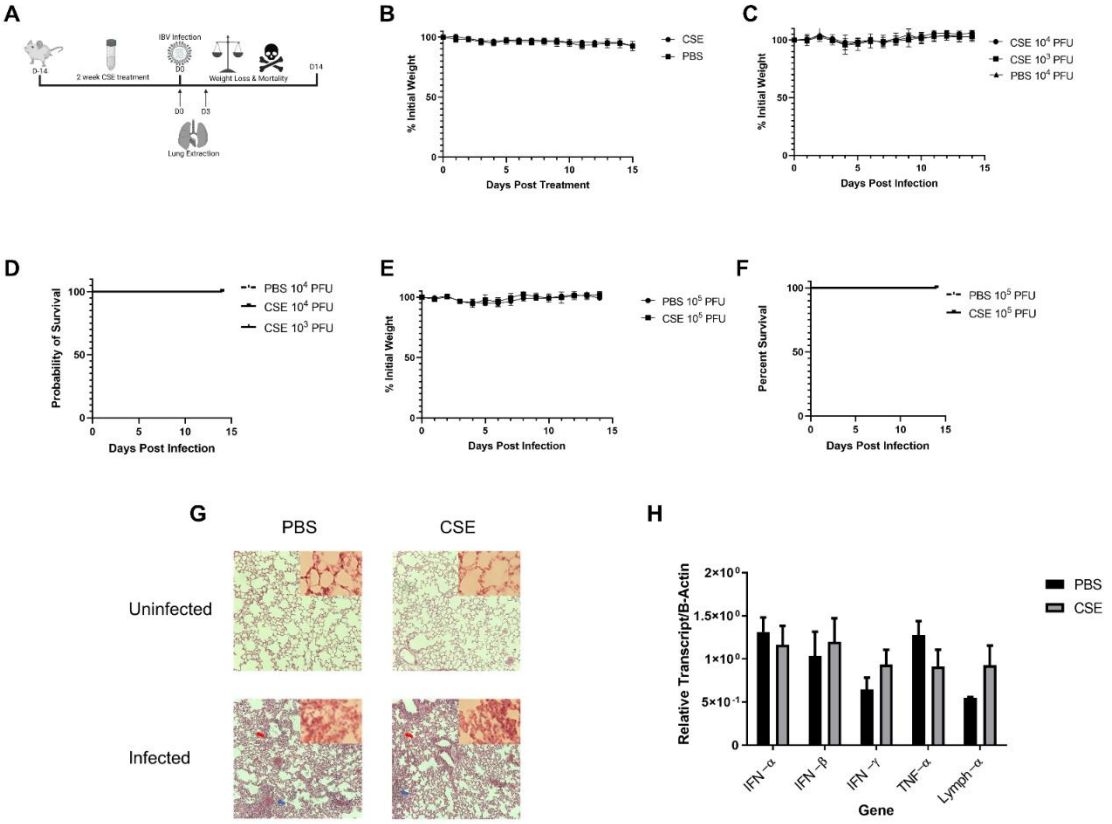

Figure 4.2 1X CSE treatment does not affect mice weight loss or survival before or after IBV infection.

A) 6–8-week-old female BALB/cJ mice were treated intranasally with 50µl of 1xCSE daily, six days per week, for two weeks total. Weights of mice were monitored during 1x CSE treatment (B) and after infection (C) with 10^3 or 10^4 PFU, or 105 (E) PFU/mouse. Survival was monitored up to 14 days post infection for D) 10^3/10^4 or 10^5 (F) PFU/mouse groups. N=5 for all groups. Lungs were harvested from 1X CSE treated mice at the day of infection, Day 0, or three days post IBV infections. For mice of 3 DPI, half of tissues were fixed for H&E staining analysis (G) and the rest were used for qPCR gene expression analysis of pro-inflammatory molecules (H). Larger lung pictures are 10X magnification, while smaller picture in upper right corner of lung histology represents 20x magnification. Red arrows indicated thickening of the alveolar septa with congestion, blue arrows indicated the infiltration of inflammatory cells. A large number of neutrophils and lymphocytes were only present in 20X pictures of infected samples. Statistical significance for figure were determined by 2-way ANOVA with multiple comparisons.

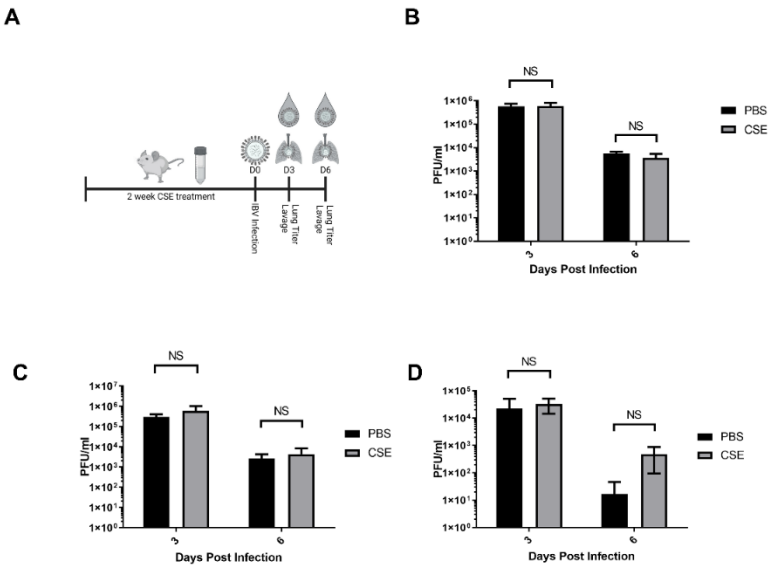

Figure 4.3 1X CSE treatment does not affect respiratory viral replication or pathological responses.

A) schematic describing 6–8-week-old female BALB/cJ mice treated with 1X CSE and infected with IBV. Virus lung replication was measured on day 3 and day 6 post $1x10^3$ (B) or $1x10^5$ PFU/mouse of IBV (C). D) Virus replication was also measured from upper airway lavage fluid collected from $1x10^3$ PFU infected mice by standard plaque assay. Significance was determined by standard students t-test.

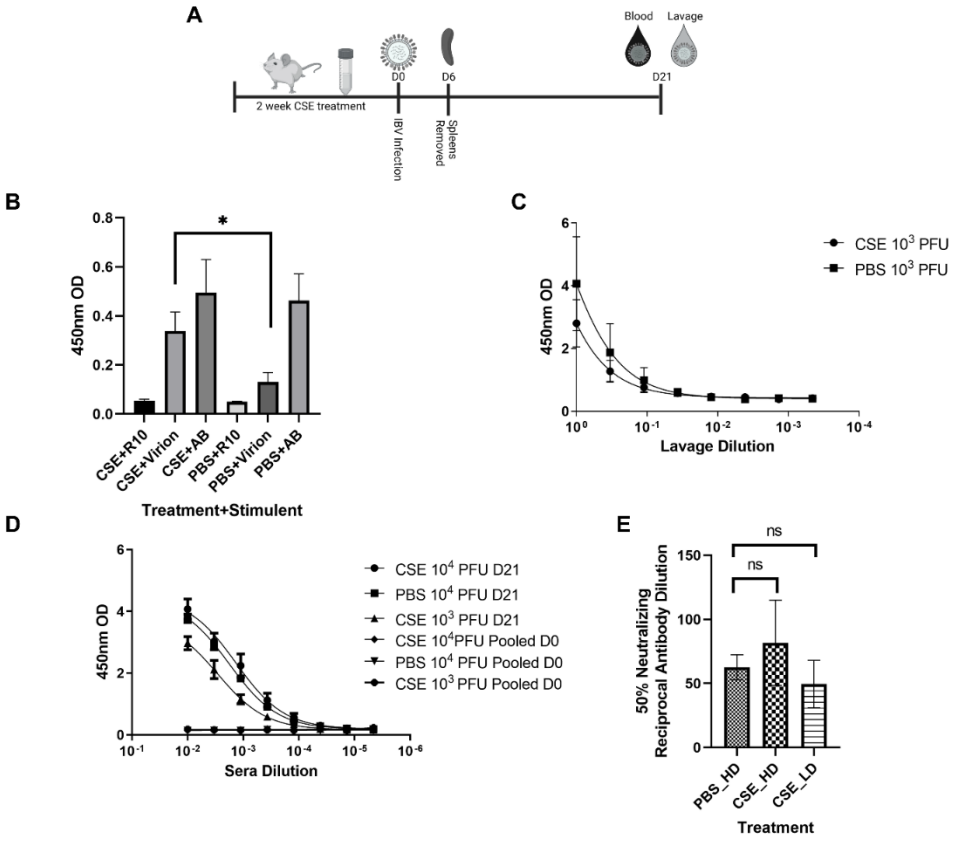

Figure 4.4 1X CSE treated mice do not exhibit altered adaptive immune responses post IBV infection.

As shown in schematic A) mice were treated with 1x CSE for two weeks and infected with either 10^3 or 10^4 PFU/mouse of IBV. Spleens from 10^3 PFU infection group were removed 6 DPI, homogenized and stimulated with either IBV virion, R10 media only, or Positive Control Antibody CD3/CD28 (AB). B) IFN-ɣ expression was measured from stimulated splenocytes by ELISA. N=3. B) Upper airway lavage fluid was used to measure IgA antibody titers 21 DPI by ELISA from mice infected with 10^3 PFU of IBV (C) Blood sera was drawn from mice infected with 10^3 or 10^4 of IBV 21 DPI to measure IBV specific IgG responses by ELISA (N=5) or (D) neutralizing antibody titers as calculated from the 50% Reciprocal Inhibition Titer. Two-way ANOVA was used to test significant differences with multiple comparisons, * indicating $p<0.5$

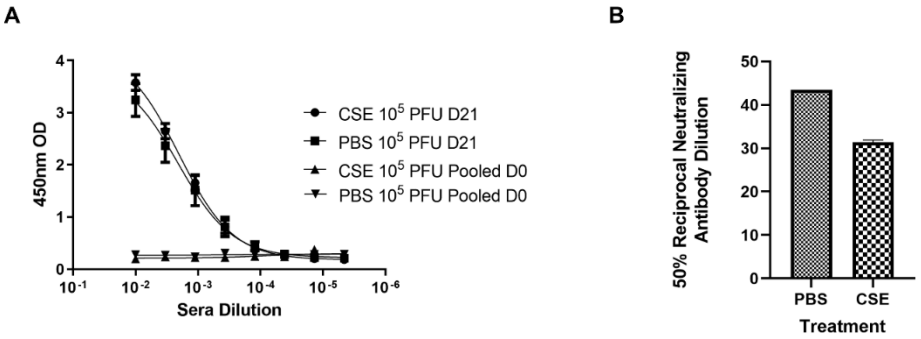

Figure 4.5 1x CSE treatment does not affect IgG or neutralizing titers of mice infected with higher doses of IBV.
Mice were infected with treated with 1x CSE as in Figure 4, and infected with 10^5 PFU/mouse of IBV. A) Blood sera was drawn from mice infected with 10^3 (LD) or 10^4 (HD) of IBV 21 DPI to measure IgG responses by ELISA (N=5) or (D) neutralizing antibody titers as calculated from the 50% Reciprocal Inhibition Titer. Two-way ANOVA was used to test significant differences.

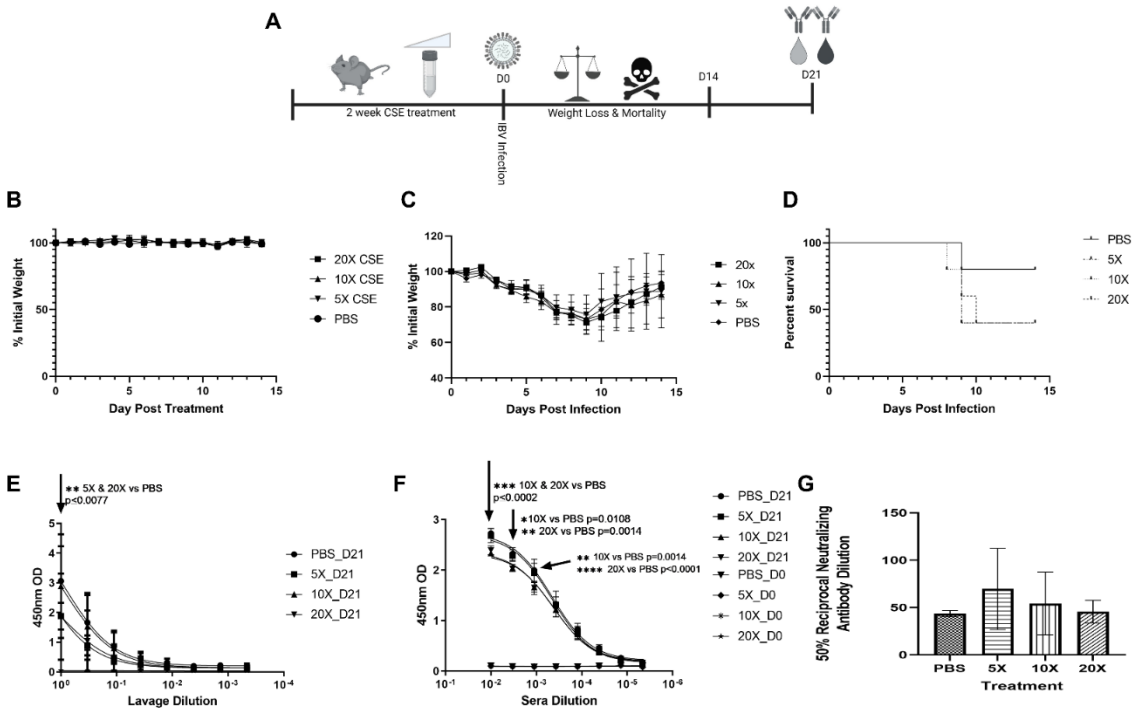

Figure 4.6 Increasing concentrations of CSE reduced survival.
A) Schematic showing 6-8-week-old female BALB/cJ mice were treated intranasally with 50µl of CSE, ranging from 5x to 20x, daily for six days per week, for two weeks total. B) Weights of mice were monitored during CSE treatment and C) after infection with 10^5 PFU/mouse of IBV for 14 days. D) Survival was monitored for up to 14 days post infection, N=5 for all groups. E) Lavage IgA or F) Sera IgG specific for IBV from samples collected at 21 DPI was determine by ELISA from surviving mice, and G) neutralizing antibody titers were calculating from microneutralization assays. Two-way ANOVA was used to test significant differences

Conclusion Chapter

In this chapter, I will summarize our main findings associated with our research aims and contextualize our results within the field. I will also discuss the limitations, possible future experiments, and applications of this work.

Influenza viruses represent a major annual public health concern. Influenza A virus (IAV) and Influenza B virus (IBV) are responsible for yearly epidemics, yet IBV remains well understudied, and potentially underutilized, compared to IAV. Broadly, we sought to fill three gaps in the field regarding IBV pathology, replication, and vaccination. First, cigarette smoking is a major risk factor of chronic and infectious disease, and while the risk and effects of CS have been modeled in IAV, there is no model regarding how IBV infections are impacted by CS. Second, the IBV nucleoprotein (BNP) remains under characterized in terms of its interactions with host proteins during replication. Third, current generation live attenuated influenza vaccines mimic real influenza virus infection, but have limited use during pandemic situation in part due to the potential reassortment event that could occur with circulating viruses, resulting in restoration of virulence to the vaccine strains. To these ends, our long-term goals were: a) better understanding the pathogenic impact CS on IBV infections in a well-controlled system b) elucidation of host-viral interactions with the BNP protein c) development of safer LAIV strategies for pandemic situations.

We sought to model the impact of IBV infection on smoker's health, virus replication and pulmonary damage in a controlled environment. To achieve this, mice were pre-treated with various concentrations of cigarette smoke extract (CSE) for two weeks prior to IBV infection. We found that low doses of CSE did not affect virulence

weight loss, survival, lung pathology, viral IBV replication in the lungs or upper airway, IgA or IgG antibody levels, or IgG neutralizing potency. Interestingly, low dose CSE did increase spleenocyte IFN-γ levels post IBV stimulation, suggesting CSE elevated cellular immune responses to IBV infection. Finally, higher doses of CSE did not affect virulence weight loss, but did significantly decrease survival post infection, IgA and IgG levels, but did not affect IgG neutralizing potency. These findings, to the best of our knowledge, represent the first animal system modeling how CS directly impacts IBV infection. Prior to this, Noah et al., had shown that young current smokers had elevated pro-inflammatory cytokine levels and higher viral RNA levels post vaccination with live attenuated IBV compared to never smoker controls (1). However, these findings are based upon human data which can be significantly affected by genetic variation, number of cigarettes smoked per day, unknown co-morbidities, diet, variation in exercise, variation in type of cigarettes smoked per day, age, and prior immunogenic exposure to IBV. Our system provides a robust platform to quickly and easily replicate experiments in a controlled environment with animals that have well controlled diets, genetic backgrounds, and equal CSE exposure. Using CSE provides three additional benefits, including a safer process for animal handling, cheaper set up, and specific understanding of water-soluble component effects. Traditional cigarette smoking models utilize plexiglass or glass chambers to expose the whole animals to side-stream smoke pumped into the chamber (similar to secondhand smoke exposure). This allows for the buildup of toxic or carcinogenic compounds on the fur and represents hazards when handling the animals. Our system utilizes CSE nasal inoculations to treat the mice, preventing personal from handling smoke covered mice. Second, because the mice are inoculated intranasally, no special chamber or equipment is necessary making our

system a cheaper option compared traditional models. Third, because the CSE we use only contains the water-soluble parts of cigarette smoke, our platform allows for future experiments to separate the effects of water-soluble from water-insoluble parts of CS by comparing to traditional chamber CS models.

To better understand the pathways perturbed by BNP in IBV infection, we conducted a yeast two hybrid (Y2H) screen using BNP as the bait. We screened BNP against both a human and mouse cDNA library. We discovered 13 human and 6 mouse proteins that potentially interact with BNP. Interestingly, KPNA3 was found among both human and mouse lists as a potential BNP interactor. KNPA3 in humans is the gene encoding the nuclear adaptor protein IMPα4, one of 7 nuclear adaptor proteins that link cellular cargo to IMPβ for nuclear import. To validate this interaction between IMPα4 and BNP in human cells, we showed that IMPα4 could be co-immunoprecipitated (Co-IP) with BNP as the bait in 293T cells. Further, BNP amino acids 44-47, the putative nuclear localization signal, were required for this interaction by Co-IP. In 293T cells, both IMPα4 and BNP co-localized to the nucleus. Interestingly, knockout of IMPα4 gene expression resulted in only a slight decrease to IBV replication. Together, our data suggests that BNP and IMPα4 likely bind in vivo, but this interaction is likely not necessary for replication. It should be noted that while this data suggests IMPα4 facilitates nuclear import similar to IAV, our current methods cannot determine if IMPα4 facilitates BNP nuclear import. Further, while IAV NP has been shown to be necessary and sufficient for import of the vRNA (2, 3), it is not clear if BNP facilitates the same process for IBV. To determine if BNP facilitates nuclear import of the vRNA, and if IMPα4 is involved in this process, an in vitro import assay system is required (4).

To better attenuate influenza live virus vaccines for pandemic situations and to improve upon previous designs (5), we by progressively introducing IBV HA amino acids into the IAV ectodomain and expressed this chimera in the IBV genetic backbone. We found that introduction of 8 and 9 amino acids from IBV HA introduced into the membrane proximal region (MPR) of IAV H9HA resulted in significant reduction in viral replication ex vivo compared to PBS or IBV backbone controls. These vaccine candidates in mice did not affect survival or weight loss post vaccination and were able to elicit both significant levels of IAV specific IgG and neutralizing IgG against the vaccine target IAV HA. Finally, these vaccine candidates were able to protect mice from lethal IAV challenge. This vaccine design represents a significant if iterative step forward from the previous design. Hai et al. (5) expressed the IAV HA ectodomain in the genetic backbone of IBV, and attenuated these vaccines viruses by truncating the NS segment. Our approach of progressive mutation of HA achieves 2 goals simultaneously. First, progressive mutation of the membrane proximal region of IAV HA attenuates replication without the need to introduce attenuation through a master donor virus like current generation live vaccines need. Second, this progressive attenuation of HA prevents the vaccine virus from restoring to a virulent state due to a reassortment event occurring between the vaccine virus and circulating IBVs. However, we did find that in vivo, viral vaccine replication was similar to the IBV backbone replication group. Even though weight loss was similar between vaccine and IBV backbone/PBS groups, it is still possible that similar pulmonary replication could suggest the vaccine candidates have pulmonary pathological effects. As such, it is critical that further analysis of the lung pathology be performed on vaccinated mice to confirm the vaccine candidates do not damage the lungs. Despite this, these attenuated viruses still represent valuable

resources as live vaccines that can elicit both humoral and mucosal immunity, without the risk of reassortment with IAV, nor restoration of virulence from IBV reassortment.

And so, a question must be asked. Given the distinct origin of each chapter topic discussed, are these projects related to each other? Superficially, these studies are interconnected through the use of IBV, both as a model to study pathology and replication, as well as serve as a viral vector for vaccination. In truth, while each project was derived separately from one another, each project is connected through the consequences of their findings. For example, the platform we developed for examining cigarette smoking on IBV infections could easily be used for examination of how CS affects IBV vaccinations. As noted in chapter three, Noah et all found that CS directly impacts the cytokine immune profiles of smokers compared to non-smokers (1). The development of our CSE/IBV platform allows for the controlled study of how CS impacts IBV vaccination efficacy and immune responses to vaccination, including how immune responses would be impacted in our rIBV vectored vaccines. For example, we noted an increase in IFN-□ production from spleenocytes due to CSE exposure in mice during infection. IFN-□ is produced from a subset of immune cells, including CD8+ and CD4+ T-Cells during activation. These cells are important for clearance of infected cells and activation and proliferation other immune cells such as B-cells. It would be important to examine what are the consequences of these immune changes in the context of vaccines as they could inform us as to how our rIBV vaccines may behave given specific lifestyle factors like CS. Additionally, BNP, its functions as a nucleoprotein, and its interactions in host cells represent a fundamental aspect underlying all IBV replication. As such, its functions and interactions would likely be integral to both vaccine replication and under smoking infection conditions. Japanese encephalitis virus NS5 protein

competitively binds to IMPα4, reducing nuclear import of its cargo NF-κB and as a consequence, reducing IFN-β, a type I interferon (IFN) (6). These IFNs during infection trigger expression of antiviral genes that are integral for the innate immune response (7). We speculate that BNP could similarly competitively inhibit NF-kB action by competing for binding to IMPα4. Interestingly, cigarette smoke extract has been shown to alter nuclear localization profiles of specific cargo proteins such as HSP10 in lung fibroblast cells, localizing to the nucleus in the presence of CSE but not without (8). This could suggest that CSE may be having an effect, directly or indirectly, on the nuclear import/export machinery and cargo. The water insoluble tar phase from cigarette smoke has been shown to increase activation of NF-kB in a dose dependent fashion in multiple cell types including T-cells and lung cells (9). If this is the case, smoking effects on NF-kB may be antagonistic to BNP's speculated competitive role. It is however not clear what the consequences are of CS induced chronic activation of NF-kB are for the host, much less during IBV infection. Further, because CS alters immune response profiles during infection, it's possible that these CS/NP specific actions could be altered in vaccinations using live attenuated viruses given they simulate real infections.

In summary, we labored to fill three specific gaps in the IBV field regarding how cigarette smoking impacted infection, how interactions between BNP and IMPα4 affected replication, and how to develop a better method for attenuation of live influenza vaccine viruses for use in pandemic situations. First, we found that high concentrations of CSE significantly reduced humoral responses to infection as well as reduced survival. This study represents the development of a robust, simple, and controlled experimental platform to further study the impact CS has on all facets of IBV replication that was not previously available, including how CS may impact vaccination responses. Second, we

confirmed that BNP and IMPα4 interact via Co-IP, but deletion of IMPα4 expression does not impact IBV replication ex vivo. This study warrants further analysis of other IMPα proteins interaction with BNP as they could collectively represent future therapeutic targets for treatments. Third, progressive introduction of IBV HA coding sequence into the IAV ectodomain resulted in attenuation of rIBVs expressing IAV HA ex vivo, elicited IAV specific antibodies that could neutralize IAV, and finally could protect mice from lethal challenge. These recombinant viruses represent promising candidate vaccines as they are incapable of reassorting with circulating IAV, and do not possess the capacity to lose their attenuation even if they reassort with circulating IBV.

References

1 Noah, T. L. et al. Tobacco Smoke Exposure and Altered Nasal Responses to Live Attenuated Influenza Virus. Environmental Health Perspectives 119, 78-83, doi:10.1289/ehp.1002258 (2011).

2 Oneill, R. E., Jaskunas, R., Blobel, G., Palese, P. & Moroianu, J. Nuclear Import of Influenza-Virus Rna Can Be Mediated by Viral Nucleoprotein and Transport Factors Required for Protein Import. Journal of Biological Chemistry 270, 22701-22704, doi:DOI 10.1074/jbc.270.39.22701 (1995).

3 Cros, J. F., Garcia-Sastre, A. & Palese, P. An unconventional NLS is critical for the nuclear import of the influenza A virus nucleoprotein and ribonucleoprotein. Traffic 6, 205-213, doi:10.1111/j.1600-0854.2005.00263.x (2005).

4 Cassany, A. & Gerace, L. Reconstitution of nuclear import in permeabilized cells. Methods Mol Biol 464, 181-205, doi:10.1007/978-1-60327-461-6_11 (2009).

5 Hai, R., Garcia-Sastre, A., Swayne, D. E. & Palese, P. A Reassortment-Incompetent Live Attenuated Influenza Virus Vaccine for Protection against Pandemic Virus Strains. Journal of Virology 85, 6832-6843, doi:10.1128/Jvi.00609-11 (2011).

6 Ye, J. et al. Japanese Encephalitis Virus NS5 Inhibits Type I Interferon (IFN) Production by Blocking the Nuclear Translocation of IFN Regulatory Factor 3 and NF-kappaB. J Virol 91, doi:10.1128/JVI.00039-17 (2017).

7 McNab, F., Mayer-Barber, K., Sher, A., Wack, A. & O'Garra, A. Type I interferons in infectious disease. Nat Rev Immunol 15, 87-103, doi:10.1038/nri3787 (2015).

8 Corrao, S. et al. Hsp10 nuclear localization and changes in lung cells response to cigarette smoke suggest novel roles for this chaperonin. Open Biol 4, doi:ARTN 140125 10.1098/rsob.140125 (2014).

9 Anto, R. J., Mukhopadhyay, A., Shishodia, S., Gairola, C. G. & Aggarwal, B. B. Cigarette smoke condensate activates nuclear transcription factor-kappa B through phosphorylation and degradation of I kappa B alpha: correlation with induction of cyclooxygenase-2. Carcinogenesis 23, 1511-1518, doi:DOI 10.1093/carcin/23.9.1511 (2002).